DISSERTATIONES
NEUROSCIENTIAE
UNIVERSITATIS
TARTUENSIS
43

LING YAN

Stress-associated immune mechanisms of schizophrenia: the importance of region-specific microglia-neurovascular interaction

DISSERTATIONES NEUROSCIENTIAE UNIVERSITATIS TARTUENSIS
43

DISSERTATIONES NEUROSCIENTIAE UNIVERSITATIS TARTUENSIS
43

LING YAN

Stress-associated immune mechanisms of schizophrenia: the importance of region-specific microglia-neurovascular interaction

UNIVERSITY OF TARTU
Press
1632

Department of Physiology, Institute of Biomedicine and Translational Medicine, University of Tartu, Tartu, Estonia.

The dissertation was accepted for the commencement of the degree of Doctor of Philosophy in Neurosciences on October 19th, 2023 by the council for the Curriculum of Neurosciences.

Supervisors:	Li Tian, PhD, Research Professor, Department of Physiology, Institute of Biomedicine and Translational Medicine, University of Tartu, Estonia
	Cai Song, PhD, Professor, Guangdong Ocean University, China
	Eero Vasar, MD, PhD, Professor, Department of Physiology, Institute of Biomedicine and Translational Medicine, University of Tartu, Estonia
Reviewers:	Martti Laan, MD, PhD, Associate Professor, Department of Medical Biology, Institute of Biomedicine and Translational Medicine, University of Tartu, Estonia
	Liina Haring, MD, PhD, Associate Professor, Department of Psychiatry, Institute of Clinical Medicine, University of Tartu, Estonia
Opponent:	Urtė Neniškytė, PhD, Associate Professor, Institute of Biosciences, Life Sciences Center, University of Vilnius, Lithuania
Commencement:	December 15th, 2023

This study was supported by the Mobilitas Pluss top researcher grant No. MOBTT77 by the European Union through the European Regional Development Fund and the personal research grant No. PRG878 from the Estonian Research Council.

ISSN 1736-2792 (print)
ISBN 978-9916-27-393-7 (print)
ISSN 2806-2418 (pdf)
ISBN 978-9916-27-394-4 (pdf)

University of Tartu Press
www.tyk.ee

TABLE OF CONTENTS

LIST OF ORIGINAL PUBLICATIONS

The thesis is based on the following original papers, referred to in the text by Roman numerals I–IV.

I. Chen S, Fan F, Xuan FL, **Yan L**, Xiu M, Fan H, Cui Y, Zhang P, Yu T, Yang F, Tian B, Hong LE, Tan Y, Tian L. Monocytic subsets impact cerebral cortex and cognition: differences between healthy subjects and patients with first-episode schizophrenia. *Front Immunol.* 2022 Jul 11;13: 900284. https://doi: 10.3389/fimmu.2022.900284.

II. **Yan L***, Li Y*, Feng W, Chithanathan K, Li W, Huang J, Li H, Chen W, Tian B, Wang Z, Tan S, Zharkovsky A, Hong LE, Tan Y, Tian L. CSF1R regulates schizophrenia-related stress response and vascular association of microglia/macrophages. *BMC Med*. 2023 Aug 4;21(1):286. https://doi:10.1186/s12916-023-02959-8.

III. Xuan FL*, **Yan L***, Chithanathan K, Gou M, Chen W, Li Y, Huang J, Wang L, Zharkovsky A, Tan T, Tian L. Adult vascular-associated $CD206^{+}$ microglia may be progenitor-like cells dampened in first episode schizophrenia. (Preprint) https://doi:10.2139/ssrn.4492077

IV. **Yan L**, Gu MQ, Yang ZY, Xia J, Li P, Vasar E, Tian L, Song C. Endogenous n-3 PUFAs attenuated olfactory bulbectomy-induced behavioral and metabolomic abnormalities in *fat-1* mice. *Brain Behav Immun.* 2021 Aug;96:143–153. https://doi: 10.1016/j.bbi.2021.05.024.
* Shared first authorship.

Contribution of the author

I. The author participated in the RNA-seq data analysis and manuscript editing.

II. The author constructed the CUS model, performed mice behavioral tests, immunohistochemistry and flow cytometry experiments, analyzed data, and wrote the manuscript.

III. The author participated in the study design, performed flow cytometry, RNA-seq, and immunohistochemistry experiments, analyzed data, and revised the manuscript.

IV. The author participated in study design, performed all experiments, analyzed data, and wrote the manuscript.

ABBREVIATIONS

ANCOVA	analysis of covariance
ANOVA	analysis of variance
BAM	border-associated macrophages
BBB	blood-brain barrier
BGI	Beijing Genomics Institute
CBM	cerebellum
Cop	coproporphyrinogen III
CSF1R	colony stimulating factor 1 receptor
CSF1Ri	CSF1R inhibitor
CTQ	childhood trauma questionnaire
Ctr	control
CTX	cortex
CUS	chronic unpredictable stress
DAPI	4′,6-diamidino-2-phenylindole
DEG	differentially expressed gene
DSM	Diagnostic and Statistical Manual of Mental Disorders
EPM	elevated plus maze
Fads	fatty acid desaturase
FDR	false discovery rate
FES	first episode schizophrenia
GO-BP	gene ontology biological pathway
HCs	healthy controls
HPA	hypothalamus-pituitary gland-adrenal gland
HPC	hippocampus
IBA1	ionized calcium-binding adapter molecule 1
ICV	intracranial volume
IFN-γ	interferon-γ
IL	interleukin
KEGG	Kyoto encyclopaedia of genes and genomes
Klf	Krüppel-like transcription factor
LC-TOF/MS	liquid chromatography-time-of-flight mass spectrometry
Log_2FC	log_2 fold changes
MCCB	MATRICS™ consensus cognitive battery
MDD	major depressive disorder
MFI	mean fluorescent intensity
MRI	magnetic resonance imaging
NMDA	N-methyl-D-aspartate
NO	nitric oxide
No.	number
NVAMs	nonvessel-associated microglia/macrophages
NVU	neurovascular unit
OB	olfactory bulb

OBX	olfactory bulbectomy
OFT	open field test
OPC	oligodendrocyte precursor cell
OPLS-DA	orthogonal projections to latent structures-discriminate analysis
PANSS	positive and negative symptom scale
PBS	phosphate buffered saline
PCA	principal component analysis
PFA	paraformaldehyde
PFC	prefrontal cortex
Pla2g	phospholipase A2 group
PPI	protein-protein interaction
PSS	perceived stress scale
PUFAs	polyunsaturated fatty acids
PVMs	perivascular macrophages
QCs	quality controls
qPCR	quantitative polymerase chain reaction
RNA-seq	ribonucleic acid sequencing
ROS	reactive oxygen species
SNS	sympathetic nervous system
SPT	sucrose preference test
SSC	somatosensory cortex
TCT	three-chamber test
TGF-β	transforming growth factor-β
TH	thalamus
TMs	total microglia/macrophages
TNF-α	tumor necrosis factor-a
TST	tail suspension test
VAMs	vessel-associated microglia/macrophages
VEGF	vascular endothelial growth factor
Veh	vehicle
VIP	variable importance for the projection
WT	wild type

1. INTRODUCTION

Psychiatric disorders, also known as mental illnesses, are a major source of disability and death for the working-age population and cause considerable economic and healthcare burdens globally (Collaborators, 2017). Psychiatric disorders can be caused by miscellaneous intrinsic and extrinsic factors that jointly impact on the brain (Uher et al., 2017; Charlson et al., 2019; Machlitt-Northen et al., 2022). Schizophrenia is a major psychiatric disorder showing psychotic and affective symptoms as well as cognitive impairment (McCutcheon et al., 2020), which can be exacerbated by stressful events (Vafadari et al., 2019; Holtzman et al., 2013; Gomes et al., 2017).

Stress-associated dystrophies of the cortical and subcortical structures are frequently observed in both psychiatric patients (Lieberman et al., 2018; Kalin, 2019; Wannan et al., 2019) and animal models (Kim et al., 2015; Sarabdjitsingh et al., 2017), due to impaired neuronal projections across different brain structures (Franklin et al., 2012). For instance, we have reported that cumulative stress is associated with cortical thinning and cognitive deficits in first episode schizophrenia (FES) patients (Zhou et al., 2021). Besides neuronal deficits, biological substrates underlying stress-induced brain changes also include compromised angiogenesis and integrity of the blood-brain barrier (BBB) (Greene et al., 2018; Dion-Albert et al., 2022), and glia-mediated neuroinflammation (Sugama et al., 2020; Maydych, 2019).

Individuals with higher levels of inflammatory biomarkers are at an increased risk of developing psychiatric disorders (Kose et al., 2021; Hughes et al., 2022). Psychiatric patients also often have inflammation-associated abnormal lipid metabolism, among others (Penninx et al., 2018; van der Spek et al., 2023). Immunometabolic alterations tip the balance of neurotransmission, and disrupt the blood and cerebrospinal fluid circulations in the brain (Hodo et al., 2020; Carmen-Orozco et al., 2019), thereby triggering and/or exacerbating psychiatric disorders (Cattaneo et al., 2015).

Microglia and borderline/barrier-associated macrophages (BAMs) are the most important regulators for neuroinflammation in the adult brain (Yang et al., 2019; Frumer et al., 2023). Their overactivation is detrimental to the brain and behaviors causing spine loss, BBB leakage, as well as anxiety and cognitive impairment (Tan et al., 2020; Yu et al., 2022). Nevertheless, glia are also beneficial for brain homeostasis with neuro-protective functions and may contribute to stress adaptation (Cătălin et al., 2013; Piirainen et al., 2021). Multiple glia-targeting anti-inflammatory drugs (Zhang et al., 2018; Zhang et al., 2019; Gao et al., 2022) have been tested to treat psychiatric disorders. However, these generic treatments have only shown limited and even debatable supplementary therapeutic effects (Nitta et al., 2013). This suggests that we still do not fully understand the temporal-spatial feature and functions of microglia/macrophages, especially concerning their subgroups and associated effector molecules, in a disease-specific context.

To better understand functions of microglia/monocytes and their subpopulations in psychiatric disorders through the lens of chronic stress, we performed a series of clinical and preclinical investigations on a cohort of FES patients and two mouse stress models, including a chronic unpredictable stress model combined with pharmacological microglial ablation, and an olfactory bulbectomy-induced stress model combined with endogenous delivery of omega-3 polyunsaturated fatty acids. Using these models, we characterized region/location-specific mechanisms of microglia/macrophages in regulating brain and behaviors by multidisciplinary *in vivo* and *in vitro* laboratory approaches. Our research findings reveal subtype-specific microglial/monocytic molecules that may be useful candidates for developing diagnostic biomarkers and therapeutic drugs for psychiatric disorders.

2. REVIEW OF LITERATURE

2.1. Overview of stress and stress-associated psychiatric disorders

2.1.1. Stress-associated psychiatric disorders: focusing on schizophrenia

Major stress-related psychiatric disorders as classified in the Diagnostic and Statistical Manual of Mental Disorders-5 (DSM-5) (First, 2013) and the International Classification of Diseases-11 (Harrison et al., 2021) include schizophrenia, bipolar disorder, anxiety disorders such as post-traumatic stress disorder, and major depressive disorder (MDD), among others. Millions of people worldwide have been reported to suffer from psychiatric disorders, which are considered serious public health problems (Collaborators, 2017). Stress is a common individual experience and an inevitable part of all human lives, but when becoming persistent, stress can cause, trigger, or exacerbate almost any mental illness, particularly psychiatric disorders, which are characterized by dysregulated stress responses (Halbreich, 2021). Stress is also a major component of many animal models recapitulating psychiatric disorders, such as olfactory bulbectomy and chronic stress rodent models (McHugh et al., 2019; Atrooz et al., 2021).

Symptoms of schizophrenia can be broadly classified into three categories: positive symptoms, negative symptoms, and cognitive symptoms (Tandon et al., 2013). The positive symptoms, such as delusions and hallucinations, are often the reason a patient presents to a clinician. The negative symptoms, such as loss of motivation and social withdrawal, and cognitive impairments, including deficits in working memory, executive function, and processing speed, are the major reason affecting social and vocational functions of a patient (Galderisi et al., 2018). Schizophrenia affects approximately 1 in 300 people (0.32%) worldwide (WHO, 2022). Its onset is most often during late adolescence and young adulthood and tends to happen with higher prevalence and earlier onset among men than women (Giordano et al., 2021; Li et al., 2022). Schizophrenia accounts for a huge healthcare burden, with annual associated costs estimated to be more than $343.2 billion in the United States in 2019, for instance (Kadakia et al., 2022). In Europe, unemployment rates of such patients run between 70% and 90% (Holm et al., 2021). The disorder is also associated with reduced life expectancy: individuals with schizophrenia have a mean life expectancy of about 15 years shorter than the general population and a 5% to 10% lifetime risk of death by suicide (Hjorthøj et al., 2017).

Schizophrenia is believed to result from a combination of genetic and environmental factors (Comer et al., 2020). While the exact mechanisms underlying schizophrenia are not fully understood, several theories have been proposed to explain the onset and progression of its symptoms. The most prominent theory on schizophrenia is disturbance of the neurotransmitter system. An

imbalance of dopamine neurotransmission in the mesolimbic system is responsible for positive symptoms (Lau et al., 2013). This hypothesis is supported by the fact that antipsychotics that block dopamine receptors are effective in reducing the positive symptoms of schizophrenia. Dysfunction in the glutamate neurotransmission system in the mesocortical pathway, including the prefrontal cortex (PFC), thalamus, and temporal lobes, induces cognitive impairments and negative symptoms of schizophrenia (Uno et al., 2019). Disturbances in glutamate signaling may affect synaptic plasticity (i.e., the ability of neurons to modify the strength of their connections with other neurons) and N-methyl-D-aspartate (NMDA) receptor functioning. As such, NMDA-receptor antagonists can induce psychotic symptoms mimicking schizophrenia (Winship et al., 2019).

There is also evidence that abnormalities in brain development may contribute to schizophrenia. For example, studies have found that individuals with schizophrenia may have smaller brain volumes, particularly in the PFC and hippocampus (HPC), brain regions that are important for cognition and memory (Kalin, 2019; Lieberman et al., 2018; Wannan et al., 2019). In addition, early-life environmental and genetic risk factors altering neurodevelopmental trajectories, which predispose an individual to the disorder, are also identified. For example, certain genetic variants, including those related to the immune system development, have been associated with an increased risk of developing schizophrenia (Comer et al., 2020). Twin studies suggest that schizophrenia has a heritability estimate of around 80%, due to not only genetic influences but also environmental effects that moderate genes (van Os et al., 2008). Environmental factors, such as prenatal stress, infection, and substance abuse, may all increase the risk of developing schizophrenia (van Os et al., 2009).

In recent years, scientists have found that exposure to psychological stress or traumatic life event(s) during perinatal or adolescent period triggers or exacerbates symptoms of schizophrenia (Vafadari et al., 2019; Holtzman et al., 2013; Gomes et al., 2017). Heightened stress response usually precedes the onset of psychosis and cognitive deficits in schizophrenia patients (Pruessner et al., 2011; Krkovic et al., 2017; Studerus et al., 2021) and induces psychiatric-like behaviors in modeled rodents (Willner, 2017; Tran et al., 2023). Our group also reported that cumulative stress was associated with cortical thinning and cognitive deficits in FES patients (Zhou et al., 2021).

All current pharmacological treatments for schizophrenia are dopamine D2-receptor blockers, many of which having extrapyramidal or metabolic side effects and work for only about half of patients, despite treating positive symptoms efficiently and enabling the patient an independent life. However, prominent negative symptoms and cognitive impairments that affect approximately 40% and 80% of people with schizophrenia, respectively, have no treatments available with proved efficiency currently (Carbon et al., 2014; McCutcheon et al., 2020). The underlying reason for this is due to incomplete understanding of the complex pathophysiology of schizophrenia, which involves many molecular targets. Therefore, more rigorous research is needed to better understand the underlying mechanisms and to develop more effective treatments.

2.1.2. Chronic unpredictable stress (CUS) model

Several rodent chronic stress models resemble human psychosocial stressors, which include both predictable and unpredictable components, such as chronic social defeat stress, chronic restraint stress, and CUS (Tran et al., 2023).

The CUS model was first described by Katz in 1981 (Katz et al., 1981) and developed further by Papp and Willner (Willner, 2017). The model involves subjecting animals to a series of unpredictable and varied stressors over an extended period. The specific stressors can vary but typically include physical stressors such as restraint, cold temperature exposure, forced swimming, or psychological stressors like social isolation or exposure to predators' odors (Nollet, 2021). Unlike acute or predictable stressors that the body can adapt to, the CUS disrupts the body's ability to respond to and cope effectively with stressors, leading to dysregulation of various physiological systems and behavioral processes (Monteiro et al., 2015; Trow et al., 2019). The CUS model is often employed to study stress-related psychiatric disorders such as depression, anxiety and cognitive impairment (Tran et al., 2023).

In line with clinical finding, exposure to chronic stressors has been demonstrated to lead to psychiatric-related behaviors by inducing neurotransmitter dysregulation (Duman et al., 2019), neuroinflammation (Wohleb et al., 2016), and impairments in neurogenesis (Franklin et al., 2012; Pittenger et al., 2008) in corticolimbic and mesolimbic brain regions, leading to structural changes in these regions (McEwen, 2006; Kim et al., 2015; Sarabdjitsingh et al., 2017). These preclinical studies demonstrate that stress-induced neurobiological effects contribute to psychiatric-like behaviors such as anhedonia, despair, anxiety, social withdrawal, and cognitive impairments (Planchez et al., 2019).

2.1.3. Olfactory bulbectomy (OBX)-induced stress model

Olfaction is indispensable for acquisition of emotions and associated memories and social behaviors (Keller et al., 2013). Convincing evidence has shown that olfactory dysfunction occurs in neurodegenerative diseases (Godoy et al., 2015). Impairment of odor discrimination in schizophrenia was first reported in late 1980s (Hurwitz et al., 1988). Since then, many studies have confirmed that olfactory performance is impaired in patients with schizophrenia and MDD (Hasegawa et al., 2022). Pathological changes in the olfactory system, such as reduction in the olfactory bulb (OB) volume and olfaction deficits, are found to be associated with negative symptoms and social and cognitive impairments in patients with schizophrenia (Corcoran et al., 2005; Yang et al., 2021).

Olfactory deficits also led to stress in mice, as evidenced by elevated plasma corticosterone levels and enhanced anxiety (Glinka et al., 2012). Reduced OB volume may compromise neural circuit established between the OB and other brain regions, such as the orbitofrontal cortex, HPC, and amygdala, thereby affecting higher-order brain functions including cognition, memory, motivation, and emotion (Croy et al., 2017; Moberly et al., 2018).

Removal of the OB in rodents, i.e., OBX, induces psychiatric-like behaviors through alterations of neuroendocrine, neurotransmission, and immune components in the corticolimbic circuit (Song et al., 2005). OBX-induced depressive-like behaviors were reported to be associated with the production of reactive oxygen species (ROS) and suppression of antioxidant enzymes (Tasset et al., 2010), and hippocampal microglial activation and neuroinflammation (Morales-Medina et al., 2017) (see also section 2.3.3). Cortical and hippocampal degenerations in association with cognitive deficits, loss of libido, reduced social, exploratory and memory deficits behaviors were found in the OBX model as well (Wang et al., 2007; Morales-Medina et al., 2013). The OBX therefore has been used to screen antidepressant drugs for the past 40 years in both rats (van Riezen et al., 1976) and mice (Han et al., 2009).

2.2. Mechanisms of stress association with psychiatric disorders

Stress induces a rapid activation of the sympathetic nervous system (SNS) and a more persisting activation of the hypothalamus-pituitary gland-adrenal grand (HPA) axis, leading to increased release of epinephrine (adrenaline) and norepinephrine (Godoy et al., 2018) and glucocorticoids (cortisol) (Stephens et al., 2012). The SNS, the HPA axis, and the internal organs all work together to mediate stress-induced changes in immune and metabolic responses in the body (Kyrou et al., 2009; Mifsud et al., 2018), thereby contributing to anxiety and other psychiatric disorders (Nandam et al., 2019) (**Fig. 1**).

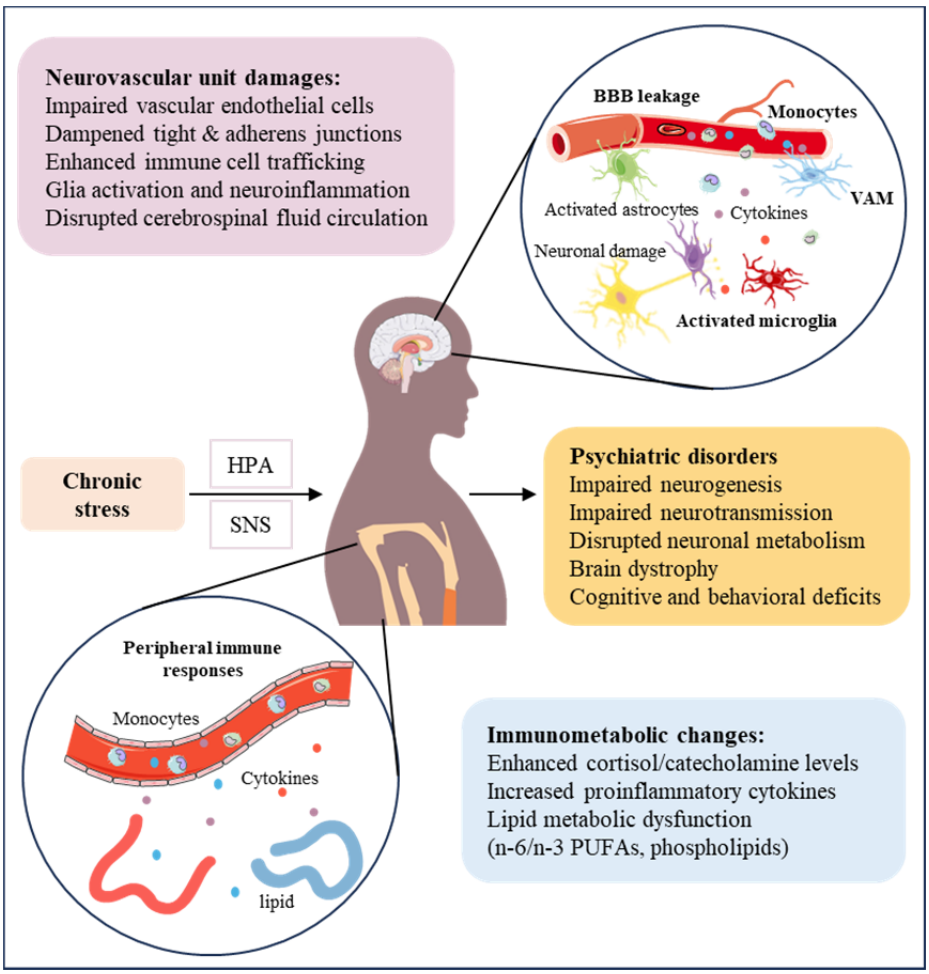

Figure 1. Mechanisms of stress-induced psychiatric disorders. Chronic stress induces psychiatric disorders due to changes in immune and metabolic responses in the periphery and the brain via activation of the sympathetic nervous system (SNS) and the hypothalamus-pituitary gland-adrenal grand (HPA) axis. In the periphery, stress-induced cortisol/catecholamines can promote immune cells such as monocytes and macrophages to produce more pro-inflammatory cytokines and disrupt lipid (omega (n)-6/n3 polyunsaturated fatty acids (PUFAs), phospholipids) metabolism in the organs. In the brain, stress can compromise neurovascular unit functions by impairing vascular endothelial cells, dampening tight and adherens junctions, enhancing immune cell infiltration, inducing glia activation and neuroinflammation, and disrupting cerebrospinal fluid circulation. Overall, through these mechanisms, stress can impair neurogenesis and neurotransmission and disrupt neuronal metabolism, resulting in brain dystrophy and cognitive and behavioral impairments. BBB: blood-brain barrier; VAM: vessel-associated microglia/macrophages. The figure is prepared using Servier Medical Art under a Creative Commons Attribution 3.0 unported license.

2.2.1. Inflammation in stress-associated psychiatric disorders

Inflammation is a physiological immune response to injury or infection in the body. However, chronic inflammation has been linked to several psychiatric disorders (Yuan et al., 2019).

Peripheral inflammatory responses are involved in psychiatric disorders including schizophrenia (Kose et al., 2021; Hughes et al., 2022). Individuals with psychiatric disorders often have higher levels of inflammatory markers in their blood and cerebrospinal fluid, such as C-reactive protein, interleukin (IL)-1β, IL-6, and tumor necrosis factor-alpha (TNF-α) produced by circulating immune cells and tissues, compared to healthy individuals (Feng et al., 2020). Chronic inflammation in the brain, or neuroinflammation, directly disrupts neurotransmission and neuroplasticity, as well as metabolism and fluid circulation (Hodo et al., 2020; Cattaneo et al., 2015; Müller, 2018).

Stress can trigger both peripheral inflammation (Elkhatib et al., 2020) and neuroinflammation (McEwen et al., 2012; Maydych, 2019). Stress-induced cortisol and noradrenergic signaling drive alterations in microglial phenotype (Frank et al., 2012; Sugama et al., 2019; Sugama et al., 2020). Prolonged stress caused for instance a release of high mobility group box 1, a damage (or danger)-associated molecular pattern molecule, which binds to the receptor for advanced glycation end products and promotes the activation of nucleotide-binding domain leucine-rich repeat and pyrin domain containing receptor 3 and pro-inflammatory cytokine production by microglia in the HPC (Weber et al., 2015). Chronic stress also increased extracellular adenosine triphosphate level, which bound to purinergic receptor P2RX7 and led to microglial activation and increased neuroinflammation (Iwata et al., 2016). Stress-induced microglial activation resulted in increased monocyte trafficking to the brain and enhanced anxiety (Wohleb et al., 2014b), and cognitive deficit along with inhibited neurogenesis (Al-Onaizi et al., 2020). Chronic stress also altered several key microglial receptor-mediated pathways, including complement component 3 – complement component 3 receptor, fractalkine – fractalkine receptor, and colony stimulating factor 1 – colony stimulating factor 1 receptor (CSF1R), leading to increased synaptic pruning and decreased dendritic branching and spine density (Bollinger et al., 2019).

2.2.2. Lipid metabolic alterations in stress-associated psychiatric disorders

Lipid metabolism involves lipids synthesis and degradation, producing among other functions energy and structural components for cells (Xie et al., 2020). Lipids, including glycerophospholipids and sphingolipids, fatty acids and their metabolites, sterols, and lipoproteins, are known to have immunomodulatory properties (Andersen, 2022).

The brain is the second most lipid-rich organ, containing abundant sphingolipids and cholesterols, and lipids take up over half of the brain's dry weight

(Cermenati et al., 2015). Lipids in the brain play important roles in myelination and action potential propagation, synaptogenesis, and neurogenesis during brain development and homeostatic maintenance (Cermenati et al., 2015). Impaired lipid metabolism is involved in oxidative stress and neuroinflammation, and disturbs neuronal energy homeostasis in the brain, leading to severe neurodevelopmental disorders and motor dysfunction (Hamilton et al., 2007; Naudí et al., 2017; Yang et al., 2022).

Studies have shown that individuals with psychiatric disorders often have abnormal levels of specific fatty acids, cholesterol, etc., and are accompanied by metabolic syndrome such as dyslipidemia (Penninx et al., 2018; van der Spek et al., 2023). For examples, increases of phospholipids were found in the gray matters of schizophrenia patients (Schwarz et al., 2008). Decreased serum levels of ether lipids and raised levels of phospholipids were also demonstrated in schizophrenia and MDD subjects (Dickens et al., 2021). Triglyceride and very low-density lipoproteins were found to be increased while low-density lipoproteins decreased in schizophrenia patients (Pillinger et al., 2017). A recent multi-omics study reported sustained metabolic disruption and increased inflammatory markers in the circulating blood of schizophrenia patients, including apolipoproteins and complement proteins (Campeau et al., 2022). Schizophrenia was also associated with decreased n-3 PUFAs and n-3/n-6 ratio in the peripheral blood (Berger et al., 2019). Knockout mice of a fatty acid binding protein 7, which modulates transportation and metabolism of fatty acids, display schizophrenia-like phenotypes and reductions in dendritic complexity and spine density (Ebrahimi et al., 2016).

Stress affects lipid metabolism in both rodents and humans. For instances, chronic stress increased lipid consumption, reduced insulin sensitivity, and promoted hepatic lipid accumulation (Dille et al., 2022), as well as disrupted endothelial lipid metabolism, hence leading to vascular injury in rodents (Abe et al., 2010). Increases of phospholipids, namely phosphatidylcholine and phosphatidylethanolamine, were found in the brains of CUS-subjected mice (Faria et al., 2014). Plasma phosphatidylcholine was associated with stress severity also in human subjects (Noerman et al., 2020). Stress affects lipid metabolism via the HPA-released cortisol (Chuang et al., 2010; Wu et al., 2019; Kivimäki et al., 2023). In return, fatty acids affect glucocorticoid receptor sensitivity and modulate the HPA axis via negative feedback on corticotropin-releasing hormone secretion (Mocking et al., 2018).

Importantly, glial cells are more vital than neurons for lipid metabolism in the brain (Barber et al., 2019). Particularly, microglial lipid metabolism was linked to both neuronal functions and brain pathology (Bruce et al., 2018; Nugent et al., 2020). Microglial depletion in adult mice by a CSF1R inhibitor (CSF1Ri) caused loss of myelin due to altered oligodendrocyte lipid metabolism (McNamara et al., 2023). Lipid metabolism was deficient in the liver of *Csf1r*-knockout mice (Keshvari et al., 2021). Furthermore, CSF1R was suggested to be associated with disrupted lipid metabolism in the corpus callosum of schizophrenia patients (Shimamoto-Mitsuyama et al., 2021).

Exact mechanisms underlying inflammation-associated alterations in lipid metabolism in stress- related psychiatric disorders are not yet fully understood, however. It is believed that both genetic and environmental factors, such as stress and diet, can contribute to these changes (Bremner et al., 2020). Understanding interrelationships between abnormal lipid metabolism and immune activation may provide new insights into the pathophysiology of stress associated psychiatric disorders and help to develop new antipsychotic therapies.

2.2.3. Cerebrovascular dysfunction in stress-associated psychiatric disorders

Angiogenesis is the process of forming new blood vessels from pre-existing vessels and plays a crucial role in normal physiological processes, including organ development, tissue growth and repair, and progression of various diseases, such as cancer, cardiovascular disease, and inflammatory disorders (Mancuso et al., 2008; Hatakeyama et al., 2020). Angiogenesis guides the development and maintenance of cerebral vasculature to ensure adequate regional blood flow and normal brain functions (Tam et al., 2010).

The neurovascular unit (NVU) is composed of vascular cells (endothelial cells, pericytes, and vascular smooth muscle cells), glial cells (astrocytes, and the more recently depicted NVU-associated microglia and oligodendrocytes), and neurons. The NVU is enclosed by tight junctions and adherens junctions and extracellular matrix components (basement membrane), with which forming the BBB (Kugler et al., 2021). The BBB is a highly selectively permeable membrane that separates the circulating blood from the brain extracellular fluid and regulates the entry of plasma substances, including nutrients and drugs, into the brain (Daneman et al., 2015). Hence, the NVU is a structural and functional complex that regulates cerebral blood flow and maintains functional integrity of the BBB and disruption of the NVU may contribute to the pathogenesis of neurodegenerative diseases (Yu et al., 2020). Dysfunction of the BBB may lead to increased inflammation and oxidative stress in the brain, which in turn may stimulate abnormal angiogenesis. Alternatively, abnormal angiogenesis may lead to disruption of the BBB, allowing harmful substances to enter the brain to trigger an inflammatory response (Carmen-Orozco et al., 2019).

In recent years, there has been an increasing interest in dysfunctions of the BBB and angiogenesis in psychiatric disorders, and accumulating evidence suggests a vital role for the NVU in modulating cognition, mood, and stress responses during the development of psychiatric disorders (Pollak et al., 2018; Morris et al., 2020; Dion-Albert et al., 2023). For instances, angiogenic genes, such as *WNT*, vascular endothelial growth factor (*VEGF*), insulin-like growth factor 1, angiopoietin, ephrin-receptor signaling, etc., were downregulated in the post-mortem brains of schizophrenia patients (Katsel et al., 2017). Lower levels of angiogenic factors, such as the VEGF, were related to abnormal brain development underlying cognitive dysfunction in schizophrenia (Zhao et al., 2019). Dampened cerebral vascular endothelial molecules and accelerated vas-

cular inflammation were found in schizophrenia patients with "high inflammation" (Cai et al., 2020). In rodent models, chronic stress was also shown to compromise the BBB and angiogenesis (Greene et al., 2018; Dion-Albert et al., 2022), and induce monocytic infiltration into the brain (Wohleb et al., 2014a).

Increased BBB permeability may allow for entry of pro-inflammatory cytokines and other immune molecules (Kealy et al., 2020) as well as monocytes (Weber et al., 2017) into the brain via the bloodstream, culminating in neuroinflammation and oxidative stress in psychiatric disorders. Vice versa, when the BBB is disrupted, astrocyte-derived S100B is released into the blood in significant amounts and has thus been regarded as a biomarker of this condition (Marchi et al., 2003). Other brain-derived BBB pathology biomarkers include glial fibrillary acidic protein, matrix metalloproteinases, tight junction molecules, and cell adhesion molecules (Sweeney et al., 2018). Blood levels of S100B, matrix metalloproteinases and cell adhesion molecules were indeed found to be altered in schizophrenia (Futtrup et al., 2020). Moreover, expression of a tight junction protein Claudin-5 was reduced in the HPC of individuals with schizophrenia (Greene et al., 2020).

Overall, molecules involved in compromised angiogenesis and BBB integrity may represent potential targets for novel therapeutic interventions in treatment of psychiatric disorders.

2.3. Microglia and microglia-like cells in psychiatric disorders: focusing on schizophrenia

As crucial myeloid cell types in the immune system, microglia and monocytes/macrophages share phenotypic similarities and yet exhibit distinct differences in terms of origin, location, and brain functions. Monocytes are originated from and replenished by hematopoietic stem cells in the bone marrow postnatally and are transported throughout the body via the bloodstream (Geissmann et al., 2010). In contrast, microglia arise from primitive myeloid progenitors in the yolk sac, which migrate into the central nervous system during embryonic development and maintain by themselves *in situ* throughout adulthood (Saijo et al., 2011). During brain homeostasis, circulating monocytes traffic to the choroid plexus and dura mater and increase the local complexity of BAMs (Van Hove et al., 2019), while their infiltration into the brain parenchyma is prevented by the BBB (Mildner et al., 2007). However, under pathological conditions, physical BBB damage and excessive inflammatory responses induce monocytes to infiltrate into the brain parenchyma and become microglia-like cells (Yamanaka et al., 2021; De Vlaminck et al., 2022). One study reported that monocytes can transit into microglia during development and after neonatal stroke, showing ramified morphology and expressing microglial marker genes (*Sall1*, *Tmem119*, and *P2ry12*) (Chen et al., 2020). Functionally, monocytes are more involved in brain pathological conditions, acting as immune surveillant in response to stimuli like inflammation or infection, and developing regulatory properties essential for tissue repair (Guilliams et al., 2018; Frumer et al., 2023).

Microglia instead play more critical roles in brain physiological conditions, including not only immune surveillance and regulation of neuroinflammation, but also synaptic pruning and support of angiogenesis and neurogenesis (Piirainen et al., 2021; Gogoleva et al., 2019; Hattori, 2023), as depicted in more details below.

2.3.1. Microglial populations and functions in the healthy brain

Microglia are the major resident innate immune cells in the brain and play a crucial role in brain development and homeostasis. One striking feature of microglia is their rapid activation in response to even minor pathological alterations/infections in the brain (Colton, 2009). In a healthy adult brain, CD45 protein amount can differentiate microglia ($CD11b^{+}/CD45^{low}$) from macrophages ($CD11b^{+}/CD45^{high}$) (Grabert et al., 2016).

Key functions of microglia in the healthy brain include: (1) Immune surveillance: microglia constantly monitor for signs of infection or injury. They are the first line of defense against pathogens and toxins that enter the brain and quickly respond to any disruption in neural functions (Nimmerjahn et al., 2005). (2) Regulation of neuroinflammation: microglia play a key role in regulating immune responses and can promote either pro-inflammatory or anti-inflammatory signaling, depending on the context (Gogoleva et al., 2019). (3) Synaptic pruning: microglia help maintain appropriate number of synapses by removing unnecessary, weak, or damaged synapses (Yu et al., 2022; Paolicelli et al., 2011). (4) Neuroprotection: microglia are responsible for clearing away debris and waste products generated by cellular metabolic processes and turnover (Cătălin et al., 2013). They can produce a variety of neurotrophic factors that promote neuronal survival and growth, such as brain-derived neurotrophic factor (Araki et al., 2021). (5) Modulation of neurotransmission: microglia are involved in regulating neurotransmission by releasing signaling molecules such as cytokines, chemokines, and neurotrophic factors (Umpierre et al., 2021). (6) Modulation of myelination: microglia synthesize growth factors that promote survival and maturation of oligodendrocyte precursor cells (OPCs) (Nicholas et al., 2001). (7) Last but not least: maintenance of angiogenesis and BBB integrity (Ronaldson et al., 2020; Hattori, 2023).

Microglia are a group of heterogenous cells, which show different temporal-spatial features depending on age, gender, brain regions, and disease conditions (Masuda et al., 2020; Tan et al., 2020). When activated, microglia can acquire different phenotypes, namely microglial polarization, depending on activating stimuli. Microglial polarization is characterized by changes in gene expression, morphology, and secretory profile. When cultured *in vitro*, microglia can be polarized into M1 or M2 type. In general, the M1-like microglia can be identified by CD16 and CD86, while the M2-like microglia by CD206, CD163, and arginase 1, among other markers (Jurga et al., 2020) (**Fig. 2**).

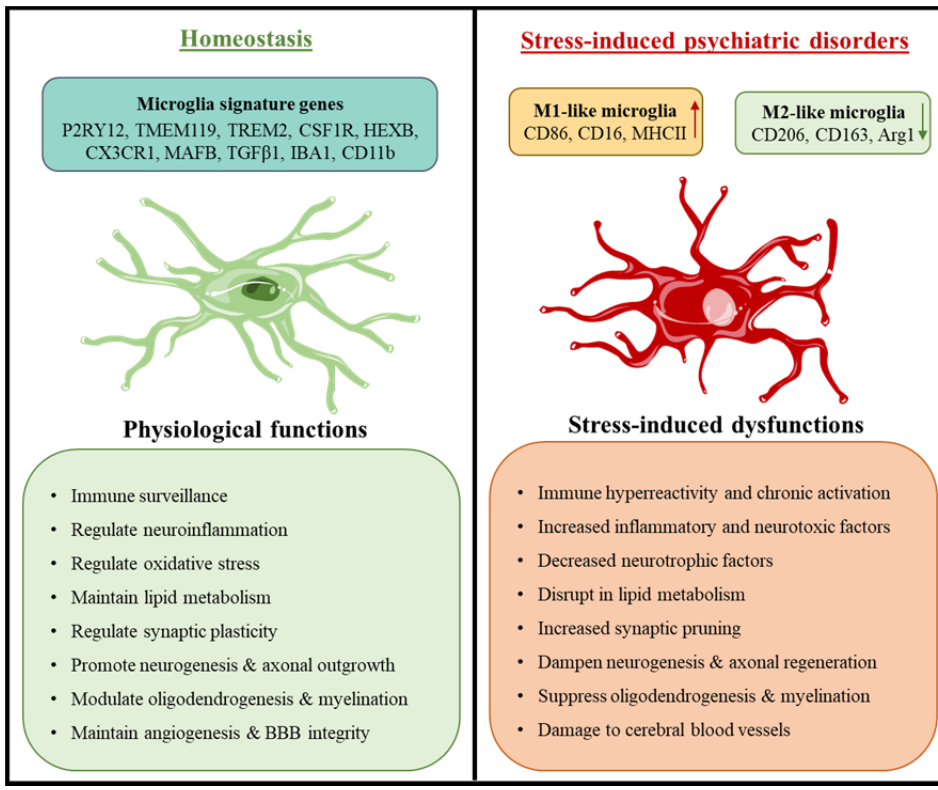

Figure 2. Phenotypic distinctions between homeostatic and stressed microglia. Under physiological conditions, ramified microglia survey the brain microenvironment with their processes to maintain brain homeostasis. Under stress, primed microglia possess an over-ramified morphology. Markers for microglial activation vary widely depending on the type (enhanced classical immune functions, and reduced homeostasis). Stressed microglia lose their homeostatic functions and lead to multiple neurobiological dysfunctions. BBB: blood-brain barrier. The figure is prepared using Servier Medical Art under a Creative Commons Attribution 3.0 unported license.

Upon infection or injury, the M1-like microglia produce pro-inflammatory cytokines, such as TNF-α and IL-1β, and induce tissue damage. Chronic activation of microglia and subsequent neuroinflammatory processes hinder neurogenesis, axonal regeneration, and synaptic plasticity (Cornell et al., 2022), and aggravate cerebral vascular damage and BBB permeability (Chen et al., 2019).

The M2-like microglia by contrast express anti-inflammatory mediators and growth factors, such as IL-10 and transforming growth factor-β (TGF-β), and are prone to remove cellular debris to promote tissue repair and neuronal survival (Hu et al., 2015; Wang et al., 2022). M2-like microglia also promote neurogenesis (Nikolakopoulou et al., 2013) and neurovascular remodeling through the release of VEGF (Zhao et al., 2018; Tian et al., 2019).

It should be emphasized, however, that this static M1-M2 division of microglial populations is oversimplistic and not well aligned with microglial molecular features *in vivo* and has been rejected by researchers nowadays (Paolicelli et al., 2022).

2.3.2. Microglia and perivascular macrophages-blood brain barrier interaction

Microglia near the cerebral blood vessels can monitor BBB integrity (Ronaldson et al., 2020; Hattori, 2023). Earlier studies observed that microglia co-cultured with endothelial cells enhanced endothelial expression of tight junction proteins Occludin and Zonula occludens-1 (Mehrabadi et al., 2017). Instead, blocking microglial process motility promoted laser-induced BBB injury, and ablation of juxta-vascular microglia abolished resolution of BBB leakage (Lou et al., 2016). Later studies demonstrated that vessel-associated microglia contacted endothelial cells in a C-C chemokine receptor type 5-dependent manner and maintained the BBB integrity via enhancing the expression of Claudin-5 (Haruwaka et al., 2019). Recently, microglia depletion was found to result in ~15% increase in diameter of the cerebral blood capillary (Bisht et al., 2021). Microglia also regulated cerebral blood flow through purinergic receptor P2ry12, whereas *P2ry12*-deficient mice showed reduced contact of microglial processes with the capillary and increased cerebral blood flow (Bisht et al., 2021; Császár et al., 2022).

In pathological conditions, morphological change of microglia near the capillary was correlated with the level of cerebral blood flow during transient ischemia (Masuda et al., 2011). Depletion of microglia caused vascular permeability to fibrinogen in chronic mild hypoxia (Halder et al., 2019). However, other studies showed that under pathological conditions, such as the white matter lesion, activated microglia interacted with vascular glycocalyx and disrupted vessel integrity (Forsberg et al., 2018), and phagocytosed astrocytic endfeet to impair BBB function (Haruwaka et al., 2019). M1-like microglia contributed to BBB permeability via the release of pro-inflammatory cytokines including TNF-α, IL-1β, IL-6, IL-12, C-C motif chemokine ligands2, ROS, and cyclooxygenase-2 (Ronaldson et al., 2020), whereas M2-like microglia-released IL-10 (Wang et al., 2016) and TGF-β facilitated BBB protection (Ronaldson et al., 2020) .

Perivascular macrophages (PVMs) are a specific type of BAMs that reside in the perivascular space that surrounds the blood arteriole and venule in the brain (Yang et al., 2019) and regulate the BBB integrity (Willis et al., 2007). PVMs also regulate cerebral blood flow (Chen et al., 2023) and arterial cerebrospinal fluid flow via remodeling of extracellular matrix in the arterial basement membrane (Drieu et al., 2022). Depletion of PVMs resulted in hyperpermeability of the BBB, which was rescued when M2-like macrophages were reconstituted through VE-cadherin expressed in vascular endothelial cells (He et al., 2016). PVMs depletion also impaired vasodilation of the arterioles (Drieu et al.,

2022). However, PVMs participated in BBB disruption under pathological conditions such as stroke (Pedragosa et al., 2018) and Alzheimer's disease, and depletion of PVMs rescued the Aβ peptide-induced attenuation of resting cerebral blood flow (Park et al., 2017).

Overall, interactions of microglia and PVMs with the BBB are critical for brain homeostasis and in various pathological conditions. More research in this new area may facilitate the development of novel therapeutic strategies for brain diseases.

2.3.3. Microglia in the olfactory bulb (OB)

Microglia are present in various regions of the brain, including the OB. Olfactory microglia play a critical role in maintaining structural and functional integrities of the OB in physiological conditions and olfactory neuroinflammation accompanied with microgliosis results in the OB damage in pathological conditions (Reshef et al., 2017; Seo et al., 2018).

In the adult rodent brain, the OB is a highly sensitive region to both inflammation and regeneration (LaFever et al., 2022), as it hosts abundant neural stem cells (Tufo et al., 2022). Indeed, new neurons were found to be constantly added to the OB from the subventricular zone via the rostral migration stream enriched with a mesh of blood vessels (Bovetti et al., 2007; Martončíková et al., 2021; Miettinen et al., 2021). Appropriate microglial activation (e.g., M2-like microglia) is essential for the survival of neuroblasts in this migratory axis (Ribeiro Xavier et al., 2015). In addition, neuroblast migration is accompanied by highly dynamic synaptic formation and pruning, which is mediated by microglia (Reshef et al., 2017).

New findings also revealed that circulation of the cerebrospinal fluid aided by PVMs was most active around the OB in mice (Drieu et al., 2022). Besides, chronic mild hypoxia induced microglia-vascular clustering particularly in the OB as compared to the CTX (Halder et al., 2020). In mice undergoing olfactory sensory deprivation by unilateral nasal occlusion, activated microglia eliminated dopaminergic neurons and their synapses in the OB, leading to reduced OB volume (Grier et al., 2016). Loss of microglia in *Csf1r*$^{-/-}$ mice resulted in volume reductions of multiple brain regions including the OB and the surrounding areas as well as impaired olfaction (Erblich et al., 2011; Nandi et al., 2012). Hence, further research in this area may benefit improved diagnosis and treatment of psychiatric disorders.

2.3.4. Microglia and monocytes in schizophrenia

Alteration in microglial functions may lead to psychiatric disorders (Tay et al., 2017). Enhanced microglial activation as detected by positron emission tomography in the cerebral grey matter of patients with schizophrenia was reported (van Berckel et al., 2008). Microglial density was significantly increased in the PFC of patients with schizophrenia (Fillman et al., 2013), and microglial

activation co-occurred with grey matter alterations in frontal and subcortical structures such as the PFC and HPC in schizophrenia (Laskaris et al., 2016). Immunohistochemical studies also found primed or reactive microglial subtypes in patients with schizophrenia. For instances, HLA-DR^{+} microglia in the dorsolateral prefrontal cortex were found to be increased and reflect impaired cerebral lateralization in chronic schizophrenia (Steiner et al., 2006). Likewise, a recent study on patients of chronic schizophrenia with active psychosis found increased CD64^{+} microglia in the post-mortem brains (De Picker et al., 2021).

Microglial dysfunction has also been demonstrated in both OBX and CUS models that are relevant for schizophrenia. In the rodent OBX model, activated microglia showed hypertrophic features of thicker processes and larger microglia soma (Takahashi et al., 2018), and produced more pro-inflammatory cytokines and ROS (Rinwa et al., 2013). Likewise, we and others showed that microglial activation was significantly increased in limbic regions and contributed to anxiety, depressive-like behaviors, and social withdrawal in the rodent CUS model (Liu et al., 2019; Yan et al., 2021).

Monocytes and monocyte-derived macrophages are major mononuclear myeloid cells that regulate infection and inflammation (Austermann et al., 2022). Human monocytes are a highly heterogeneous population, as evidenced by the relative expression levels of CD14 and the low-affinity Fc-III receptor (CD16), which divide monocytes into classical (CD14^{++}CD16^{-}), intermediate (CD14^{++}CD16^{+}), and nonclassical (CD14^{+}CD16^{++}) subsets, which account for ~85%, 5%, and 10% of total circulating monocytes, respectively (Ziegler-Heitbrock et al., 2010; Wong et al., 2011). Each of these subsets is thought to be phenotypically distinct, with distinct signature genes and nonoverlapping roles in a wide range of chronic inflammatory and autoimmune diseases, including neurological diseases (Schmidl et al., 2014; Narasimhan et al., 2019).

The classical monocytes have the most prominent phagocytic capacity and antimicrobial function (Wong et al., 2011). The nonclassical monocytes, as a highly complex functional subset, are on the other hand thought to be anti-inflammatory and patrol the vasculature, playing an important role in maintaining vascular homeostasis (Narasimhan et al., 2019). The nonclassical monocytes can also be pro-inflammatory and susceptible to immune senescence after stimulation (Ong et al., 2018). The intermediate monocytes are thought to be a transitional state between classical and nonclassical monocytes, sharing some phenotypic and functional characteristics with both subsets (Ziegler-Heitbrock et al., 2010). They are involved in antigen presentation to induce T-cell proliferation in infectious (Kapellos et al., 2019) and inflammatory conditions (Passos et al., 2015).

Previous studies produced some knowledge on monocytes in contribution to chronic low-grade inflammation in psychiatric disorders (Weber et al., 2018). When compared to healthy controls (HCs), schizophrenia patients had a higher monocyte count (Mazza et al., 2020) and increased monocytic subcellular organelles such as the nucleolus, mitochondria, and lysosomes (Uranova et al., 2017). Patients with schizophrenia also had more inflammatory gene finger-

prints in their monocytic transcriptomes (Drexhage et al., 2010). Higher level of toll-like receptor 4 on $CD14^+$ monocytes was detected in drug-naïve or chronic schizophrenia patients compared with HCs (Muller et al., 2012; Keri et al., 2017) and was correlated with more severe cognitive deficits in drug-naïve schizophrenia patients (Keri et al., 2017). Elevated level of soluble CD14 in blood samples drawn from individuals who were subsequently diagnosed with schizophrenia was detected, implicating an advantageous monocytic activation before disease onset (Weber et al., 2018).

Overall, increasing evidence suggests that microglia and monocytes may play a significant role in the development and progression of schizophrenia.

2.3.5. Pharmaceutical modulation of microglia in psychiatric disorders

Pharmaceutical modulators of microglia have shown some promise in treating psychiatric disorders. Evidence suggests that anti-inflammatory medications, such as nonsteroidal anti-inflammatory drugs and cytokine inhibitors, may be effective in treating psychiatric disorders (Köhler et al., 2014; Cho et al., 2019). For example, the anti-inflammatory drug aspirin was shown effectiveness in treating schizophrenia by reducing microglial activation and inflammation in the brain (Schmidt et al., 2019).

Minocycline, an antibiotic of the tetracycline family that inhibits M1 microglia and activates M2 microglia, when combined with antipsychotic medications, can rescue negative symptoms and cognitive deficits of schizophrenia (Zhang et al., 2018; Zhang et al., 2019). Minocycline can inhibit microglial phagocytic function (Mattei et al., 2017), reduce microglia-mediated synaptic uptake (Sellgren et al., 2019), and upregulate arginase 1 in schizophrenia (Xia et al., 2020). Moreover, it protects from grey matter loss in the cortical regions of patients with schizophrenia (Chaves et al., 2015).

Another pharmaceutical microglial modulator is CSF1Ri, such as PLX3397 or PLX5622, which can ablate microglia without producing gross behavioral changes in adult animals (Green et al., 2020). Recent studies nevertheless showed that microglial ablation resulted in enhanced anxiety (Elmore et al., 2014), impaired spatial memory (Torres et al., 2016), and enhanced hippocampal lesion-induced fear learning and memory (Rice et al., 2015) or hampered fear memory elimination (Wang et al., 2020) in adult mice. Mice subjected to CSF1Ri at embryonic age showed anxiolytic-like behavior later in adulthood (Rosin et al., 2018). Corroboratively, microglial repopulation upon CSF1Ri withdrawal corrected repetitive behavior and social deficits induced by maternal immune activation (Ikezu et al., 2021) and improved spatial memory in aged mice (Elmore et al., 2018). Notably, microglial repopulation has been demonstrated on a beneficial therapeutic effect for many neurological diseases (Han et al., 2019). Furthermore, CSF1 ameliorated depressive-like behavior in mice after CUS (Kreisel et al., 2014). On the contrary, some studies found that microglial ablation by CSF1Ri abrogated the recurrence of anxiety (Weber et al.,

2019) and social behavior deficits (Lehmann et al., 2019) in stress-sensitized mice. Lower CSF1R in the post-mortem brains (López-González et al., 2019; Shimamoto-Mitsuyama et al., 2021; Snijders et al., 2021) and spleens (Zhang et al., 2020) of chronic schizophrenia patients were reported. However, the effect of the CSF1R or the CSF1Ri on schizophrenia is still unknown.

Besides the above microglial modulators, other pharmacological interventions on neuroinflammation have also been extensively tested. For instances, dietary supplementation with n-3 PUFAs can rescue depressive behavior and neuropathological changes due to their anti-inflammatory and anti-oxidative properties (Gao et al., 2022; Watanabe et al., 2004; Song et al., 2016). A previous study also showed that the dietary n-3 PUFAs (eicosatetraenoic acid and docosahexaenoic acid) improved cognitive functions and reduced psychosis severity in adolescents with schizophrenia (Hsu et al., 2020). The best understood mechanism underlying attenuated depression induced by the n-3 PUFAs is its inhibition of transformation of an n-6 PUFA - arachidonic acid - into eicosanoid (a precursor of pro-inflammatory mediators) through cyclooxygenase and lipoxygenase (Kuehl et al., 1980; Choi et al., 2008). Arachidonic acid signaling was reported to be upregulated in OBX rats (Skelin et al., 2011). The arachidonic acid precursor linoleic acid is also convertible into pro-inflammatory mediators (Saraswathi et al., 2004; Raphael et al., 2013). In contrast, alpha-linolenic acid, an n-3 PUFA, can down-regulate inflammatory and oxidative factors by blocking NF-κB and MAPKs (Jie et al., 2007).

Notably, an earlier study showed that generic anti-inflammatory drugs had only limited supplementary therapeutic effects (Nitta et al., 2013). A recent systematic review however reported that anti-inflammatory drugs combined with antipsychotics had a favorable treatment effect in psychotic disorders, particularly for positive and negative symptoms as well as working memory deficit in schizophrenia. Nevertheless, the improved effects of some medicines may not be fully attributable to immunomodulation (Jeppesen et al., 2020). This suggests that we still do not fully understand the brain immunomodulation mediated by microglia/macrophages, especially concerning temporal-spatial features and functions of their subgroups in a disease-specific context, and therefore more research is needed to help develop more effective anti-psychotic treatments.

3. AIMS OF THE STUDY

The general aim of this study was to uncover schizophrenia-related stress-coping mechanisms mediated by microglia in FES patients and animal models. These results may help improve the understanding of mechanisms underlying ontogenesis and pathophysiological development of stress-related schizophrenia as well as its treatment.

More specific objectives of my study were:

1. To characterize monocytic subsets and myeloid genes in association with brain atrophy and cognitive dysfunction in FES patients.
2. To explore mechanisms underlying microglia-mediated stress modulation in mouse models and FES patients.
3. To discover region- and location-specific functions of microglia and micro-glial receptors.
4. To characterize anti-inflammatory and anxiolytic effects of endogenous n-3 PUFAs in mice.

4. MATERIALS AND METHODS

4.1. Human subjects' demographic and clinical measures

FES Patients (n = 128) recruited for this study were from the Beijing Hui Long Guan Hospital. Patients were diagnosed with schizophrenia according to the Structured Clinical Interview for DSM-4 (First, 2013) independently by two experienced psychiatrists. Inclusion criteria were: (1) Han Chinese and aged 18 – 55 years old; (2) illness duration ≤ 3 years (< 1 year on average); and (3) education equal or greater than 8 years; (4) right handedness, and physically healthy in the past; (5) un-medicated or < 2 weeks of anti-psychotic medication at the time of blood draw; (6) receiving no immunomodulators, immune-suppressive or anti-inflammatory agents in the past 6 months; (7) no substance and alcohol abuse/dependence. Candidates who unmet recruitment criteria were excluded. Additional exclusion criteria included: (1) other psychiatric disorders diagnosed according to the DSM-IV Axis I; (2) severe physical illness; (3) recent infection or treatment with physiotherapy or psychotherapy; (4) mental retardation or serious nervous system disease; and (5) lactation or pregnancy.

Age- and sex-matched HCs (n = 111) were recruited from the local community simultaneously. Complete medical histories of HCs were collected, and physical examinations were conducted for all participants to identify those with chronic medical or psychiatric conditions. Potential control participants who had previously been diagnosed with an Axis I psychiatric disorder based on Structured Clinical Interview for DSM-IV criteria or had experienced substance abuse or dependence within the previous six months, and those who had a history of autoimmune disorders or other significant medical conditions or received anti-inflammatory medications were excluded. The other general criteria were the same as for FES patients. Candidates who unmet the recruitment criteria were excluded. All participants provided written informed consents. The study was approved by the Institutional Ethical Committee of Beijing Huilongguan Hospital with license No. 2017-49.

Participants' (51 FES patients and 46 HCs) past traumatic experiences were evaluated by childhood trauma questionnaire (CTQ)-short form, a 29-item self-reported questionnaire that includes physical abuse, emotional abuse, sexual abuse, physical neglect, and emotional neglect. Each factor has five corresponding items with five possible responses, ranging from 1 (never) to 5 (always), with the total overall trauma score ranging from 25 to 125, where a higher score means more severe trauma (Bernstein et al., 2003). Reliability and validity in the general Chinese population and Chinese patients with mental disorders have been demonstrated (Jiang et al., 2018).

Participants' (51 FES patients and 46 HCs) stress levels were evaluated based on the perceived stress scale (PSS), a 14-item self-reported questionnaire, each item has five possible responses, ranging from 0 (never) to 4 (very often), where a higher score indicates higher perceived stress, measuring feelings and thoughts during the last month (Cohen et al., 1983). Reliability and validity in

the general Chinese population and Chinese patients with mental disorders have been demonstrated (Leung et al., 2010). Scores of the positive and negative syndrome scale (PANSS) (Kay et al., 1987), which was validated in Chinese patients (Si et al., 2004), were measured independently by two psychiatrists.

The MATRICS™ consensus cognitive battery (MCCB) test was applied to assess the cognitive functioning of 58 FES patients and 52 HCs. It consists of ten tests encompassing seven cognitive domains, and domain scores as well as a composite score were computed using the MCCB scoring program. The clinical validity and reliability of the Chinese version of MCCB had been previously established in both healthy volunteers and schizophrenia patients (Shi et al., 2015).

4.2. Magnetic resonance imaging (MRI) acquisition and processing

Brain structural MRI data were acquired using a Siemens Prisma 3.0T MRI scanner (Siemens, Germany) with a 64-channel head coil. Foam pads were used to minimize head motions. Sagittal three-dimensional magnetization-prepared rapid acquisition gradient echo was used to collect each participant's anatomical data following the ENIGMA protocol with FreeSurfer software (Fischl et al., 2002; Fischl, 2012): repetition time = 2,530 ms, echo time = 2.98 ms, field-of-view = 256 × 224 mm, flip angle = 7°, field of view = 256 × 224 mm^2, matrix size = 256 × 224 bit, thickness/gap = 1/0 mm, and inversion time = 1100 ms. After scanning, two radiologists evaluated image quality and if there were significant artefacts, images were recollected. Bi-hemispheric cerebral cortical/ subcortical structures were measured.

After imputing corresponding internal anatomical instructions, 70 Desikan-Killiany atlas-based cortical and subcortical regions were extracted and data were processed with FreeSurfer software (http://surfer.nmr.mgh.harvard.edu) following the ENIGMA pipeline, e.g., region-by-region visual checking and removal of incorrect values for brain segmentations (http://enigma.usc.edu/ protocols/imaging-protocols). Bi-hemispheric regional areas and thicknesses were measured, regional volumes and intracranial volumes (ICV) (mm^3) were calculated, and no data were excluded. Brain images were obtained within 7 days after signing an informed consent form, and 60 FES patients and 54 HCs from the total cohort, including the subjects in the flow cytometric experiment, completed the MRI scan.

4.3. Blood bulk RNA sequencing (RNA-seq)

Human blood (5 ml) was collected between 7 and 9 a.m. after overnight fasting in PAXgene™ blood ribonucleic acid (RNA) tubes (Applied Biosystems, USA). Tubes were shaken vigorously for at least 10 s after sampling and immediately stored at -80 °C. Total RNAs were extracted using Mag-MAX™ RNA Isolation

Kit (Applied Biosystems, USA) by following the manufacturers' instructions from human blood. RNAs were quantified and assessed for purity by optical density ratios of 260 nm/280 nm and 260 nm/230 nm using NanoDrop spectrophotometry (ThermoFisher), and samples (1 μg) were immediately sent on dry ice to the laboratory of the Beijing Genomics Institute (BGI) for messenger RNA sequencing (RNA-seq) on the BGIseq-500 platform. Quality controls (QCs) on RNA samples (RIN/RQN ≥ 7.0, 28S/18S ≥ 1.0) were confirmed by BGI, followed by globin mRNA removal and cDNA library construction. Clean data of at least 4 Gb (20 M clean reads) per sample were collected. After QC of fastq files, an mRNA-seq count table was obtained from bam files.

Gene expression analysis was done on the NetworkAnalyst platform using DESeq2 (Zhou et al., 2019). Counts with variance percentile rank < 15% and counts < 4 were filtered out, transformed, and normalized to Log2 reads per million values. Log2 fold changes (Log2FC) were calculated for differentially expressed genes (DEGs) with a significance of $p < 0.05$ adjusted by Benjamini-Hochberg's false discovery rate (FDR). Monocyte-specific DEGs were selected according to the relevant literatures of monocytic transcriptomic profiling (Zawada et al., 2011; Villani et al., 2017; Kapellos et al., 2019). DEGs were analyzed for gene ontology biological pathway (GO-BP) in DAVID (https://david.ncifcrf.gov/) and protein-protein interaction (PPI) in STRING (https://string-db.org/cgi/input.pl).

GeneWeaver, a database for the integration and analysis of heterogeneous functional genomics data (https://geneweaver.org/), was explored to dig out CSF1R-associated gene sets annotated to contribute to human brain development. Annotated gene series GS393224 (Abnormality of brain morphology), GS393415 (Hydrocephalus), and GS393709 (Abnormality of neuronal migration) were retrieved for further comparisons to overlapping blood RNA-seq DEGs and GO-BP analysis as described above.

4.4. Blood flow cytometry

Five ml of fresh heparin lithium-anticoagulated peripheral blood samples were collected from 29 FES patients and 27 HC subjects after an overnight fasting, and processed within 30 minutes for fluorescent staining of cell surface receptors as described previously (Chen et al., 2019b). The fluorochrome-conjugated antibodies used in this study were 10 μl FITC-labeled mouse anti-human CD14 (Clone M5E2; Catalog Number 555397; BD Biosciences) and 3 μl PerCP-Cy™5.5-labeled mouse anti-human CD16 (Clone B73.1; Catalog Number 565421; BD Biosciences). The percentages of classical ($CD14^{++}CD16^{-}$), intermediate ($CD14^{++}CD16^{+}$), and non-classical ($CD14^{+}CD16^{++}$) subsets among the total monocyte population were determined based on the corresponding gating. Single cells were filtered through cell strainers, carefully suspended, and immediately acquired by a BD FACSCalibur flow cytometer, and the analyses were performed with FlowJo V10 software. Corresponding isotype control antibodies (all BioLegend) were also tested.

4.5. Plasma colony stimulating factor 1 receptor (CSF1R) protein detection

Five ml of fresh heparin lithium-anticoagulated peripheral blood samples were collected from 126 FES patients and 102 HC subjects after an overnight fasting. Plasma samples were separated by centrifugation at 4000 rpm for 10 minutes, which were immediately stored at -80 °C until assayed. CSF1R protein was measured by sandwich enzyme-linked immunosorbent assay (ELISA) kit (#RX-XQ-EN13238, Beijing Rongxin Zhihe Biotechnology Co. Ltd.). Each sample was measured in duplicates. The intra-plate and inter-plate variation coefficients for the ELISA were 10% and 15%, respectively.

4.6. Experimental Animals

4.6.1. Mouse breeding

Wild type (WT) C57BL/6NTac male mice (3-month-old, Taconic) from different litters were housed in 1264C Euro standard type II cages (Tecniplast) measuring 268 × 215 × 141 mm dimensions. Cages containing aspen chips and wool for bedding and nesting were replaced once a week. Each cage contained 9 – 10 animals based on allocation after weaning. Mice were kept under standard conditions with unlimited access to food and water on a 12/12-hour light/dark cycle (light on 7 a.m. – 7 p.m.). All animal procedures in this study were performed in accordance with the European Communities Directive with license No. 171 (01.07.2020) issued from the Estonian National Board of Animal Experiments.

Male mice of a *C. elegans fat-1* transgenic line, which can convert n-6 PUFAs to n-3 PUFAs endogenously in the brain (Kang et al., 2004), were mated with WT C57BL/6 female mice to obtain *fat-1* positive C57BL/6 mice (Fat-1) and WT C57BL/6 mice. The presence of the *fat-1* gene in each mouse was confirmed by genotyping. Male mice at age of 2 months old were divided into four groups: WT/Sham, WT/OBX, Fat-1/Sham, and Fat-1/OBX (n = 5 in each group). Mice were fed with a diet of 10% safflower oil for 3 months and housed at room temperature (20~22 °C) with a 12:12 hour light-dark cycle (lights on at 07:00), in pathogen-free condition with humidity level at 50 ± 10% and free access to food and water. The size of each cage, which contained 3 mice and was cleaned twice a week, was 290 × 178 × 160 mm. Experimentations were conducted between 9:00 a.m. and 5:00 p.m. in compliance with the Chinese National Institutes of Health guide for the care and use of laboratory animals and approved by the Local Bioethics Committee (Guangdong Ocean University, China; document number: SYXK2014-0053).

For *fat-1* PCR, DNAs were extracted from approximately 2-3 mm of the mouse toe by Mouse Tail SuperDirect™ PCR kit (FOREGENE, Chengdu, China). Primers used for the *fat-1* gene were forward: 5′-CTGCACCACGCCTT CACCAACC-3′ and reverse: 5′-CACAGCAGCAGATTCCAGAGATT-3′. PCR

was performed with a Super cycler (Kyratec, Mansfield, Australia) with a program at 95 °C for 15 minutes, followed by 30 cycles of 94 °C for 30 seconds, 62 °C for 30 seconds, 72 °C for 60 seconds, and a final extension at 72 °C for 10 minutes. Amplified PCR products were analyzed on 1% agarose gels and amplified bands were visualized by the automatic gel system (Tanon 3500, Shanghai, China).

4.6.2. Mouse CUS and CSF1R inhibitor (CSF1Ri) treatment procedures

After a week of transfer adaptation, mice were randomly assigned into 4 groups (n = 9~10/group): Control (Ctr)-Vehicle (Veh), CUS-Veh, Ctr-CSF1Ri, and CUS-CSF1Ri treatment for 14 days, PLX3397 (HY-16749/CS-4256, MedChem Express) was dissolved at 200 mg/ml in DMSO (D8418, Sigma-Aldrich) stock solution and an aliquot was freshly diluted with corn oil (#8267, Sigma-Aldrich) by 1:6.5 before use. Drug-treated mice were daily fed with Veh (100 µl 15% DMSO/85% corn oil + 0.5 g Nutella/mouse/day or PLX3397 (120 mg/kg bodyweight, e.g., 3 mg in 100 µl 15% DMSO/85% corn oil + 0.5 g Nutella/mouse/day) added onto polystyrene Petri dishes, which were provided to mice individually for voluntary ingestion before they returned to home cages. All mice were fed daily with an equal dose of Veh for 2 days in advance to get accustomed to the novel taste. Voluntary Nutella-feeding is less stressful compared to gavage for mice (Spiller et al., 2018; Cangalaya et al., 2020).

Mice were subject to CUS/Ctr and CSF1Ri/Veh treatments. For the CUS procedure (Yan et al., 2021), mice were exposed to a variable sequence of 7 mild and unpredictable stressors once per day for 8 consecutive weeks, including food and water deprivation overnight, rat odor and isolation overnight, restraint in 50 ml tube for 2 hours, wet bedding and tilted cage, stroboscopic illumination overnight, flipped light/dark exposure, and swimming at 18 °C for 10 minutes. All stressors were randomly scheduled and changed daily to sustain an unpredictable procedure. Mice were fed with PLX3397 starting from the 7th week of CUS with the same treatment dosage and duration as described above. Behavioral experiments were performed on the 8th week.

4.6.3. OBX surgical procedure

Mice were randomly divided into 4 groups (n = 5 per group). To set up the OBX model, each mouse was placed in a stereotaxic apparatus (RWD Life Science Co., Ltd, 68001, Shenzhen, China) after being anesthetized with a mixture of salbutamol hydrochloride [15 mg/kg, intraperitoneal (i.p.)], zolazepam (15 mg/kg, i.p.), and hydrochloride xylazine (23 mg/kg, i.p.). After exposure of the skull, 1.8 mm-diameter holes were drilled on the midlines of the skull covering both the OBs, which were then suctioned by a blunt hypodermic needle attached to a 1-ml syringe. The holes were filled with gelatin to stop bleeding. Sham mice were operated similarly, but their bulbs were left intact.

Mice were kept on a heating pad to maintain their body temperatures after the operation and recovered for 21 days before experimentation.

4.7. Behavioral testing

4.7.1. Open field test (OFT)

Mice were habituated to ~250 lux room light for 1 hour. The individual mouse was measured for distance, time traveled in different zones of a digital box (44.8 × 44.8 × 45 cm) (a novel and stressful environment), and rearing activity via software (Technical & Scientific Equipment GmbH and Shanghai Xinruan Information Technology Co., Ltd) for 5–30 minutes. The floor of the box was cleaned with 70% ethanol and dried thoroughly after each mouse.

4.7.2. Elevated plus maze (EPM)

EPM consisted of open and closed arms (30 × 5 cm each) intersected at a central 5 × 5 cm square platform elevated to a height of 80 cm. Mice were habituated to ~40 lux room light for 1 hour. The individual mouse was placed on the central platform facing the open arm and recorded for time spent on open/close arms by software (EthoVision XT, Noduls) for 5 minutes. The arms were cleaned with 70% ethanol and dried thoroughly after each mouse.

4.7.3. Three-chamber test (TCT)

A rectangular three-chamber box made from clear Plexiglas was divided into an open middle section and two other identical side sections, which each accommodated a lid-covered and wire-structured cup-like container large enough to enclose a single mouse, allowing free exchange of air but not direct physical contacts between the mice on either side of it. A test mouse was first habituated in the central chamber for 5 minutes, then introduced to a stranger mouse located in a container for a sociability test. Mice were left to freely explore the three chambers for the next 10 minutes. All stranger mice were the same age as test mice and habituated to the apparatus 1 d earlier (30 minutes habituation for 3 times). The box and wire containers were cleaned with 70% ethanol and dried thoroughly after each test. Social exploration was defined as time spent in each chamber and social interaction as the number of contacts when the head and front paws of a test mouse were within 3 cm vicinity of the container wall as recorded by a camera (Noldus). The ratio of time spent in the stranger or empty chamber was calculated as sociability indices.

4.7.4. Tail suspension test (TST)

In TST, animals were hung with their tail tips stuck onto a wooden bar by adhesive tapes. During a 6-minute test period, mice were recorded with a camera and the duration of immobility was measured. Immobility was defined as a complete lack of movement other than respiration. However, small movements of the forefeet and swinging of the body caused by earlier movements were also scored as immobility.

4.7.5. Sucrose preference test (SPT)

Prior to the test, mice were single caged and habituated to the presence of two drinking bottles (fresh water in paper II and 1% sucrose in paper IV) for 24 hours. On the next day, one bottle of 1% sucrose and one bottle of fresh water were provided for 12 hours in paper II and for 4 hours in paper IV. Liquid consumption was measured before and afterwards. In paper IV, 24-hour food deprivation was also applied. Sucrose preference = sucrose intake / (sucrose intake + water intake) × 100%.

4.8. Brain flow cytometry

Hippocampal and olfactory bubal homogenates were washed and centrifuged at 500 g for 5 minutes, fixed with phosphate buffered saline (PBS) and 4% paraformaldehyde (PFA), washed, and centrifuged again, permeabilized with 0.05% Triton-X100 for 1 h at 4 °C, washed and centrifuged again, and blocked with PBS + 10% rat serum for 1 hour. In paper II, stained with flow markers (BioLegend and Miltenyi) of anti-mouse Csf1r-Brilliant Violet (BV)605 (#135517), CD11b-BV421 (#101251), CD45-BV650 (#103151BioLegend), Glast-APC (#130-123-555), and O4-PE (#130-117-357) for 1 hour. Cell acquisition and data analysis were done as described above. Astrocytes were defined as $Glast^{+}$ cells, OPCs as $O4^{+}$ cells, and microglia as $CD45^{low}CD11b^{hi}$ cells. The % of glia among total brain cells and mean fluorescent intensity (MFI) of Csf1r per microglia were measured. Corresponding isotype control antibodies (all BioLegend) were rat IgG2b-BV605 (#135517), IgG2b-BV421 (#400639), IgG2b-BV650 (#400651), IgG2b-APC (#400219), and IgM-PE (#401611). In paper III, stained with flow markers (BioLegend, Miltenyi, and Millipore) of anti-mouse CD11b-Brilliant Violet (BV)421 (#101251), CD206-PE/Cy7 (#141720), CD45-BV650 (#103151), and Vglut2-Alexa488 (#MAB5504A4) for 1 hour. Washed cells were resuspended in 500 µl PBS and acquired with a Fortessa flow cytometer (BD Bioscience). Data were analyzed by Kaluza v2.1 software (Beckman Coulter). Macrophages were defined as $CD45^{hi}CD11b^{hi}$ cells, microglia as $CD45^{low}CD11b^{hi}$ cells, $CD206^{+}$microglia as $CD45^{low}CD11b^{hi}CD206^{hi}$ and $Vglut2^{+}$microglia as $CD45^{low}CD11b^{hi}Vglut2^{hi}$. Corresponding isotype control antibodies (all BioLegend) were rat IgG2b-BV605 (#135517), IgG2b-BV421 (#400639), IgG2b-BV650 (#400651), IgG2a-PE/Cy7 (#400521), IgG-Alexa488 (#400132).

4.9. Brain RNA-seq

Mice were euthanized with CO_2 and the PFCs and OBs were dissected and immediately stored at -80 °C. Total RNAs were extracted using Trizol (Molecular Research Center and Life, USA). RNAs were quantified and assessed for purity by optical density ratios of 260 nm/280 nm and 260 nm/230 nm using NanoDrop spectrophotometry (ThermoFisher), and samples (1 μg) were immediately sent on dry ice to the laboratory of the BGI for messenger RNA-seq on the BGIseq-500 platform. Quality controls (QCs) on RNA samples (RIN/RQN ≥ 7.0, 28S/18S ≥ 1.0) were confirmed by BGI, followed by globin mRNA removal and cDNA library construction. Clean data of at least 4 Gb (20 M clean reads) per sample were collected. After QC of fastq files, an mRNA-seq count table was obtained from bam files.

Gene expression analysis was done on the NetworkAnalyst platform using DESeq2 (Zhou et al., 2019). Counts with variance percentile rank < 15% and counts < 4 were filtered out, transformed, and normalized to Log2 reads per million values. Log2FC were calculated for differentially expressed genes (DEGs) with a significance of $p < 0.05$ adjusted by BFDR. DEGs were analyzed for GO-BP in DAVID (https://david.ncifcrf.gov/) and PPI in STRING (https://string-db.org/cgi/input.pl).

4.10. Quantitative polymerase chain reaction (qPCR)

Total RNAs of brain tissues were reversely transcribed with a RevertAid First Strand cDNA Synthesis Kit (Thermo Scientific and Vazyme, Nanjing, China). qQPCR was performed by using corresponding primers and 5x HOT FIREPol® EvaGreen® qPCR Supermix (Solis BioDyne) on a PCR instrument equipped with QuantStudio 12Kflex Software v.1.2.2 (Applied Biosystems) and CFX Connect™ Real-Time system (Bio-Rad laboratories, Hercules, CA, USA) according to the respective manufacturers' instructions. Gene expression levels were quantified by normalizing the Ct values of target genes to Ct values of the reference gene (β-actin) in fold changes with the ΔΔCt method. The primers were purchased from TAG Copenhagen A/S and Sangon Biotech (Shanghai, China) (**Table 1**).

Table 1. Mouse gene qPCR primers

Gene	Primer	Sequence
Actin	Forward	ACTGAGCTGCGTTTTACACCC
	Reverse	GCCTTCACCGTTCCAGTTTT
Ang	Forward	CCAACAGGAAGGAAGGAGTGA
	Reverse	CTGGGCTTATCGCCATCTCTT
CD11b	Forward	CCCATGACCTTCCAAGAGAA
	Reverse	AGAGGGCAAATGTCTGGTTA
Csf1r	Forward	TGGCGAGGGTTCATTATCCG
	Reverse	CCAGCTTGCTAGGCTCCAAT
Cspg4	Forward	TAGGGAGCAGGCAAACGAAG
	Reverse	AAACTCAAACGACGCACAGC
Cyp2c29	Forward	CATCGACCTCCTCCCCACTA
	Reverse	AAAGTGCCCAGGGTCAAACA
Fads	Forward	CTGCCAATCTAGCCAGCACT
	Reverse	TTGAAGGCGAAGCCTAGCTC
Il1b	Forward	TGAAATGCCACCTTTTGACAGTG
	Reverse	ATGTGCTGCTGCGAGATTTG
Il6	Forward	GTCCTTCCTACCCCAATTTCCA
	Reverse	TAACGCACTAGGTTTGCCGA
Klf2	Forward	AAGAGCTCGCACCTAAAGGC
	Reverse	CTTTCGGTAGTGGCGGGTAA
Pik3cg	Forward	GAAGGGAGCCCCAGAAAAGAG
	Reverse	GTGATGCGGAGGAGGATCATT
Pla2g6	Forward	AGACCAACTGGTATGGCGTG
	Reverse	CCTGTCCCCAGAGAAACGAC
Pla2g4a	Forward	CCCCTCCAAGTAGCAAAGACT
	Reverse	GTGGCACGTAGAACCACAAC
Ptk2b	Forward	CTACACGGAGTTCACAGGGC
	Reverse	TACACGAGGTCATCGGTCCT
Tnf	Forward	GGTGCCTATGTCTCAGCCTCTT
	Reverse	GCCATAGAACTGATGAGAGGGAG
Actin	Forward	GTCGTACCACTGGCATTGTG
	Reverse	CTCTCAGCTGTGGTGGTGAA

4.11. Brain immunohistochemistry

Mice were anesthetized with intraperitoneal ketamine/xylazine and transcardially perfused with PBS and 4% PFA. After dissection, the brains were post-fixed in 4% PFA at 4 °C for 1 day, followed by PBS washing and 30% sucrose for cryoprotection. The brains were stored at -80 °C before cryosectioning

Coronal cryosections at -20 °C containing the PFC, HPC, OB in 40 μm thickness. Brain sections were washed in PBS for 5 minutes × 3 times with gentle rotation, followed by 15 minutes incubation in 0.5% Triton-X100. After PBS washings, slices were incubated with primary antibodies including rabbit anti-ionized calcium-binding adapter molecule 1 (IBA1, #SKL6615, Wako), rat anti-CD31 (#553370, BD Pharmingen) or mouse anti-CD31 (#sc-376764, Santa Cruz Biotechnology), and rat anti-CD206 (#MAB-16871, Invitrogen) in PBS blocking buffer overnight at 4 °C, followed by goat anti-rabbit IgG H&L-AlexaFluor488 (#ab175471, Abcam), goat anti-rat IgG H&L-AlexaFluor546 (#119170, Jackson ImmunoResearch), and goat anti-mouse IgG H & L-PECy7 (#D2110, Sant Cruz) for 2 hours at room temperature and then in 0.1 μg/ml 4′,6-diamidino-2-phenylindole (DAPI, #ACRO202710100, VWR) for 5 minutes, and finally mounted to glass slides with Fluoromount™ Aqueous Mounting Medium (# F4680-25ML, Sigma-Aldrich).

Images were taken in 1024 × 768 pixels at a scanning velocity of 8.0 pixel/μm with Z-stacks (step = 0.5 μm, depth = 25 μm) at 60× magnification or without Z-stacks at 20× magnification by FV1200MPE laser scanning microscope (Olympus). After $CD31^+$-area/whole image area × 100% was calculated. $IBA1^+$-microglia/macrophages whose cell soma located within the range of vascular radius surrounding a $CD31^+$-blood vessel were defined as vessel-associated microglia/macrophages (VAMs) and others as nonvessel-associated microglia/ macrophages (NVAMs). Fluorescent intensities of $CD31^+$- and $IBA1^+$-areas and microglial number (No.) and morphology were measured using ImageJ (n = 3-mice/12-sections/40~200 cells per group). Images were converted into an 8-bit format and “analyze particles” was used to measure whole cell and cell soma sizes. The threshold of intensity was set automatically by ImageJ for the whole cell and was increased by 20% with minimal size filter set at 2.5 pixels for cell soma.

4.12. Plasma metabolomics

4.12.1. Sample pre-treatment

To extract metabolites and remove proteins, 300 μl methanol-acetonitrile (2:1, v/v), including 10 μl internal standard (0.3 mg/mL 2-chloro-L-phenylalanine in methanol) was mixed with 100 μl serum. After vortex for 1 minute, the mixture was ultrasonically extracted in ice-cold water for 10 minutes, followed by standing for 30 minutes at -20 °C and centrifugation for 15 minutes at a speed of 14,000 g at 4 °C (Peng et al., 2015). Equal aliquots of each serum sample were taken to generate a QC sample. Pre-treatment of QC was the same as for

samples. A QC was inserted after every ten samples throughout an analytical run to provide a set of data from which repeatability can be assessed (Want et al., 2010).

4.12.2. Liquid chromatography-time-of-flight mass spectrometry (LC-TOF/MS)

To measure metabolites, LC-TOF/MS was performed by a Waters ACQUITY UPLC system coupled with an AB SCIEX Triple TOF 5600 (AB SCIEX, Framingham, USA). The system utilized an ACQUITY UPLC BEH C18 column (100 mm × 2.1 mm, 1.7 μm). The column temperature was maintained at 45 °C. Mobile phases of (A) 0.1% formic acid-contained water and (B) 0.1% formic acid-contained acetonitrile were used in both positive and negative ionization modes. Gradient elution was initially started from 95% A, which was linearly decreased to 80% A within 2 minutes, to 40% A within another 2 minutes, then to 0% A within 7 minutes and was maintained for 2 minutes, and finally returned to the initial ratio within 30 seconds and at equilibrium for 1 minute. Data acquisition was performed in a full scan mode (m/z ranges from 50 to 1000). Parameters of MS were followed as: ion spray voltage of 5500 V (+) and 4500 V (−); curtain gas of 35 PSI; declustering potential of 100 V (+) and −100 V (−); collision energy of 10 V (+) and −10 V (−); and interface heater temperature at 550 °C (+) and 600 °C (−).

4.12.3. LC-TOF/MS data processing

Raw data were imported to progenesis QI (Waters Corporation, Milford, USA) for raw peaks exaction, data baselines filtration and calibration, peak alignment and identification, and peak area integration and normalization. The resulting three-dimensional data, including the peak number, sample name, and normalized peak area, were entered into the SIMCA14.3 software package (Umetrics, Umea, Sweden) for principal component analysis (PCA) and orthogonal projections to latent structures-discriminate analysis (OPLS-DA). PCA was used to display natural separation among groups by visual inspection of score plots, as well as to identify clustering trends. OPLS-DA was used to validate the interpretation (R2) and prediction (Q2) of a model. To obtain a higher level of group separation and a better understanding of the variables responsible for the classification, potential candidates were chosen based on their contribution of variable importance for the projection (VIP) extracted from the first principal component in the OPLS-DA analysis. VIP > 1.0 was first selected, and the remaining variables were then assessed by Student's t-test, with $p < 0.05$ considered as statistically significant between the two compared groups (Han et al., 2017).

4.12.4. Metabolites identification and correlational analysis

Identification of different metabolites was performed as follows. First, the elemental compositions of compounds were determined by the exact mass and isotope pattern. Second, a candidate elemental composition was compared with those deposited in the databases of HMDB (http://www.hmdb.ca), Metlin (http://metlin.scripps.edu), and Lipidmaps (http://www.lipidmaps.org). Pearson's correlation analysis was conducted between the total locomotor distance and the metabolite level, with the statistical significance set at coefficient $|r| > 0.5$ and $p < 0.05$. Selected metabolites were further validated and cross-referenced for metabolic pathways in the Kyoto Encyclopaedia of Genes and Genomes (KEGG), and finally sketched according to the analysis.

From the above analysis, coproporphyrinogen III (Cop), a precursor of heme that acts as a pro-inflammatory factor and promotes the production of lipid peroxides (Ortiz de Montellano, 2008; Kumar et al., 2005) outstood. The relationship between Cop and the activation of microglia was further explored by *in vitro* cell culture study.

4.13. Microglia cell culture

To further confirm the Cop function, BV-2 microglial cell line was obtained from the National Infrastructure of Cell Line Resource (Shanghai, China). Cells were seeded in 96-well culture plates at 1×10^3 cells/well ($n = 7$) and maintained in Dulbecco's modified Eagle's medium High Glucose (Hyclone, Logan, UT, USA) containing 10% fetal bovine serum (GIBCO, Invitrogen, Karlsruhe, Germany) at 37 °C in a humidified atmosphere of 5% CO_2 and 95% air for 12 hours, then treated with Cop (1 and 10 μM) (J&K Scientific Ltd, Shanghai, China) or vehicle solution (0.1% DMSO) for 24 hours. BV-2 cell viability was analyzed by a cell counting kit-8 (Dojindo Laboratories, Kunming, China) following the manufacturer's instruction. Briefly, cells treated with or without Cop were incubated with 10 μl of cell counting kit-8 solution at 37 °C for 2 hours. The absorbance of the mixture was measured at 450 nm by a microplate reader. After Cell culture media were collected. Nitric oxide (NO) was detected by using the Griess reagent system (Promega Co., Madison, USA). Interferon-γ (IFN-γ) and IL-1β were measured by ELISA kits (Beijing Dongge Biotechnology Co., Ltd, Beijing, China) according to the manufacturer's instructions. Averaged values for each measurement were calculated and normalized against the cell viability in each group.

4.14. Data presentation and statistical analysis

Data distributions were examined by Shapiro-Wilk's test. For human data, analysis of variance (ANOVA) or Mann-Whitney U test was used for continuous variables and chi-squared tests for categorical variables. Analysis of covariance

(ANCOVA) with age and sex as covariates were conducted for plasma CSF1R and MRI data, with white blood cell counts and ICV included as additional covariates for them, respectively, and p values for multiple comparisons were corrected by FDR. The correlation was analyzed by Pearson's or Spearman's method. Relationships among CSF1R level, cortical size, and PSS score were evaluated using linear regression and moderator analysis by PROCESS-v3.5 in SPSS-v27.0 (IBM), controlled by age, sex, and ICV. For animal data, two-way analysis of variance was used to examine the interaction between CUS and CSF1Ri, with Tukey's or Bonferroni's correction for post hoc comparisons. One-way ANOVA with Tukey's correction for post hoc comparisons was used to analyze the BV2 cell experiment. Figures were prepared in GraphPad Prism-v8.0.1 and online (http://www.bioinformatics.com.cn/). Data were presented as mean ± standard error of mean and p or FDR < 0.05 was considered statistically significant.

5. RESULTS

5.1. Psychoneuroimmunological changes in first episode schizophrenia (FES) patients (Papers I and II)

5.1.1. FES patients showed worse perceived stress and cognitive impairments (Papers I and II)

A total of 128 FES patients and 111 HCs were recruited according to the inclusion and exclusion criteria. No differences were observed between the groups for age, sex, and smoking status (all $p > 0.05$) (**Table 2**). Years of education was less in FES patients than that in HCs ($p < 0.01$) (**Table 2**).

Table 2. Participants' demographic and clinical characteristics of the entire cohort of first episode schizophrenia (FES) patients and healthy controls (HCs). Data are reported as mean ± standard error of mean. Significant *p* values are shown in bold. NA, not applicable.

Characteristics	FES (*n* = 128)	HC (*n* = 111)	Z/χ2	*p*
Age (years)	30.64 ± 9.53	32.99 ± 9.57	-1.937	0.053
Males/Females	55/73	56/55	1.338	0.247
Education (years)	12.76 ± 3.41	13.79 ± 2.59	-2.612	**0.009**
Smoker/Non-smoker	18/110	23/88	1.854	0.173
Illness duration (months)	12.28 ± 12.25	NA	NA	NA
PANSS total	76.45 ± 12.94	NA	NA	NA
P subscore	22.21 ± 5.10	NA	NA	NA
N subscore	17.41 ± 6.22	NA	NA	NA
G subscore	36.85 ± 7.17	NA	NA	NA

As expected for MCCB test, a smaller cohort of FES patients who could be further screened with MCCB from the above big cohort showed significantly lower total MCCB scores and domain-specific subscores compared to the HCs after controlling for age, sex, and education years (all FDR < 0.001) (**Table 3**).

Table 3. MCCB cognition scores in a sub-cohort of first episode schizophrenia (FES) patients and healthy controls (HCs). Data are reported as mean ± standard error of mean. Values in bold indicate statistically significant differences.

MCCB domains	FES (*n* = 58)	HC (*n* = 52)	F	*p*
Verbal learning	48.72 ± 10.98	57.37 ± 7.78	17.24	**6.58×10^{-5}**
Reasoning/problem solving	46.98 ± 10.33	56.63 ± 7.40	32.04	**1.24×10^{-7}**
Visual learning	45.53 ± 9.78	55.02 ± 7.22	28.97	**4.26×10^{-7}**
Social cognition	46.32 ± 11.16	54.46 ± 10.08	12.41	**6.25×10^{-4}**
Attention/vigilance	40.50 ± 11.91	57.17 ± 10.83	49.71	**1.71×10^{-10}**
Processing speed	44.32 ± 11.05	57.50 ± 8.73	42.71	**2.38×10^{-9}**
Working memory	46.00 ± 10.94	57.55 ± 7.17	37.92	**1.28×10^{-8}**
Composite score	44.93 ± 9.30	58.69 ± 6.98	76.40	**4.05×10^{-14}**

We next selected a sub-cohort of those patients who showed higher PSS stress scores than HCs. Participants' demographic and clinical data are listed in **Table 4**. FES patients and HCs were not statistically different in age, sex, education years, and CTQ score (all $p > 0.05$). Compared with HCs, FES patients had a higher averaged PSS score (**Fig. 3A, Table 4**), which was positively correlated with PANSS total score (r = 0.334, $p < 0.05$; **Fig. 3B**).

Table 4. Demographic and clinical characteristics of a sub-cohort of first episode schizophrenia (FES) patients with high PSS scores and healthy controls (HCs). Data are reported as mean ± standard error of mean (ANCOVA or Mann-Whitney U test); CSF1R (ANCOVA controlled by age, sex, and white blood cells); Significant *p* values are shown in bold. NA, not applicable.

Demographics	FES (*n* = 51)	HC (*n* = 46)	F or $\chi 2$	*p*
Sex (M/F)	18/33	23/23	2.143	0.143
Age (years)	30.59 ± 1.18	34.00 ± 1.46	1388.000	0.120
Education (years)	12.75 ± 0.49	13.28 ± 0.33	1298.500	0.354
CTQsum	81.55 ± 5.49	70.02 ± 4.78	727.500	0.125
PSSsum	23.14 ± 0.99	21.39 ± 0.67	893.000	**0.043**
Age of illness onset (years)	29.27 ± 1.17	NA	NA	NA
Illness duration (months)	11.70 ± 2.09	NA	NA	NA
PANSS total	75.69 ± 2.03	NA	NA	NA
White blood cells (10^6/ml)	7.60 ± 1.08	6.01 ± 0.25	856.000	0.085
Plasma CSF1R (ng/ml)	18.55 ± 1.03	21.26 ± 0.766	5.539	**0.021**

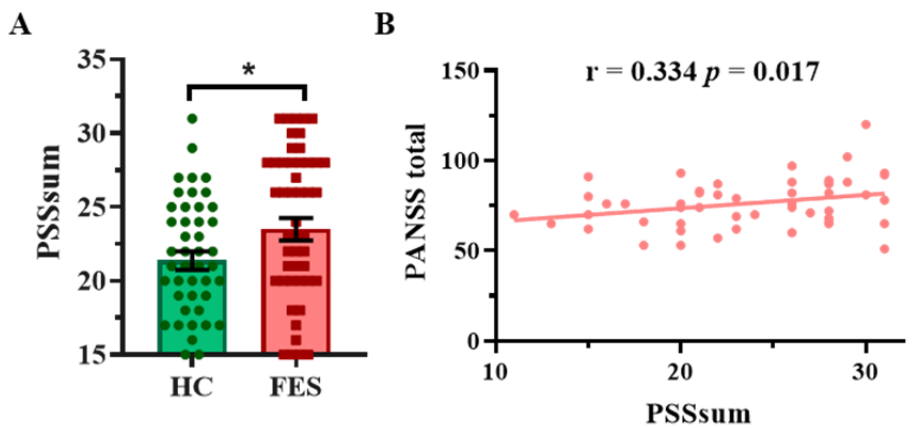

Figure 3. Perceived stress scale (PSS)sum average score was higher in first episode schizophrenia (FES) patients than healthy controls (HCs) and was correlated with PANSS score. (**A**) PSSsum scores in FES patients and HCs (n = 51 + 46); (**B**) correlation of positive and negative symptom scale (PANSS) total and PSSsum in FES patients (Spearman's correlation). Data are presented as mean ± standard error of mean; *$p < 0.05$ Mann-Whitney U test.

5.1.2. FES patients showed cerebral cortical atrophy (Paper II)

We further studied those participants in the PSS sub-cohort with MRI. We measured 8 key stress-related brain regions, including the PFC subareas, HPC, and HPC-associated entorhinal and parahippocampal gyri (**Fig. 4A**, **Table 5**), and observed reduced volumes in the superior frontal gyrus ($p < 0.005$, FDR = 0.02; **Fig. 4B**) and parahippocampal gyrus ($p < 0.004$, FDR = 0.032; **Fig. 4C**) in FES patients compared to HCs. The orbitofrontal gyrus also showed a nominal reduction in FES patients compared to HCs ($p < 0.05$, **Table 5**). The HPC and other cortical structures did not show significant differences, however (**Table 5**).

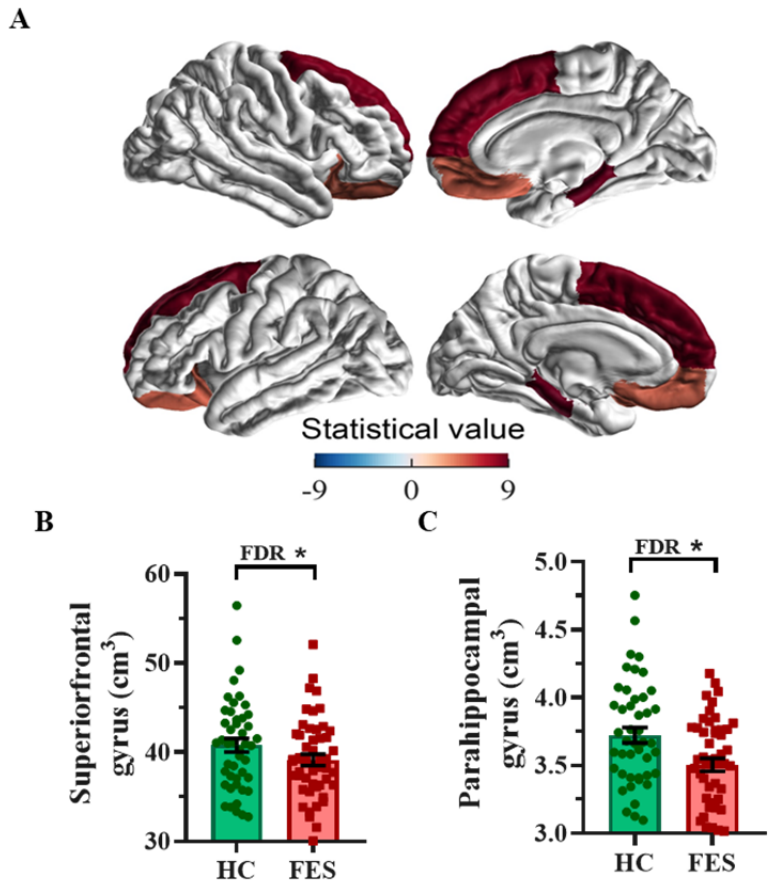

Figure 4. Cerebral cortical gyri were smaller in first episode schizophrenia (FES) patients with high PSS than healthy controls (HCs). (**A**) Exemplary magnetic resonance imaging (MRI) images, color gradient is based on the statistical *F* values (detailed in **Table 5**) of group comparison, volumes of the superior frontal (**B**) and parahippocampal gyri (**C**). Data are presented as mean ± standard error of mean; *false discovery rate (FDR) or $p < 0.05$, ANCOVA controlled by age, sex, and intracranial volume (ICV). $N = 51 + 46$

Table 5. Cerebral cortical volumes (cm^3) in first episode schizophrenia (FES) patients with high PSS and healthy controls (HCs). Data are reported as mean ± standard error of mean (ANCOVA controlled by age, sex, and intracranial volume (ICV) and corrected for multiple comparisons); Bold texts indicate significant *p* and false discovery rate (FDR) values.

	FES (*n* = 51)	HC (*n* = 46)	F	*p*	FDR
Anteriocingulate gyrus	7.729 ± 0.126	7.927 ± 0.133	1.124	0.292	0.467
Entorhinal gyrus	3.152 ± 0.069	3.136 ± 0.069	0.442	0.508	0.581
Hippocampus	8.039 ± 0.084	8.109 ± 0.096	0.156	0.694	0.694
Inferiorfrontal gyrus	19.233 ± 0.296	19.679 ± 0.313	1.031	0.312	0.416
Middlefrontal gyrus	40.051 ± 0.502	41.388 ± 0.530	3.23	0.076	0.152
Orbitofrontal gyrus	23.791 ± 0.203	24.445 ± 0.214	4.706	**0.033**	0.088
Parahippocampal gyrus	3.505 ± 0.048	3.723 ± 0.058	8.791	**0.004**	**0.032**
Superior frontal gyrus	39.134 ± 0.641	40.803 ± 0.760	8.327	**0.005**	**0.020**

5.1.3. Nonclassical monocytes were decreased in FES patients (Paper I)

We first studied molecular signatures of circulating leukocytes and identified 9062 DEGs (FDR < 0.05) between FES patients and HCs (of the entire cohort), including 4479 upregulated and 4583 downregulated genes in the big cohort. To get a better insight into the transcriptomic changes among CD14/CD16-subsets of monocytes in schizophrenia, 79 subset-specific signature genes were chosen based on recent monocytic transcriptomic profiling works (Zawada et al., 2011; Kapellos et al., 2019), among which 54 were found to have FDR < 0.05 in our RNA-seq datasets. These 54 DEGs belonged to all (7.4%), classical (16.7%), intermediate (37.0%), and nonclassical (38.9%) monocytes, respectively (**Fig. 5A**). Among these subclasses, the majority of DEGs belonging to the classical monocytes (6 out of 9, i.e., 66.7%) were downregulated and that of DEGs belonging to the nonclassical monocytes (13 out 21, i.e., 61.9%) were upregulated, while the proportions of up- and down-regulated genes (45% vs. 55%) were more equal in the intermediate monocytes (**Fig. 5A**). Notably, among the DEGs with the most magnified change of expressions (|Log2FC| > 0.5), downregulated *S100A8*, *S100A9* belonging to intermediate monocytes and upregulated *IFITM2* and *IFITM3* belonging to nonclassical monocytes outstood (**Fig. 5B**). Moreover, we noticed that *CSF1R* and *PECAM1*(*CD31*) mRNAs were decreased in the FES patients compared to the HCs (**Fig. 5B**).

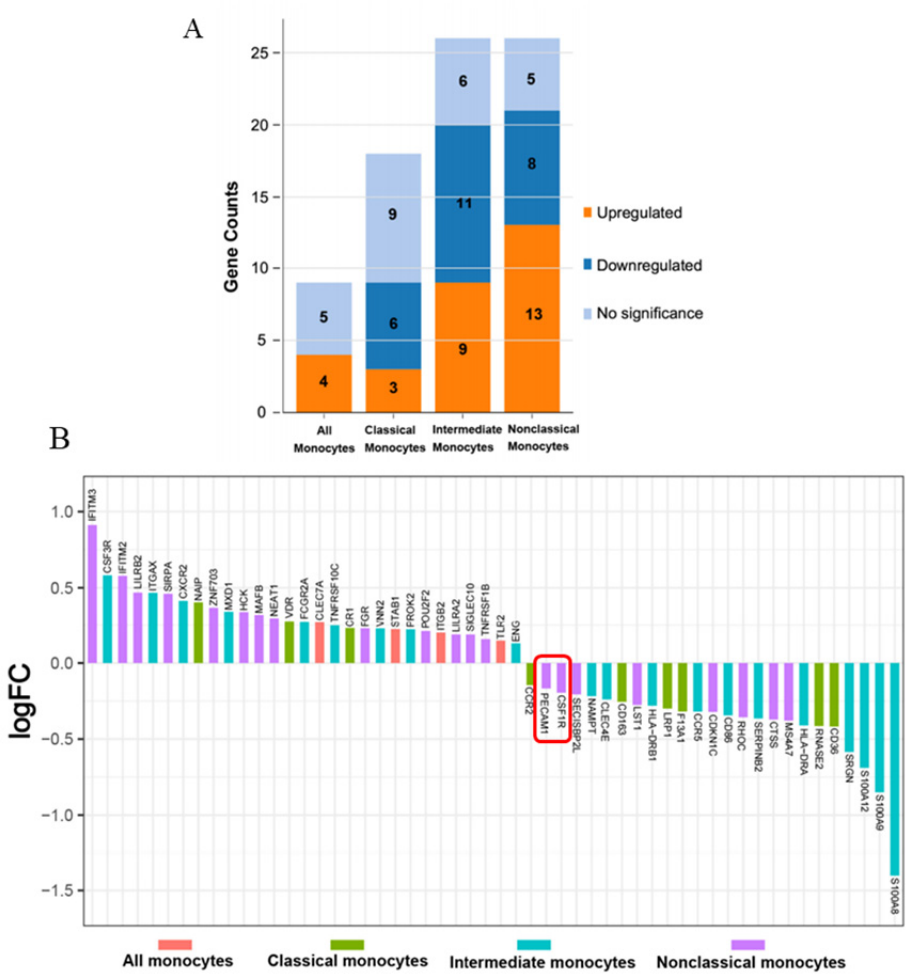

Figure 5. Peripheral blood RNA-seq transcriptomic profiling between first episode schizophrenia (FES) patients (*n* = 128) and healthy controls (HCs) (*n* = 111). (**A**) There were 54 monocytic differentially expressed gene (DEG)s (false discovery rate (FDR) < 0.05). (**B**) They were especially enriched in intermediate and nonclassical monocytes. Downregulation of *PECAM1* and *colony stimulating factor 1 receptor* (*CSF1R)* genes enriched in nonclassical monocytes is highlighted.

A subgroup consisted of 29 FES patients and 27 HCs, of whom 23 FES patients and 26 HCs were also included in the big cohort, was used to explore the distribution of monocytic subsets by flow cytometry as shown (**Fig. 6A**). There were no significant differences in age, sex, education years, or smoking status between the FES patients and HCs in this subgroup (data not shown here but reported in Paper I). Interestingly, the FES patients had a decreased percentage of the nonclassical monocytes compared to the HCs after controlling for age and sex (5.27 ± 3.01% vs. 7.61 ± 3.21%, F = 8.736, FDR = 0.015) (**Fig. 6B**). By

contrast, we found no group differences in the percentages of the classical and intermediate monocytes.

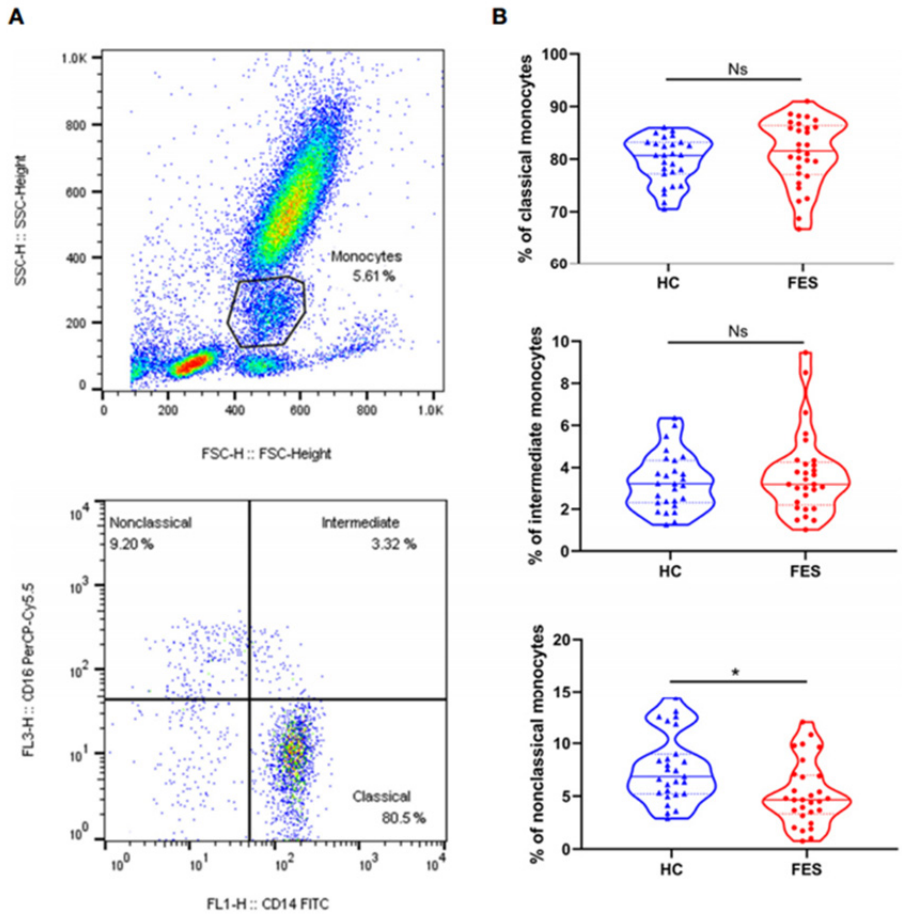

Figure 6. Nonclassical monocytes were decreased in the peripheral blood of first episode schizophrenia (FES) patients (*n* = 29) compared to healthy controls (HCs) (*n* = 27). (**A**) Dot plots show gating strategy. Monocytes were first selected based on size (forward scatter height) and granularity (side scatter height), and then monocytic subsets were defined according to surface expressions of CD14 and CD16. (**B**) $CD14^{++}CD16^{-}$ classical monocytes, $CD14^{++}CD16^{+}$ intermediate monocytes, and $CD14^{+}CD16^{++}$ nonclassical monocytes were quantitated, respectively. Solid and dotted lines represent the median and upper/lower quartile values, respectively. Ns, not significant. * false discovery rate (FDR) < 0.05.

5.1.4. Blood CSF1R mRNA and protein levels were lowered in FES patients (Paper II)

As CSF1R is critical for the development of microglia as well as the brain, we found its decrease in the blood of FES patients compared to HCs (of the entire cohort) **(**FDR = 0.003; **Fig. 5B & 7A)** particularly interesting. To validate its RNA-seq result, we measured plasma CSF1R protein and confirmed it in both the big and small patient cohorts (both $p < 0.05$; **Fig. 7B, Table 4**).

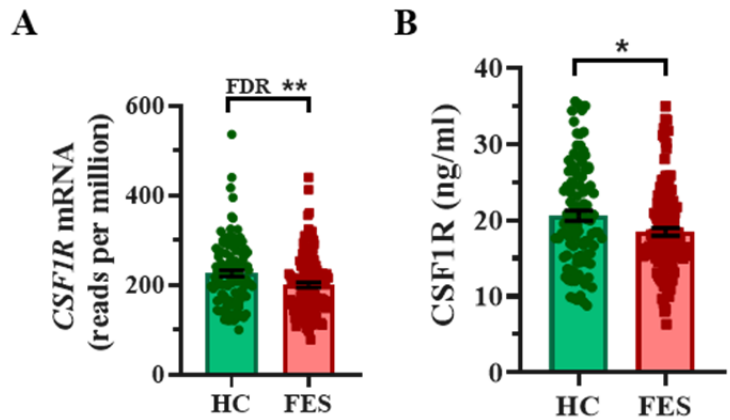

Figure 7. Blood colony stimulating factor 1 receptor (CSF1R) was decreased in first episode schizophrenia (FES) patients (*n* = 128) compared to healthy controls (HCs) (*n* = 111). (**A**) CSF1R mRNA level in blood cells; (**B**) CSF1R protein level in the plasma ($n = 126 + 102$). Data are presented as mean ± standard error of mean; *$p <$ 0.05, **false discovery rate (FDR) < 0.01 (ANCOVA controlled by age, sex, and white blood cells).

We further explored functional genomic data in GeneWeaver and retrieved 64 *CSF1R*-associated brain genes involved in human brain development. To better depict which of them were changed in our patients' blood, we overlapped them with blood RNA-seq DEGs and found 11 up-regulated DEGs and 17 down-regulated DEGs including the *CSF1R* (**Fig. 8A & 8B**). To depict functional relationships among the 28 DEGs, we checked their interactions and GO enrichment by PPI analysis, showing three different functional clusters, with *PIK3CA*, *AKT1,* and *CSF1R* as hub genes, respectively (**Fig. 8C**). The top-ranking GO-BP pathway is the regulation of developmental process (**Fig. 8D**).

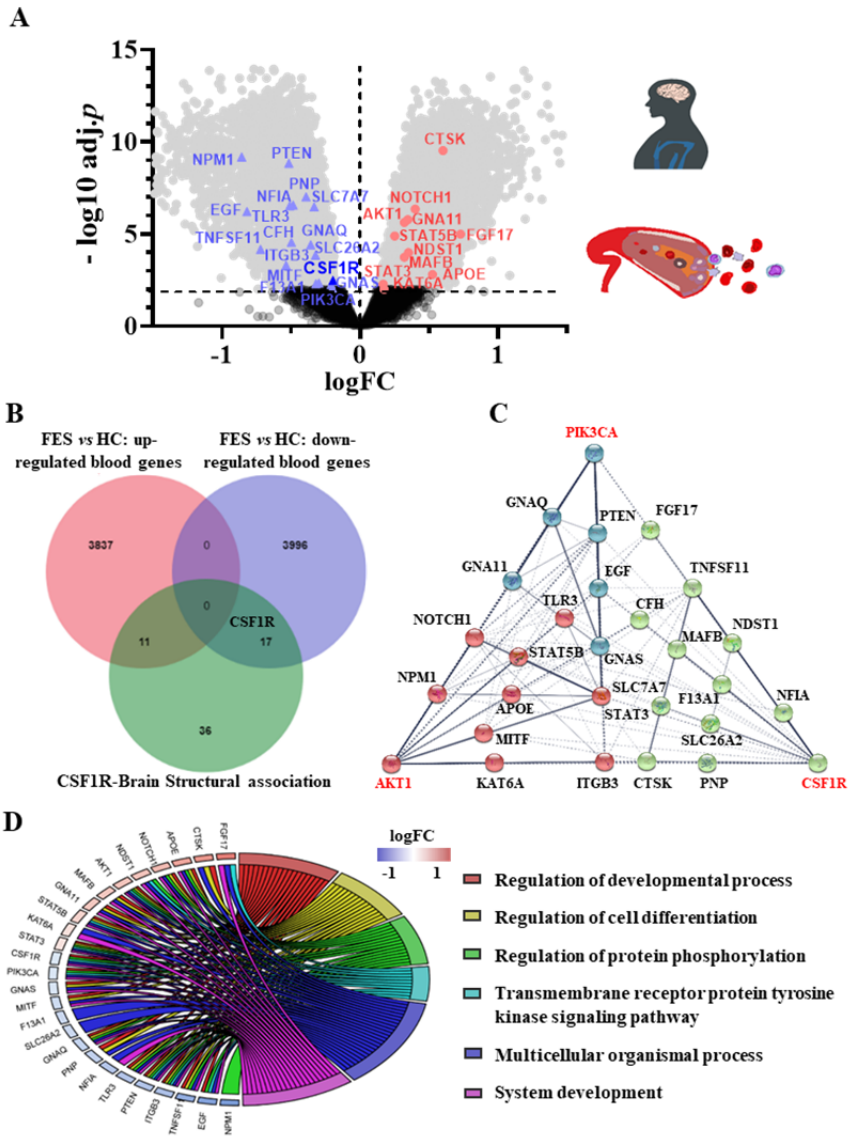

Figure 8. Blood *colony stimulating factor 1 receptor* (*CSF1R)* was decreased in FES patients along with some blood DEGs related to brain development. (**A**) A volcano plot highlights 28 blood differentially expressed gene (DEG)s in first episode schizophrenia (FES) patients versus healthy controls (HCs). Genes with FDR < 0.01 are colored (n = 128 + 111). (**B**) Venn diagram illustrates the 28 DEGs that are annotated to be associated with human brain structural development in GeneWeaver. (**C**) Protein-protein interaction (PPI) analysis shows functional interactions among the 28 DEGs, with confidence threshold = 0.4 and cluster k-means = 3. (**D**) A chord plot shows the top 6 overrepresented gene ontology biological pathway (GO-BP) subontology for the 28 DEGs associated with brain development. Genes are ordered according to the observed Log2FC and linked to their assigned terms via colored ribbons.

5.1.5. CSF1R fully moderated a negative association of the superior frontal gyrus with stress perception in healthy controls (HCs) (Paper II)

We next explored inter-relationships among the cortical structures, CSF1R mRNA or protein level, and PSS (of the PSS sub-cohort) with linear regression and moderator analyses controlled by age, sex, and ICV, predicting that brain structural deficit underlies stress susceptibility and CSF1R is one of the molecular machineries modulating brain and behavior, e.g., PSSsum as the dependent variable, cortical volumes the independent variables, and CSF1R level the moderator. The model showed that in HCs (**Fig. 9**) but not FES patients, the *CSF1R* mRNA was negatively associated with the PSSsum (β = -9.784, p < 0.05). The *CSF1R* also interacted with the superior frontal gyrus (R^2 = 0.083, p < 0.05) and since the direct association of the superior frontal gyral size with the PSSsum was insignificant (β = -5.335, p = 0.25), this demonstrates that the *CSF1R* had a full moderator effect on the superior frontal gyral correlation with the PSSsum (β = 6.109, 95% confidence interval (CI) = 1.642~10.578, p < 0.01). Additionally, the CSF1R mRNA and protein also moderated negative associations of the middle frontal gyrus (β = 0.383, p < 0.05) and the HPC (β = 0.477, p < 0.05) with the PSSsum in HCs, respectively (**Fig. S1A**). We also found that in the FES patients, the *CSF1R* mRNA was negatively correlated with the PSS score (r = -0.249, p < 0.05; **Fig. S1B**) and the PANSS total score (r = -0.365, p < 0.01; **Fig. S1C**).

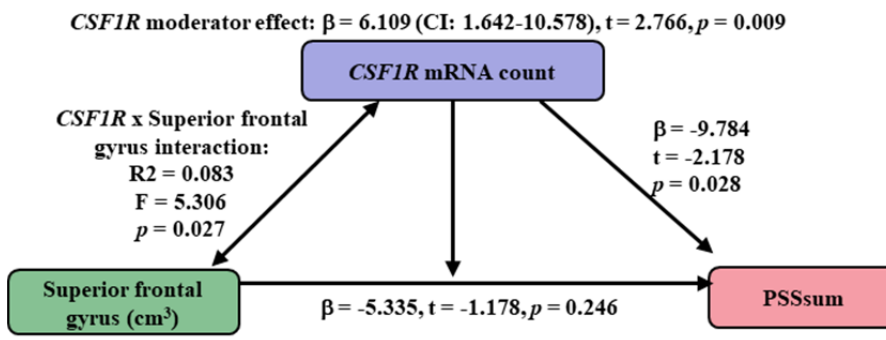

Figure 9. ***Colony stimulating factor 1 receptor*** **(*CSF1R*) facilitated a negative association of the superior frontal gyrus with the perceived stress scale (PSS)sum in healthy controls (HCs).** Blood *CSF1R* mRNA level fully moderated a negative association of the superior frontal gyral volume (independent variable) with the PSSsum score (dependent variable), controlled by age, sex, and intracranial volume (ICV).

5.2. Stress-induced psychiatric-like behaviors (Papers II and IV)

5.2.1. CUS and CSF1Ri induced psychiatric-like behaviors in mice (Paper II)

We applied a CUS mouse model (lasting 8 weeks) combined with a CSF1Ri to investigate the effect of Csf1r on stress coping (3mg PLX3397/mouse/day for 2 weeks), with the experimental design shown below (**Fig. 10**).

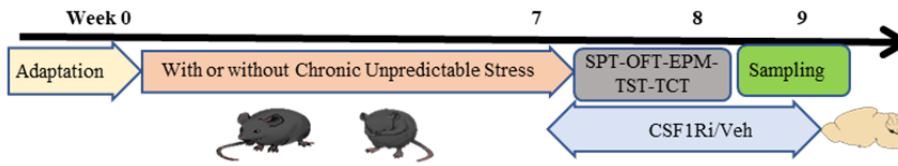

Figure 10. Schema representing mouse chronic unpredictable stress (CUS)+CSF1R inhibitor (CSF1Ri) experimental design.

We first evaluated their anxiety in OFT and EPM tests. Interactions between the CUS and CSF1Ri on ratio of corner distance/total distance in the OFT ($F(1, 35) = 4.255$, $p < 0.05$) and ratio of open/close arms time in the EPM ($F(1, 35) = 5.083$, $p < 0.05$) were observed. Both the CUS and CSF1Ri had significant main effects on the ratio of corner distance/total distance (CUS main effect: $F(1, 35) = 6.433$, $p < 0.05$; CSF1Ri main effect: $F(1, 35) = 4.773$, $p < 0.05$) and the ratio of open/close arms (CUS main effect: $F(1, 35) = 9.462$, $p < 0.01$; CSF1Ri main effect: $F(1, 35) = 27.28$, $p < 0.001$). Anxiety was enhanced by the CUS, CSF1Ri, or CUS-CSF1Ri combination (all $p<0.05$), compared to Ctr-Veh. No cumulative effect of the CUS-CSF1Ri combined treatment was found (**Fig. 11A & 11B**).

For depressive-like behaviors, we found an interaction between the CUS and CSF1Ri ($F(1, 35) = 4.353$, $p < 0.05$) and significant main effect of the CSF1Ri ($F(1, 35) = 6.184$, $p < 0.05$) in SPT. Sucrose preference was decreased by the CUS, CSF1Ri, or CUS-CSF1Ri combination (all $p < 0.05$), compared to the Ctr-Veh (**Fig. 11C**). We also observed an interaction between the CUS and CSF1Ri on immobility time, i.e., learned helplessness in TST ($F(1, 35) = 5.300$, $p < 0.05$), where the CUS triggered an increase in the immobility time compared to Ctr-Veh ($p < 0.05$) but CSF1Ri did not affect it (**Fig. 11D**). Similarly, the CUS affected sociability, i.e., less preferential entry into a social chamber in TCT (CUS main effect: $F(1, 35) = 5.555$, $p < 0.05$), but the CSF1Ri did not affect it (**Fig. 11E**). These results indicate that like the CUS, the CSF1Ri enhanced anxiety and anhedonia. But the CSF1Ri did not affect despair and sociability.

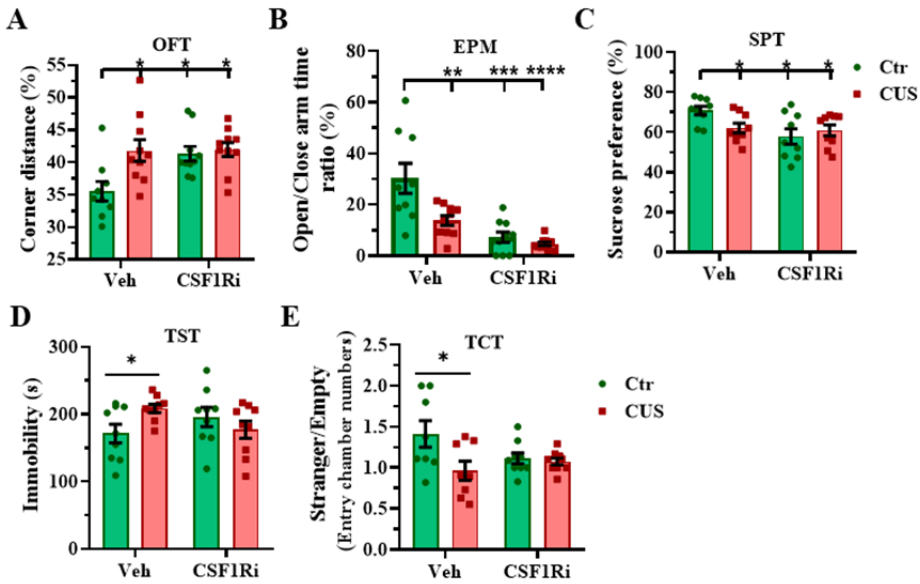

Figure 11. **Chronic unpredictable stress (CUS) and CSF1R inhibitor (CSF1Ri) enhanced anxiety and depression in mice.** (**A**) Ratio (%) of travel distance in the corners (m) against total travel distance (m) in an open field test (OFT); (**B**) Ratio (%) of time spent in an open arm against a closed arm in an elevated plus maze (EPM); (**C**) sucrose preference test (SPT) (%); (**D**) Immobility time (s) in tail suspension test (TST); I Ratio of entry numbers in a stranger chamber against an empty chamber in a three-chamber test (TCT). Data are presented as mean ± standard error of mean; *$p < 0.05$, **$p < 0.01$, ***$p < 0.001$, ****$p < 0.001$; compared to Ctr-Veh; two-way ANOVA with Bonferroni's correction; $n = 9 – 10$ per group.

5.2.2. OBX-induced psychiatric-like behaviors were attenuated in *fat-1* mice (Paper IV)

We used an OBX-induced mouse stress model created in WT and *fat-1* transgenic mice to study the role of endogenous n-3 PUFA in rescue of psychiatric-like behaviors, with the experimental design shown in **Fig. 12A**. Four weeks after the OBX, there were significant interaction effects between OBX and *fat-1* gene on total travel distance ($F (1, 16) = 4.736$, $p < 0.05$) and number of rearing ($F (1, 16) = 8.629$, $p < 0.01$). Both OBX and *fat-1* gene significantly affected the total travel distance (OBX main effect: $F (1, 16) = 39.84$, $p < 0.001$; *fat-1* gene main effect: $F (1, 16) = 16.80$, $p < 0.001$) and the number of rearing (OBX main effect: $F (1, 16) = 8.629$, $p < 0.01$; *fat-1* gene main effect: $F (1, 16) = 21.56$, $p < 0.001$). Significant increases in the total travel distance ($p < 0.001$, **Fig. 12B & 12C**) and the number of rearing ($p < 0.001$, **Fig. 12D**) in OBX group compared to Sham group in WT mice were observed. However, these hyperactive behaviors were significantly rescued by the *fat-1* gene in Fat-1/OBX group compared to WT/OBX group ($p < 0.001$, **Fig. 12B – D**). Under

the OBX condition, body weight dropped 8-16 days post operation in both the WT and *fat-1* mice and then gradually rose to the same levels as in Sham mice **(Fig. S2)**. No significant differences were observed between WT/Sham and Fat-1/Sham mice in the total travel distance and the number of rearing. We also found a significant interaction between OBX and *fat-1* gene in sucrose preference ($F(1, 16) = 4.736$, $p < 0.05$) and OBX significantly affected the sucrose preference (OBX main effect: $F(1, 16) = 12.50$, $p < 0.01$). A significant decrease in sucrose consumption in the OBX group compared to the Sham group in the WT mice was seen ($p < 0.01$, **Fig. 12E**), which significantly recovered by the *fat-1* gene in the Fat-1/OBX group compared to the WT/OBX group ($p < 0.05$, **Fig. 12E**).

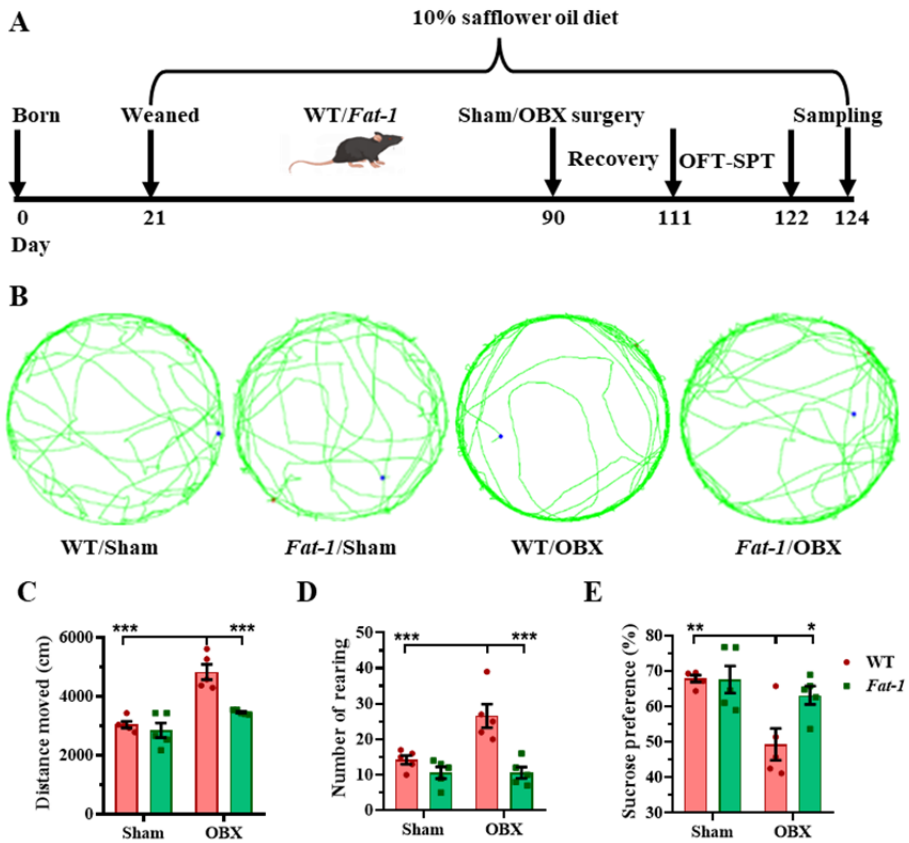

Figure 12. **Olfactory bulbectomy (OBX)-induced psychiatric-like behaviors were attenuated in *fat-1* transgenic mice**. (**A**) Schema representing OBX in *fat-1* mice experimental design. (**B**) The representative tracks; (**C**) the total travel distance, (**D**) the number of rearing in the open field test (OFT) are shown, and (**E**) the sucrose preference (%) in the sucrose preference test (SPT). Data are presented as mean ± standard error of mean; *$p < 0.05$, **$p < 0.01$, ***$p < 0.001$; two-way ANOVA with Tukey's correction; $n = 5$ per group.

5.3. Mechanisms of stress-induced psychiatric-like behaviors (Papers II–IV)

5.3.1. CUS and CSF1Ri dampened angiogenesis and CD31 expression in the mouse brain (Paper II)

We studied the PFC tissues by RNA-seq and identified 2750 DEGs including 1204 upregulated and 1546 downregulated DEGs among the four Ctr/CUS/Veh/CSF1Ri groups (see **Fig. 13A**). GO-BP enrichment analysis of these DEGs showed cell adhesion and angiogenesis as the top-ranking pathways (**Fig. 13A & 13B & S3A**), with most of the angiogenic DEGs downregulated by the CSF1Ri or CUS-CSF1Ri and a few by CUS, compared to the Ctr-Veh (**Fig. 13A & 14**). A few tight junction molecules were also downregulated by the CUS or CSF1Ri (**Fig. S3A**). These suggest that the CUS and CSF1Ri affect cerebral vasculature.

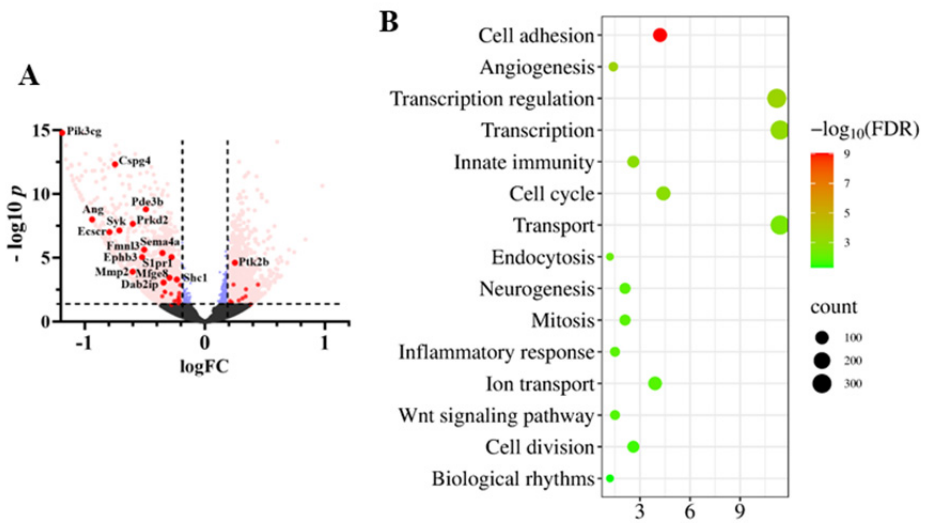

Figure 13. Chronic unpredictable stress (CUS) and CSF1R inhibitor (CSF1Ri) inhibited angiogenic genes in mice. (**A**) Volcano plot shows these differentially expressed gene (DEG)s, which are colored in pink if -Log_{10} adj. $p \geq 1.3$ and $|Log_2FC| \geq 0.2$ and in blue if $|Log_2FC| < 0.2$. Angiogenic DEGs are highlighted by red dots with gene symbols when -Log_{10} adj. $p \geq 3$. (**B**) Gene ontology biological pathway (GO-BP) enrichment analysis shows top-ranked pathways of DEGs derived from group comparisons. $N = 7$ per group.

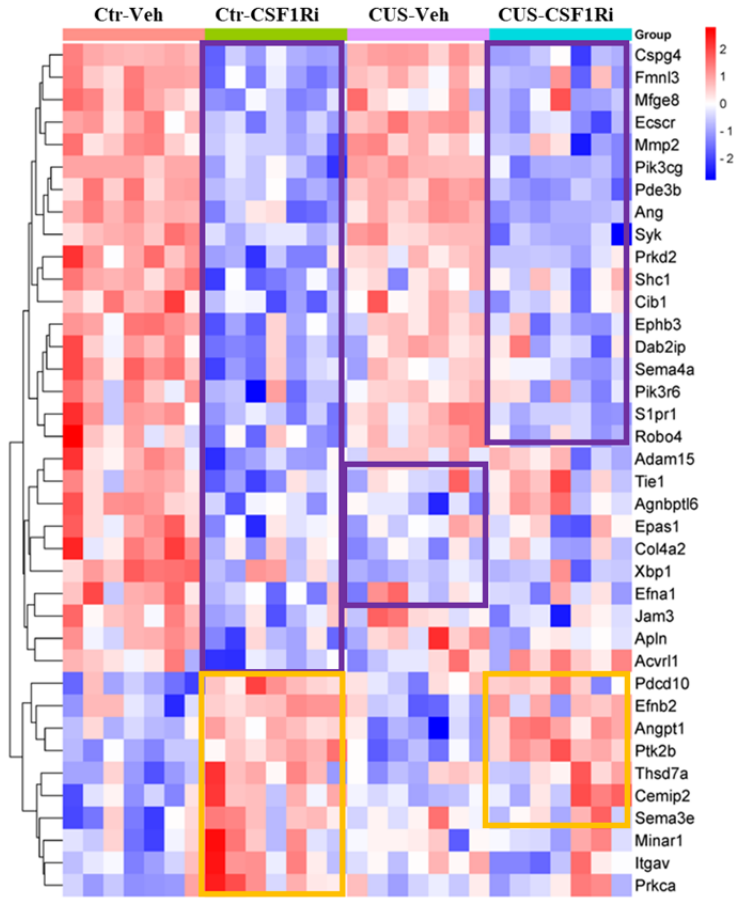

Figure 14. Angiogenic genes are inhibited by CSF1R inhibitor (CSF1Ri) and Chronic unpredictable stress (CUS) in mice. Heatmap shows 38 angiogenic differentially expressed gene (DEG)s. Downregulated (in purple frame) and upregulated (in orange frame) genes are highlighted in the heatmap. $N = 7$ per group.

To validate the RNA-seq data, we measured *Csf1r* and top-ranking angiogenic genes (*Ang*, *Cspg4*, *Pik3cg*, *Ptk2b*) in the PFC by RT-QPCR. Significant interactions existed between CUS and CSF1Ri on the expressions of *Csf1r* ($F(1, 24) = 7.797$, $p < 0.05$) and *Pik3cg* ($F(1, 24) = 10.19$, $p < 0.05/0.01$). Both the CUS and CSF1Ri affected the expressions of *Csf1r* (CUS main effect: $F(1, 24) = 18.21$, $p < 0.001$; CSF1Ri main effect: $F(1, 24) = 733.4$, $p < 0.001$) and *Pik3cg* (CUS main effect: $F(1, 24) = 11.08$, $p < 0.05$; CSF1Ri main effect: $F(1, 24) = 464.8$, $p < 0.05$). The CUS, CSF1Ri, or CUS-CSF1Ri combination reduced the expressions of *Csf1r* (**Fig. 15A**) and *Pik3cg* (**Fig. 15B**), compared to the Ctr-Veh ($p < 0.01/0.001/0.001$ for both genes). The CSF1Ri also reduced the *Ang* and *Cspg4* (both $p < 0.001$) expressions while enhanced the *Ptk2b* ($p < 0.01$) expression, compared to the Veh (**Fig. S3B-D**).

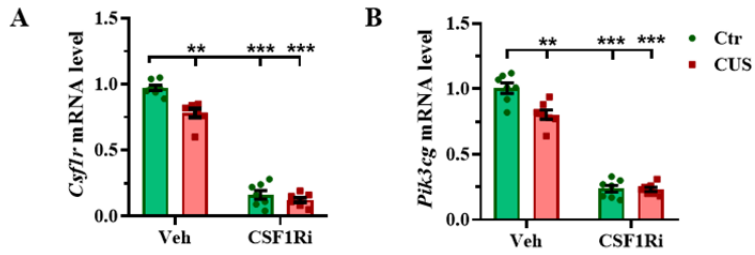

Figure 15. Chronic unpredictable stress (CUS) and CSF1R inhibitor (CSF1Ri) inhibited colony stimulating factor 1 receptor (*Csf1r*) and angiogenic genes in mice. (**A**) mRNA expressions of *Csf1r* and (**B**) *Pik3cg* in the prefrontal cortex (PFC). Data are presented as mean ± standard error of mean; **p* < 0.05, ***p* < 0.01, ****p* < 0.001; two-way ANOVA with Bonferroni's correction; *n* = 7 per group.

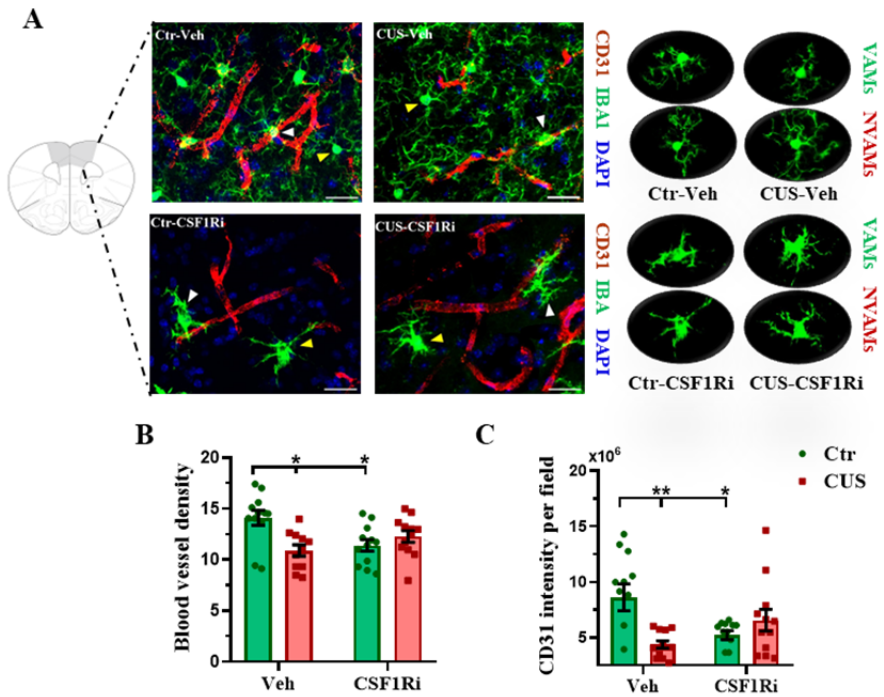

Figure 16. Chronic unpredictable stress (CUS) and CSF1R inhibitor (CSF1Ri) reduced CD31$^+$-blood vessels and differentially affected vessel-associated microglia/macrophages (VAMs) and nonvessel-associated microglia/macrophages (NVAMs) in mice. (**A**) Representative staining of CD31 and IBA1 in the prefrontal cortex (PFC) (scale bar = 10 µm). VAMs and NVAMs (indicated by white and yellow arrowheads, respectively) are shown with enlarged images; (**B**) Blood vessel density (e.g., vessel area/total area*100%) and (**C**) total CD31 intensity. Data are presented as mean ± standard error of mean; **p* < 0.05, ***p* < 0.01, ****p* < 0.001; two-way ANOVA with Bonferroni's correction; *n* = 3 mice/12 sections per group.

We further stained the PFC sections for CD31 and IBA1 by immunohistochemistry (**Fig. 16A)**. There were interactions between the CUS and CSF1Ri on blood vessel density ($F(1, 44) = 10.34$, $p < 0.01$) and total CD31 intensity ($F(1, 44) = 11.42$, $p < 0.01$). Both parameters were decreased by the CUS ($p < 0.05/0.001$) or CSF1Ri (both $p < 0.05$) compared to the Ctr-Veh, whereas no cumulative effect of CUS-CSF1Ri combined treatment existed, compared to the Ctr-Veh or single treatment (**Fig. 16B & 16C**). Hence, CD31 intensity reduction was due to decreased blood vessel density and CUS and CSF1Ri seemed not to facilitate each other on affecting angiogenesis.

5.3.2. CUS decreased microglial abundancy and Csf1r expression in the mouse hippocampus (Paper II)

We further validated CSF1Ri by quantifying microglia along with other glial populations, namely astrocytes and OPCs, in the HPC by flow cytometry. A hierarchical gating strategy is shown by representative dot plots in **Fig. 17A** and negative staining by isotype control antibodies is shown in **Fig. S4**.

Remarkably, there were interactions between CUS and CSF1Ri here on the percentage (%) of total hippocampal microglia ($F(1, 24) = 6.432$, $p < 0.05$) and Csf1r protein level ($F(1, 24) = 6.447$, $p < 0.05$). The CSF1Ri but not CUS affected the microglia % (CSF1Ri main effect: $F(1, 24) = 498.4$, $p < 0.001$) and Csf1r protein level (CSF1Ri main effect: $F(1, 24) = 109.0$, $p < 0.001$). The CUS, CSF1Ri, or CUS-CSF1Ri combination reduced the Csf1r level (due to loss of microglia and in line with RNA-seq/QPCR results, **Fig. 17B**) and the microglia% (**Fig. 17C**) compared to the Ctr-Veh ($p < 0.05/0.001/0.001$ for both parameters). Furthermore, measuring the MFI of Csf1r on each survived microglia, we observed its significant decrease induced by the CUS compared to the Ctr-Veh ($p < 0.01$; **Fig. S3E**), recapitulating our clinical data.

We also observed an additional interaction of the CUS and CSF1Ri on OPCs % ($F(1, 24) = 12.12$, $p < 0.01$). The CUS and CSF1Ri markedly affected the OPCs % (CUS main effect: $F(1, 24) = 5.292$, $p < 0.05$; CSF1Ri main effect: $F(1, 24) = 8.942$, $p < 0.01$). The CUS-CSF1Ri jointly increased the OPCs compared to the Ctr-Veh, CUS-Veh, or Ctr-CSF1Ri ($p < 0.01/0.001/0.01$), while single treatment did not affect the OPCs compared to the Ctr-Veh, indicating a boosting effect of the CUS-CSF1Ri combination on the OPCs compared to single treatments (**Fig. 17D**). Nevertheless, the CUS and CSF1Ri did not affect the abundancy of astrocytes (**Fig. 17E**).

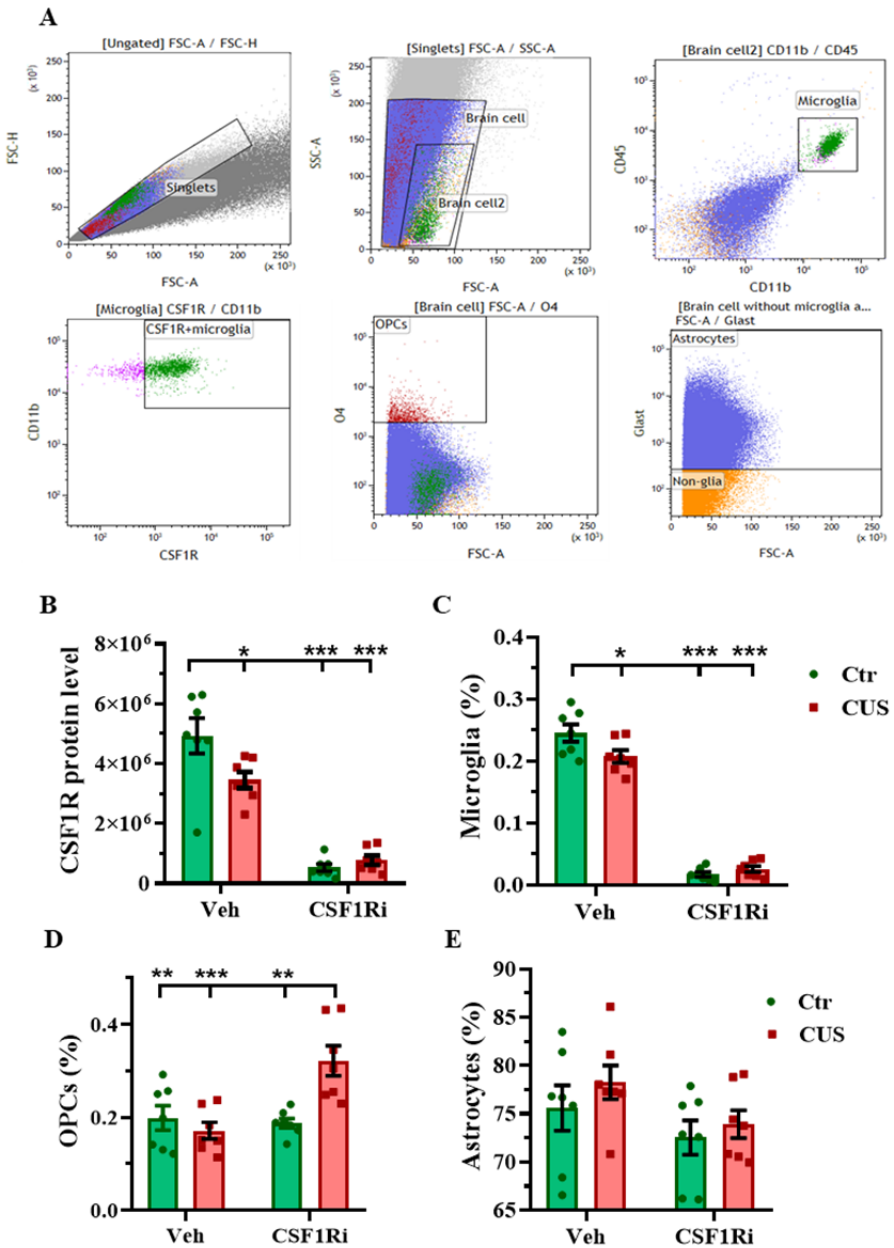

Figure 17. Chronic unpredictable stress (CUS) and CSF1R inhibitor (CSF1Ri) reduced microglia and colony stimulating factor 1 receptor (Csf1r) level in mice. (**A**) Representative flow cytometry dot plots showing gating strategy for hippocampal microglia, Csf1r^{+}-microglia, oligodendrocyte precursor cell (OPC)s, and astrocytes; (**B**) Csf1r protein level expressed by total microglia. (**C-E**) % of total microglia, OPCs, and astrocytes. Data are presented as mean ± standard error of mean; *$p < 0.05$, **$p < 0.01$, ***$p < 0.001$; two-way ANOVA with Bonferroni's correction; $n = 7$ per group.

5.3.3. CSF1Ri preferentially decreased juxta-vascular microglia/macrophages in the mouse brain (Paper II)

For $IBA1^+$-microglia/macrophages, we classified them into VAMs (e.g., juxta-vascular microglia/macrophages) and NVAMs (e.g., non-vessel associated microglia/macrophages) among the total microglia/macrophages (TMs). Although myeloid ablation by CSF1Ri has been abundantly used in the literature, to our knowledge, the only effect on total myeloid populations has been reported and very little is known about those microglia/macrophages that survive and are believed to repopulate the brain as microglial progenitor cells (Green et al., 2020; Zhan et al., 2020). We hence endeavored to characterize VAMs and NVAMs further.

Interactions between CUS and CSF1Ri on IBA1 intensities ($F(1, 44) = 4.571$, $p < 0.05$) and cell numbers ($F(1, 44) = 5.347$, $p < 0.05$) were found. The CUS and CSF1Ri obviously affected TMs (CUS main effect: $F(1, 44) = 22.29$, $p < 0.001$; CSF1Ri main effect: $F(1, 44) = 497.6$, $p < 0.001$) and microglia IBA1 intensities (CUS main effect: $F(1, 43) = 7.597$, $p < 0.01$; CSF1Ri main effect: $F(1, 44) = 25.12$, $p < 0.001$). The CUS, CSF1Ri, or CUS-CSF1Ri combination decreased the TMs-No. ($p < 0.05/0.001/0.001$; **Fig. 18A**) and total IBA1 intensity due to the loss of TMs ($p < 0.01/0.001/0.001$; **Fig. 18B**), compared to the Ctr-Veh.

Interestingly, interactions between the CUS and CSF1Ri existed on ratios of VAMs-No./TMs-No. ($F(1, 44) = 4.900$, $p < 0.05$) and IBA1 intensity in VAMs/TMs ($F(1, 44) = 6.108$, $p < 0.05$). CSF1Ri markedly changed the ratios of VAMs-No./TMs-No. (CSF1Ri main effect: $F(1, 44) = 7.992$, $p < 0.01$) and IBA1 intensity in VAMs/TM (CSF1Ri main effect: $F(1, 44) = 6.174$, $p < 0.05$). Both two parameters were dampened especially by the CSF1Ri ($p < 0.05/0.01$; **Fig. 18C & 18D**), compared to the Ctr-Veh. This implies a preferential elimination of the VAMs by the CSF1Ri, possibly due to the blood-route of drug delivery and/or the specific sensitivity of the VAMs. The CUS or CUS-CSF1Ri combination showed a similar suppressive effect as the CSF1Ri on the ratios of IBA1 intensity, compared to the Ctr-Veh (all $p < 0.05$; **Fig. 18D**). These results indicate that the CSF1Ri and CUS both dampen the VAMs more preferentially than the NAVMs.

For microglial morphometrics, interactions between the CUS and CSF1Ri on cell size ($F(1, 44) = 4.224$, $p < 0.05$) and branch size were found ($F(1, 44) = 13.91$, $p < 0.001$). The CSF1Ri markedly affected the microglia cell size ($F(1, 44) = 43.08$, $p < 0.001$) and branch size (CSF1Ri main effect: $F(1, 44) = 74.50$, $p < 0.001$). The CUS but not the other 3 conditions caused enlargement of both the cell and branch sizes in the NVAMs compared to the VAMs (both $p < 0.05$; **Fig. 18E & 18F**). Furthermore, regarding the VAMs + NVAMs together, the CUS induced enlargement of both the cell and branch sizes compared to the Ctr-Veh (both $p < 0.05$), whereas the CSF1Ri or CUS-CSF1Ri combination had opposite effects compared to the Ctr-Veh (all $p < 0.05$) (**Fig. 18E & 18F**). Cell soma size was grossly enlarged by the CSF1Ri compared to the Veh (CSF1Ri

main effect: F (1, 44) = 50.68, $p < 0.001$; **Fig. 18G**). These data overall demonstrate that the CSF1Ri preferentially eliminates the VAMs and de-ramifies both the VAMs and NVAMs, and unlike the NVAMs, the VAMs are resistant to CUS-induced ramification.

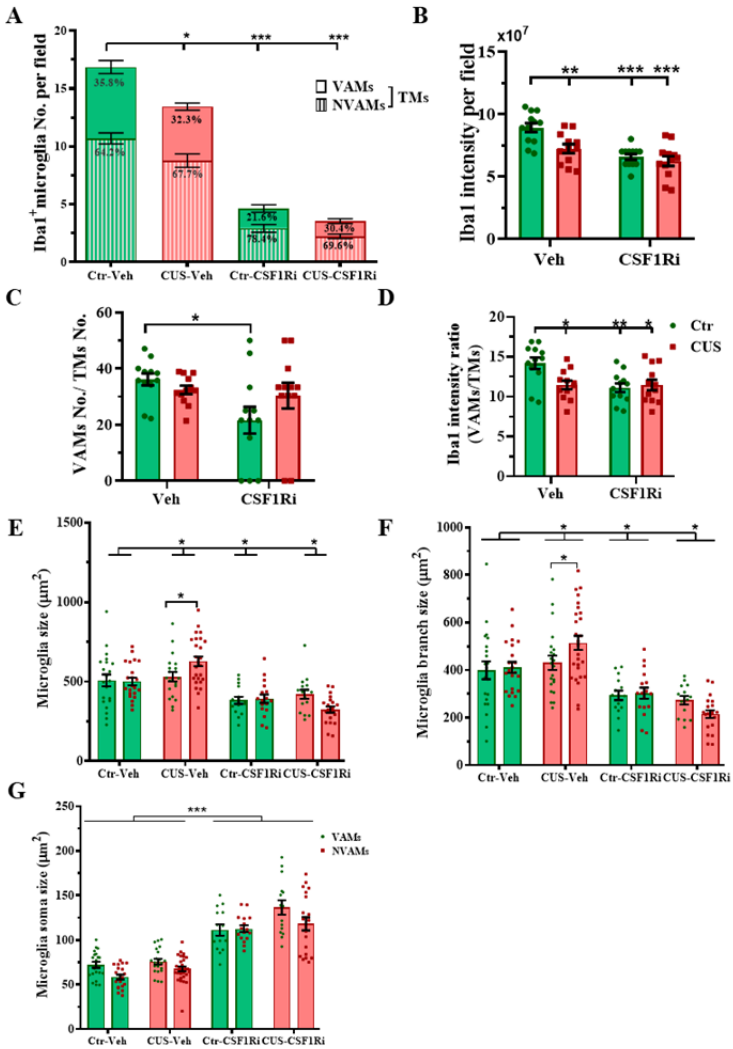

Figure 18. Chronic unpredictable stress (CUS) and CSF1R inhibitor (CSF1Ri) reduced CD31$^+$-blood vessels and differentially affected VAMs and NVAMs in mice. (**A**) Total microglia/macrophages (TMs)- number (No.) (including No. of both vessel-associated microglia/macrophages (VAMs) and nonvessel-associated microglia/macrophages (NVAMs)) and (**B**) total IBA1, (**C**) Ratios of VAMs-No./TMs-No. and (**D**) IBA1 intensity in VAMs/TMs. (**E**) Microglia cell size, (**F**) branch size, and (**G**) cell soma size. Data are presented as mean ± standard error of mean; *$p < 0.05$, **$p < 0.01$, ***$p < 0.001$; two-way ANOVA with Bonferroni's correction; n = 3 mice/12 sections per group.

5.3.4. Fatty acid metabolic genes were enriched in the mouse OB (Paper III)

To better understand the difference between OB and PFC, we studied the OB and PFC tissues by RNA-seq and identified 10723 DEGs including 5396 up-regulated and 5327 downregulated differentially expressed genes (DEGs) among the two groups **(Fig. 19**). GO-BP enrichment analysis of these DEGs showed overlapping pathways such as fatty acid metabolisms and cell adhesion (**Fig. 20A & 20B**). Apart from these, OB-enriched DEGs were involved in angiogenesis (**Fig. 20A**), while PFC-enriched DEGs in neurogenesis and endocytosis (**Fig. 20B**). The fatty acid metabolism-related DEGs were upregulated (dark red dots) while lipid metabolism-related DEGs were downregulated (dark blue dots) in the OB compared to the PFC (**Fig. 19**). Besides, angiogenesis regulating DEGs were also upregulated in the OB compared to the PFC (data not shown).

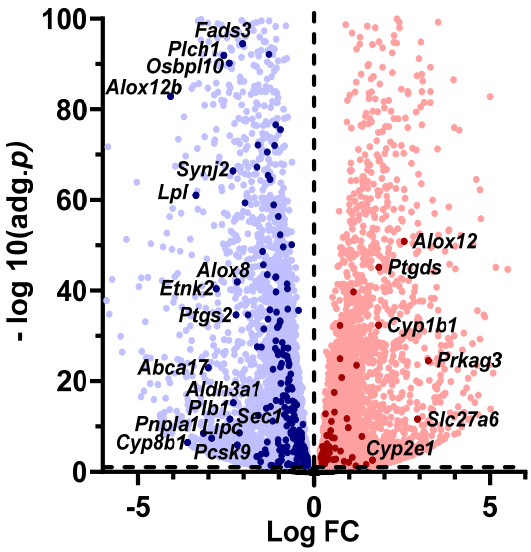

Figure 19. **Murine olfactory bulb (OB)-enriched differentially expressed gene (DEG)s are involved in fatty acid metabolism and angiogenesis.** A volcano plot of DEGs in the OB versus the prefrontal cortex (PFC), lipid metabolism DEGs with $|\log_2 FC| > 2$ are in dark blue dots and fatty acid metabolism DEGs with $|\log_2 FC| > 1$ are in dark red dots with gene symbols. $N = 7$ per group.

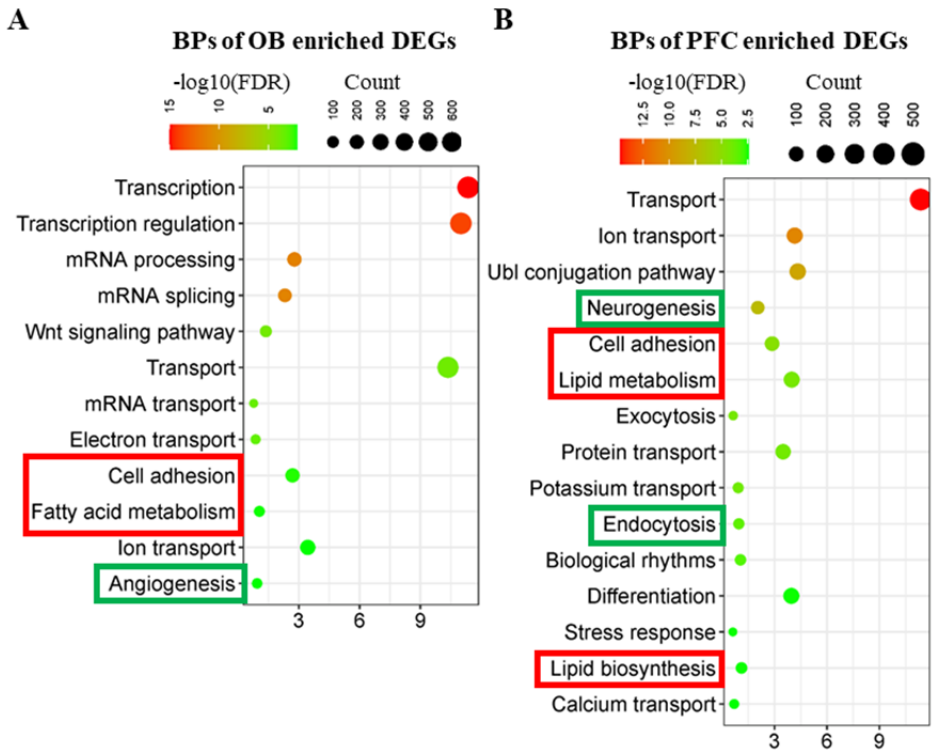

Figure 20. Murine olfactory bulb (OB)-enriched differentially expressed gene (DEG)s are involved in fatty acid metabolism and angiogenesis. Gene ontology biological pathway (GO-BP) enrichment analysis shows top-ranked pathways of OB-enriched DEGs (**A**) and prefrontal cortex (PFC)-enriched DEGs (**B**). $N = 7$ per group.

5.3.5. Lipid metabolic genes and angiogenic genes were increased by CSF1Ri treatment in the mouse OB (Paper III)

To understand the effects of CSF1Ri on OB and PFC DEGs, we studied RNA-seq data after CSF1Ri treatment for 2 weeks and identified 480 DEGs including 305 upregulated and 175 downregulated DEGs among the four groups (**Fig. 21A**). Main GO-BP pathways for these DEGs also involved fatty acid and lipid metabolisms, angiogenesis, and cell adhesion (**Fig. 21B**). Almost all DEGs involved in the fatty acid (red dots) and lipid (dark red dots) metabolisms as well as angiogenesis (green dots) were upregulated after CSF1Ri treatment in the OB, while they were downregulated in the PFC (**Fig. 21A & 21C**). These results demonstrate that lipid/fatty acid metabolism and angiogenesis processes after CSF1Ri treatment were more active in the OB, in contrast to the PFC.

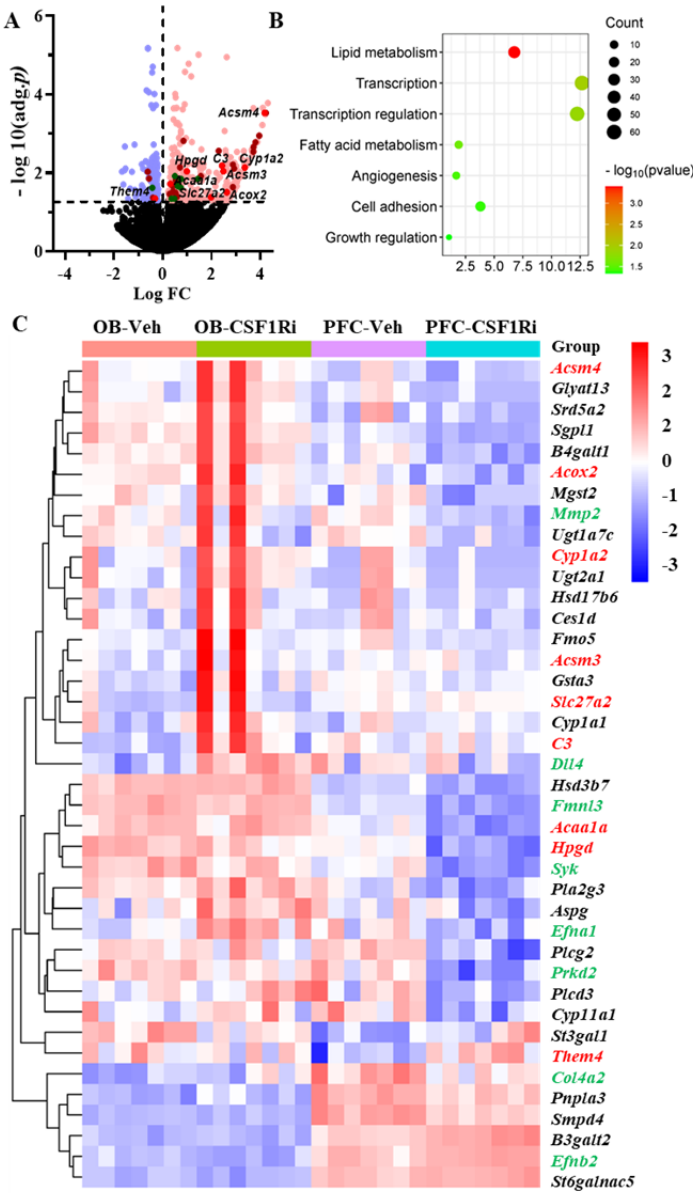

Figure 21. The murine olfactory bulb (OB) showed different responses to CSF1R inhibitor (CSF1Ri) than the prefrontal cortex (PFC) in lipid metabolism and angiogenesis. (**A**) A volcano plot of all DEGs among four groups: (1) OB-vehicle (Veh), (2) OB-CSF1Ri, (3) PFC-Veh, and (4) PFC-CSF1Ri. Lipid metabolism-related DEGs are in dark red dots, fatty acid metabolism-related differentially expressed gene (DEG)s are in red dots, and angiogenesis-regulating DEGs are in green dots with gene symbols. (**B**) gene ontology biological pathway (GO-BP) enrichment analysis shows pathways of all DEGs. (**C**) A heatmap of DEGs involved in lipid (or fatty acid, colored in red) metabolism and angiogenesis (colored in green). $N = 7$ per group.

5.3.6. CD206$^+$ and Vglut2$^+$ microglia were enriched in the mouse OB (Paper III)

To quantitate myeloid cells in different brain regions, we analyzed macrophages, microglia, and CD206$^+$/Vglut2$^+$ microglia by flow cytometry, the gating strategy is shown in **Fig. 22** and negative staining by isotype control antibodies is shown in **Fig. S5**.

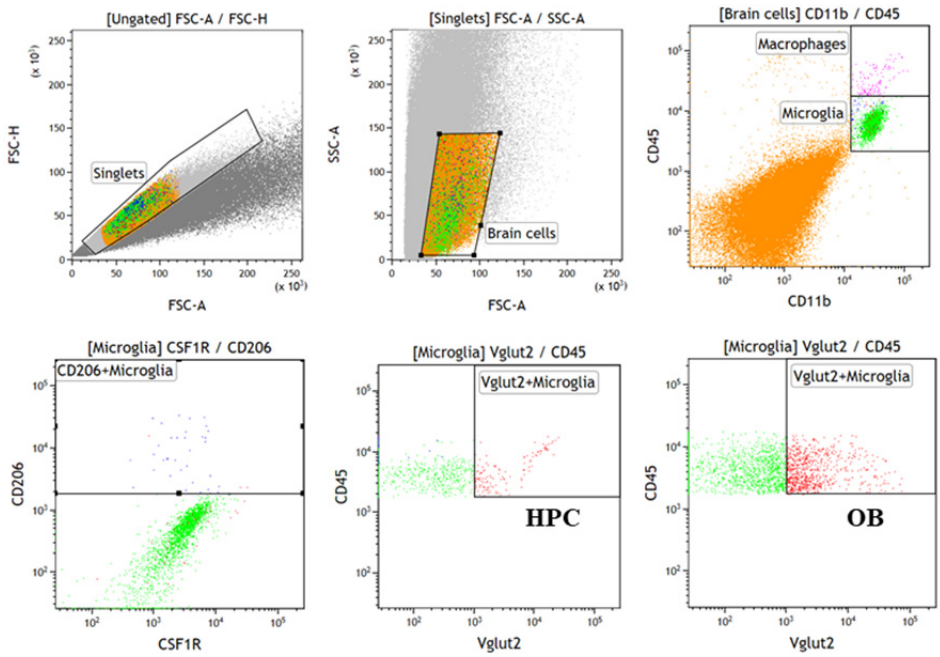

Figure 22. Representative flow cytometry dot plots showing gating strategy for murine microglia, macrophages, CD206$^+$microglia, Vglut2$^+$microglia.

We observed that the HPC (all $p < 0.001$), OB (all $p < 0.001$), and somatosensory cortex (SSC) (all $p < 0.01$) had higher percents of microglia than the cerebellum (CBM) and thalamus (TH) (**Fig. 23A**). The OB had a higher percent of macrophages than the HPC, SSC, CBM, and TH (all $p < 0.001$) (**Fig. 23B**). The OB expressed more CD206$^+$ microglia than the HPC, SSC, CBM and TH (all $p < 0.001$) (**Fig. 23C**). The Vglut2$^+$ microglia were more abundant in the OB than the HPC and SSC (all $p < 0.05$) (**Fig. 23D**). These results indicate that the OB has more M2-like microglia and OB microglia engulf more presynaptic Vglut2 than those in the other regions.

To confirm if the OB displayed more CD206$^+$ microglia, we use IHC to stain the brain tissues with IBA1 and CD206, as shown in **Fig 23E**. We found that the HPC, OB, and cortex (CTX) did not show any difference in the abundancy

of IBA1^{+} microglia (**Fig. 23F**), while the OB and HPC expressed higher amount of CD206^{+}IBA1^{+} microglia (**Fig. 23G**).

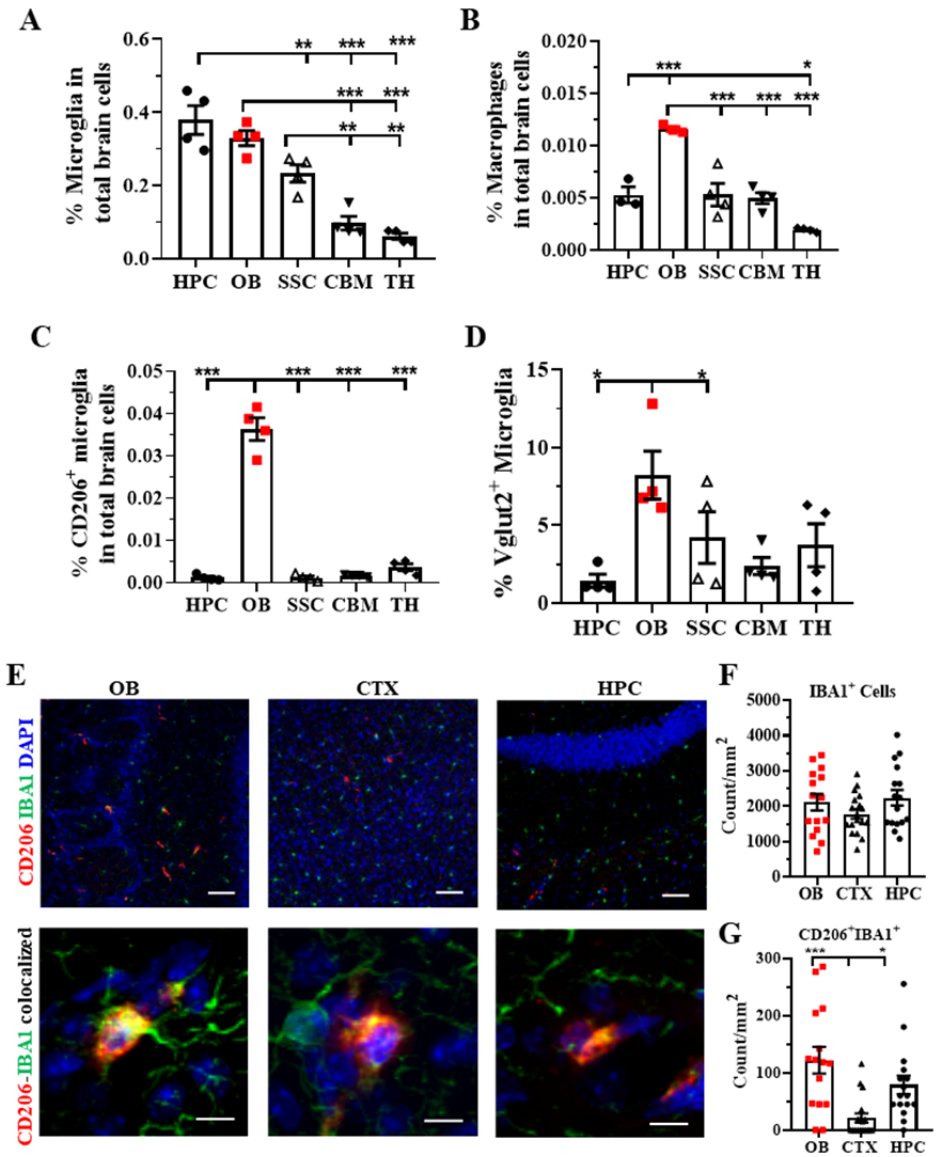

Figure 23. The murine olfactory bulb (OB) has higher abundancies of CD206^{+} and Vglut2^{+} microglia, and macrophages than the other brain regions. (**A**) microglia %, (**B**) macrophages %, (**C**) CD206^{+} microglia, (**D**) Vglut2^{+} microglia %; (**E**) Representative staining of IBA1and CD206 in the OB, CTX, HPC; (**F**) All IBA1^{+} microglia; (**G**) CD206^{+}IBA1^{+} microglia (scale bar = 10 µm). Data are presented as mean ± standard error of mean; *p < 0.05, **p < 0.01, ***p < 0.001; one-way ANOVA with Tukey's correction; n = 4 per group.

In studying myeloid response to CSF1Ri, we observed interactions between brain region and CSF1Ri on microglia % ($F(1, 24) = 5.615$, $p < 0.05$), $CD206^+$ microglia % ($F(1, 24) = 147.3$, $p < 0.001$) and $Vglut2^+$ microglia % ($F(1, 24) = 9.793$, $p < 0.01$). Both brain region and CSF1Ri significantly affected the percentage of microglia (Region main effect: $F(1, 24) = 18.99$, $p < 0.001$; CSF1Ri main effect: $F(1, 24) = 521.4$, $p < 0.001$) and $CD206^+$ microglia (Region main effect: $F(1, 24) = 206.7$, $p < 0.001$; CSF1Ri main effect: $F(1, 24) = 160.3$, $p < 0.001$), as well as $Vglut2^+$ microglia (Region main effect: $F(1, 24) = 87.38$, $p < 0.001$; CSF1Ri main effect: $F(1, 24) = 19.76$, $p < 0.001$). OB-Veh had higher microglia than HPC-Veh/CSF1Ri and OB-CSF1Ri (all $p < 0.001$), and HPC-Veh displayed more microglia than Abl groups (both $p < 0.001$) (**Fig. 24A**). OB-Veh showed higher $CD206^+$ microglia % than HPC-Veh/CSF1Ri and OB-CSF1Ri (all $p < 0.001$) (**Fig. 24C**). OB-Veh showed higher $Vglut2^+$ microglia % than HPC-Veh/CSF1Ri ($p < 0.05/0.001$) (**Fig. 24D**). For macrophages % in total brain cells, the brain region significantly affected it ($F(1, 24) = 77.57$, $p < 0.001$), while the OB had higher macrophages % than the HPC both in Veh and CSF1Ri (**Fig. 24B**). Furthermore, CSF1Ri displayed a trend of decreasing it but without significance. The results demonstrate that the OB had more microglia, $CD206^+$ microglia, and $Vglut2^+$ microglia than the HPC. CSF1Ri ablated microglia both in the OB and HPC while deleting $CD206^+$ microglia in the OB but not in the HPC, indicating the anti-inflammatory subtype microglia is more sensitive in the OB than the HPC. The remaining microglia exhibited more Vglut2 pruning ability both in the OB and the HPC.

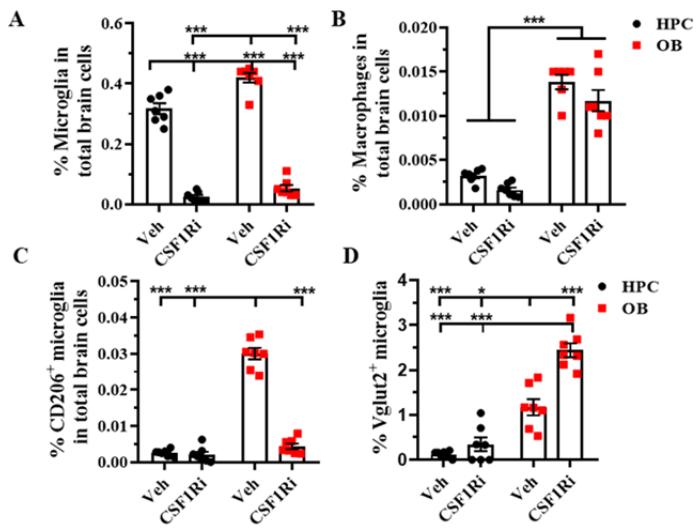

Figure 24. Mouse olfactory bulb (OB) and hippocampus (HPC) microglia respond to CSF1R inhibitor (CSF1Ri) treatment. (**A**) microglia %, (**B**) macrophages %, (**C**) $CD206^+$ microglia %, (**D**) $Vglut2^+$ microglia %. Data are presented as mean ± standard error of mean; $*p < 0.05$, $***p < 0.001$; two-way ANOVA with Tukey's correction; $n = 7$ per group.

5.3.7. CD206^{+}IBA1^{+} microglia located more at the blood vessels (Paper III)

We further characterized myeloid cells using CD206 and IBA1 antibodies in the adult cerebral cortex by immunohistochemistry. As CD206 is a perivascular macrophage marker, we also studied the relationship of CD206^{+}IBA1^{+} microglia and IBA1^{+} microglia with blood vessels marked by CD31 in the cortex (**Fig. 25A-C**). We observed CD206^{+}IBA1^{+} cells （$p < 0.001$, **Fig. 25B**） were notably co-stained with CD31, while IBA1^{+} cells were mostly non-CD31-associated ($p < 0.001$, **Fig. 25C**), demonstrating that CD206^{+}IBA1^{+} microglia located more at the brain blood vessels.

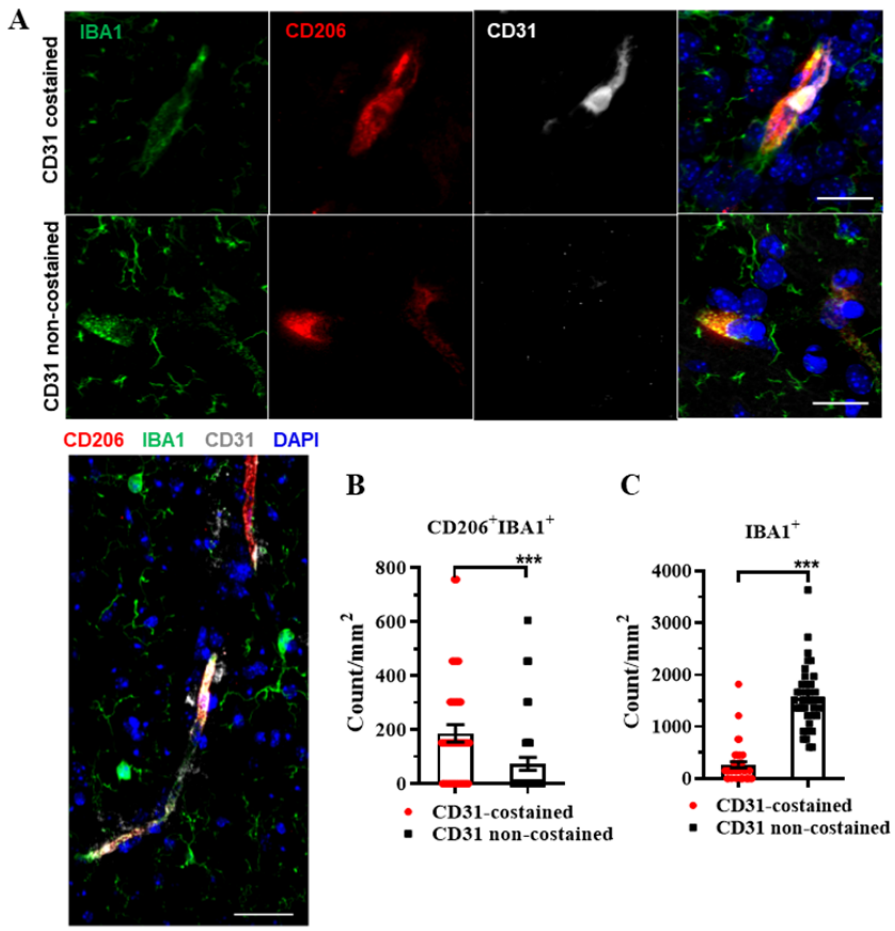

Figure 25. CD206^{+}IBA1^{+} cells are associated with CD31 in the murine cerebral cortex. (**A**) Representative images of the CD206^{+}IBA1^{+} cells and CD31 colocalization, quantification of CD206^{+}IBA1^{+} cells (**B**) and IBA1^{+} cells (**C**) Microglia costained or non-costained with CD31 in the parenchyma of the adult cortex. Data are presented as mean ± standard error of mean; Mann Whitney U-test. ***$p < 0.001$; $n = 4$ per group.

5.3.8. OBX-induced dysregulation of phospholipid metabolic pathways was rectified in *fat-1* mice (Paper IV)

To corroborate lipid metabolism, we measured lipid metabolites in the serum of *fat-1* mice with the OBX model by LC/MS (see **Fig. 12A**). Detected metabolic features from different experimental groups were classified and separated by PCA and OPLS-DA for multivariate data analyses. Robustness of analytical procedures was checked by inspecting the grouping of QC samples in score scatter plots. Good clustering of the QC samples was observed in the PCA (**Fig. 26A**), indicating stability during the analyses.

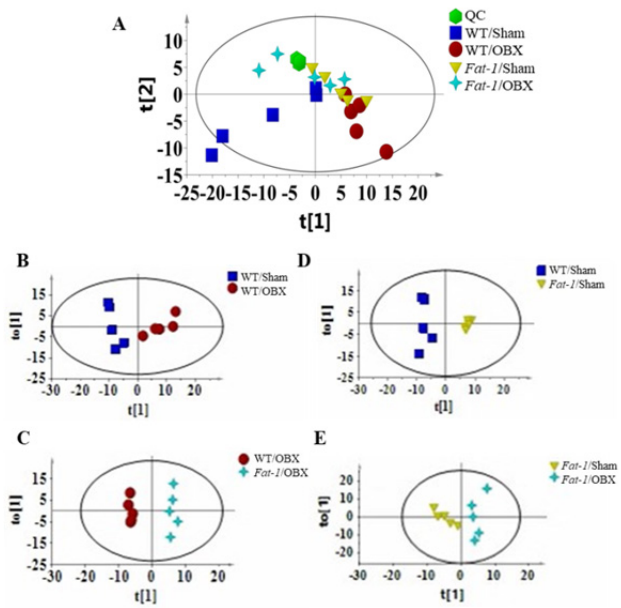

Figure 26. Principal component analysis (PCA) score plots of serum metabolites among wild type (WT)/Sham, WT/olfactory bulbectomy (OBX), Fat-1/Sham, and Fat-1/OBX mouse groups. (**A**) Samples from different groups were scattered into different regions, except the Fat-1/Sham and Fat-1/OBX groups. Score scatter plots of orthogonal projections to latent structures-discriminate analysis (OPLS-DA) (**B-E**) analyses with all metabolites. OPLS-DA showed that the samples from different groups were scattered into different regions. Fat-1/Sham (▼), WT/Sham (■), WT/OBX (●), Fat-1/OBX (✦), the quality control (QC) samples (⬣). *N* = 5 per group.

The OPLS-DA showed a clear separation between different groups (**Fig. 26B-26E**). The OPLS-DA revealed that 55 of these metabolites (**Fig. S6A**) were different between WT/Sham and WT/OBX mice, 44 between Fat-1/Sham and Fat-1/OBX mice (**Fig. S6D**), 74 between WT/OBX and Fat-1/OBX mice (**Fig. S6B**), and 70 between WT/Sham and Fat-1/Sham mice (**Fig. S6C**). The total altogether 145 endogenous metabolites in the serum changed among the four animal groups (**Fig. 27**).

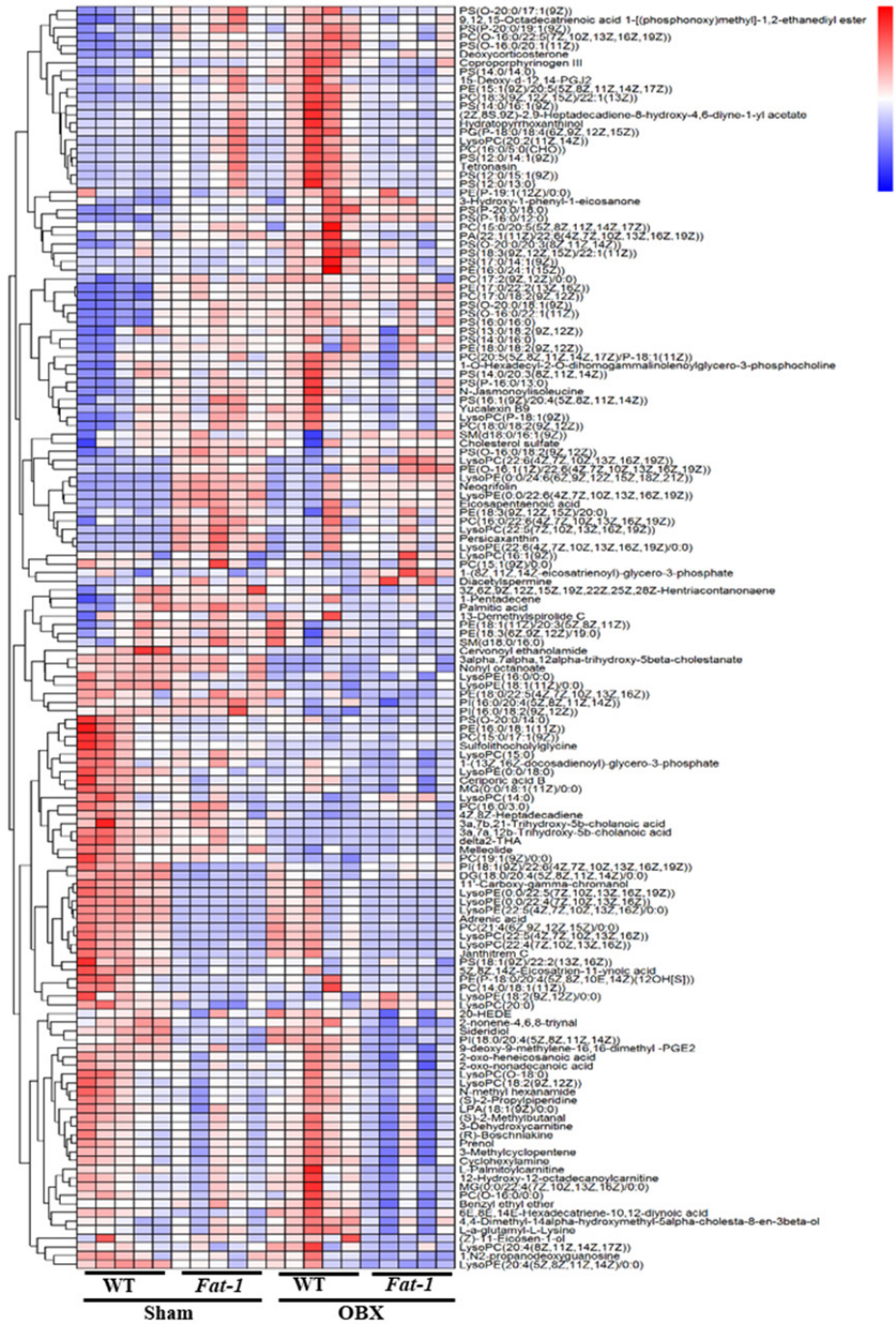

Figure 27. Heat map of serum lipid metabolites produced in wild type (WT)/Sham, WT/olfactory bulbectomy (OBX), Fat-1/Sham, and Fat-1/OBX mice. *N* = 5 per group.

Venn diagrams indicate that the most unique change in serum metabolic feature came from a comparison of the WT mice with the *fat-1* mice after the OBX, with 28 non-overlapping metabolites detected (**Fig. 28A**, green). By contrast, the least striking change was found within the WT between the Sham and OBX groups, with only 6 unique metabolites (**Fig. 28A,** purple). Furthermore, among the 26 overlapping metabolites detected both in the WT/OBX *vs* WT/Sham groups and the WT/OBX *vs* Fat-1/OBX groups, 10 metabolites were also involved in the WT/Sham *vs* Fat-1/Sham groups (**Fig. 28A**, yellow). Finally, the remaining 16 chemicals were changed by the OBX in the WT, while 15 were unchanged in *fat-1* mice. Changes of these metabolites were summarized in **Table 6**. Namely, phospholipids (phosphoserine, phosphatidylcholine, phosphatidylethanolamine, phosphatidylglycerol), L-a-glutamyl-L-lysine, hydratopyrrhoxanthinol, benzyl 3-(((benzyloxy)carbonyl)amino)acrylate, tetronasin, and Cop were the outstanding ones. Apart from a decreased level of the phosphatidylcholine (19:1(9Z)/0:0), levels of the other endogenous phospholipids were all elevated after the OBX in the WT. By contrast, all these changes were normalized in the OBX-operated *fat-1* mice.

Table 6. Serum lipid metabolites changed by olfactory bulbectomy (OBX) in wild type (WT)s but not *fat-1* mice.

Metabolites	WT/OBX *vs* WT/Sham			WT/OBX vs Fat-1/OBX		
	VIP	FC	*p*	VIP	FC	*p*
Phosphoserine (18:1(9Z)/22:2(13Z,16Z))	2.74	6.41	0.01	2.99	0.20	0.01
phosphatidylglycerol (P-18:0/18:4(6Z,9Z,12Z,15Z))	2.41	21.60	0.05	3.18	0.03	0.05
phosphoserine (12:0/15:1(9Z))	1.94	8.42	0.01	2.24	0.30	0.04
phosphatidylethanolamine (P-19:1(12Z)/0:0)	1.96	1.67	0.02	2.07	0.69	0.05
phosphoserine (12:0/14:1(9Z))	1.38	11.08	0.01	1.67	0.21	0.03
phosphatidylcholine (19:1(9Z)/0:0)	1.39	0.74	0.00	2.43	1.13	0.01
phosphoserine (12:0/13:0)	1.62	11.85	0.03	2.07	0.16	0.04
Phosphatidylcholine (20:5(5Z, 8Z,11Z,14Z,17Z)/P-18:1(11Z))	3.24	2.31	0.01	30.22	0.39	0.01
phosphoserine (14:0/16:1(9Z))	1.12	8.99	0.02	1.42	0.19	0.03
phosphatidylcholine (18:3(9Z,12Z,15Z)/22:1(13Z))	1.14	14.64	0.00	1.15	0.31	0.01
L-a-glutamyl-L-Lysine	1.23	1.48	0.00	1.76	0.59	0.01
Hydratopyrrhoxanthinol	1.17	16.83	0.04	1.69	0.10	0.04
Benzyl 3-(((benzyloxycarbonyl) amino)acrylate	1.27	3.76	0.03	4.64	0.20	0.02
Coproporphyrinogen III	1.33	4.08	0.01	1.47	0.31	0.04
Tetronasin	1.05	7.89	0.01	1.09	0.30	0.03

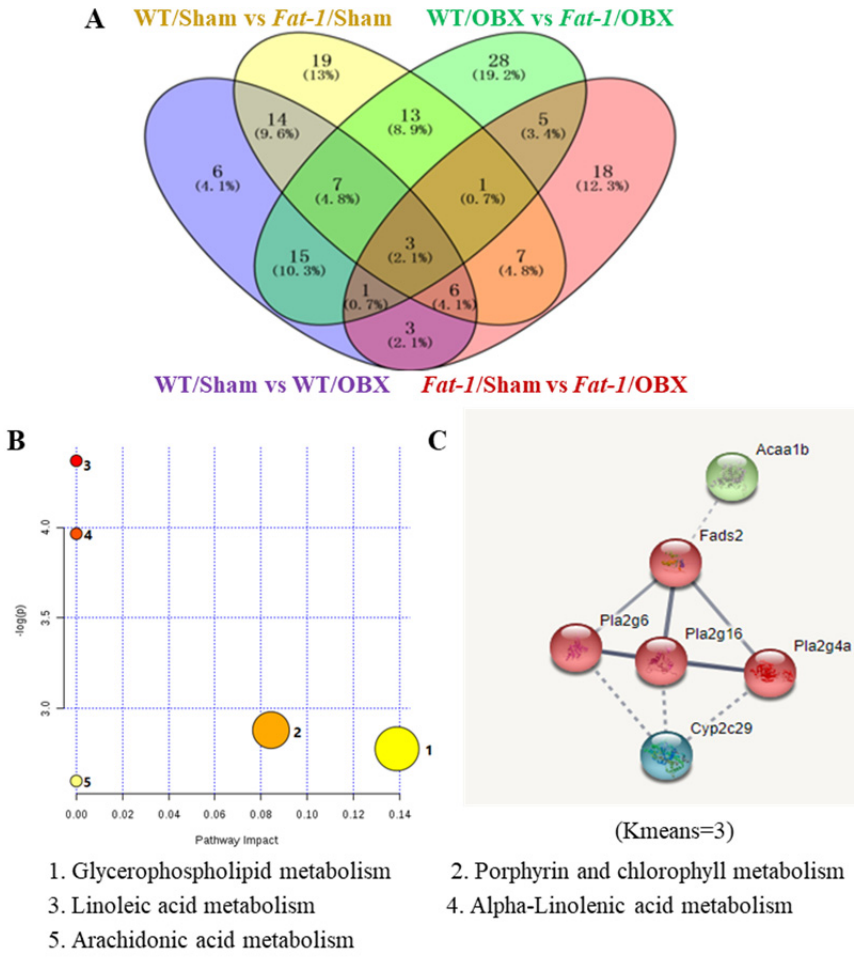

Figure 28. Serum lipid metabolites changed by olfactory bulbectomy (OBX) in wild type (WT) and *Fat-1* mice and related anti-inflammatory lipid genes. (**A**) A Venn diagram summarizes different lipid metabolites in each pair-wise comparison among WT/Sham, WT/OBX, Fat-1/Sham, and Fat-1/OBX mouse groups. Among them, 15 (10.3%) phospholipid metabolites were elevated in WT/OBX mice but normalized in Fat-1/OBX mice (see also **Table 6**). (**B**) Kyoto encyclopaedia of genes and genomes (KEGG) pathway analysis showed lipid metabolic pathways in which these 15 metabolites were involved, and (**C**) the involved anti-inflammatory lipid genes in these pathways.

Subsequently, five major metabolic pathways were found by KEGG analysis: (1) Glycerophospholipid metabolism, (2) Porphyrin and chlorophyll metabolism, (3) Linoleic acid metabolism, (4) Alpha-Linolenic acid metabolism, and (5) Arachidonic acid metabolism (**Fig. 28B**). All genes involved in the five pathways were further analyzed for functional clustering and protein-protein interactions by String v11 (**Fig. 28C**). Genes involved in inflammatory path-

ways such as fatty acid desaturase (*Fads)*, phospholipase A2 group *(Pla2g)4a*, *Pla2g6*, *Pla2g16*, *Cyp2c29*, and *Acaa1b*, as well as pro-inflammatory cytokines were chosen for validation.

5.3.9. OBX-induced pro-inflammatory cytokines were dampened in *fat-1* mice (Paper IV)

Next, we used qPCR to explore the pro-inflammatory cytokines in the HPC among four groups of mice. An interaction between OBX and *fat-1* gene was significant on mRNA expressions of *Itgam* (*CD11b*) ($F(1, 16) = 5.68$, $p < 0.05$), *Tnf* ($F(1, 16) = 5.491$, $p < 0.05$) and *Il6* ($F(1, 16) = 26.06$, $p < 0.001$). The OBX significantly affected the expressions of *CD11b* (OBX main effect: $F(1, 16) = 4.31$, $p < 0.05$) and *Tnf* (OBX main effect: $F(1, 16) = 10.67$, $p < 0.01$). Moreover, both the OBX and *fat-1* gene significantly affected the mRNA expression of *Il6* (OBX main effect: $F(1, 16) = 10.20$, $p < 0.01$, *fat-1* main effect: $F(1, 16) = 6.673$, $p < 0.05$). These three genes were significant increased ($p < 0.05$, 0.01, 0.01, respectively) in the OBX group compared to the control Sham group in WT mice, which were significantly attenuated in *fat-1* mice ($p < 0.05/0.05/0.01$, respectively (**Fig. 29A & 29B, 29D**). After the OBX, the *fat-1* but not WT mice exhibited a decrease in *Il1b* ($p < 0.05$) (**Fig. 29C**).

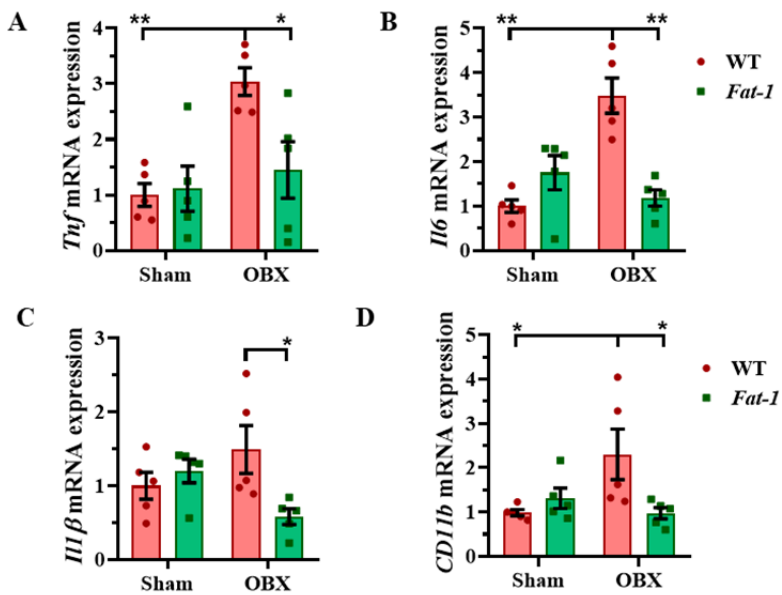

Figure 29. Olfactory bulbectomy (OBX)-induced microglial activation and pro-inflammatory cytokines were attenuated in *fat-1* mice. Expressions of *tumor necrosis factor* (*Tnf)* (**A**), *interleukin* (*Il)6* (**B**), *Il1β* (**C**), and *CD11b* (**D**) mRNAs in the hippocampus (HPC) are shown. Data are presented as mean ± standard error of mean; $*p < 0.05$, $**p < 0.01$; two-way ANOVA with Tukey's correction; $n = 5$ per group.

5.3.10. Anti-inflammatory lipid metabolic genes were highly expressed in *fat-1* mice (Paper IV)

No significant interaction existed between OBX and *fat-1* gene. However, the *fat-1* gene affected mRNA expressions of hippocampal *Fads* (*fat-1* main effect: F (1, 16) = 29.69, $p < 0.001$), (*Pla2g6)* (*fat-1* main effect: F (1, 16) = 13.60, $p < 0.01$, and Krüppel-like transcription factor- (*Klf)2* (*fat-1* main effect: F (1, 16) = 29.48, $p < 0.001$). The *Fads* and *Klf2* mRNA levels were both higher in Sham (both $p < 0.05$) and OBX groups (both $p < 0.01$, **Fig. 30A & 30C**) in *fat-1* mice compared with WT mice. In parallel, the OBX enhanced the *Pla2g6* expression ($p < 0.01$) (**Fig. 30B**) in the *fat-1* mice compared to the WT mice. There were no significant differences of *Pla2g4a* and *Cyp2c29* gene expression between the *fat-1* and WT mice in neither the OBX nor the Sham group (**Fig. S7**).

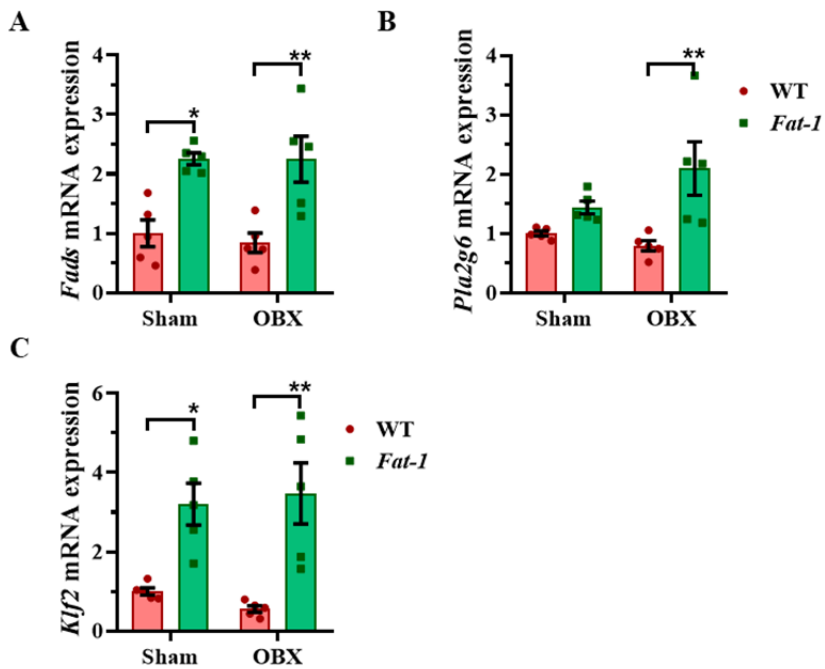

Figure 30. *Fat-1* mice had high anti-inflammatory lipid genes expression than WT mice. Expressions of *fatty acid desaturase (Fads)* (**A**), *phospholipase A2 group* (*Pla2g)6* (**B**), and *Krüppel-like transcription factor* (*Klf)2* (**C**) mRNAs in the hippocampus (HPC). Data are presented as mean ± standard error of mean; *$p < 0.05$, **$p < 0.01$; two-way ANOVA with Tukey's correction; $n = 5$ per group.

5.3.11. Lipid metabolite coproporphyrinogen III (Cop) enhanced pro-inflammatory response in BV2 microglia cell line (Paper IV)

Cop was elevated in WT after OBX, decreased in Fat-1/OBX mice (see **Fig. 27**) and was positively associated with hyperactivity behavior ($r = 0.524$, $p = 0.018$) (**Fig. 31A**). We used the Cop to treatment BV2 microglia cell line and found that cell viability was decreased after the Cop treatment (1 and 10 μM) for 24 h (**Fig. 31B**), while secretions of pro-inflammatory cytokines IFN-γ (**Fig. 31D**) and IL-1β (**Fig. 31E**) at protein levels, as well as NO (**Fig. 31C**), were remarkably increased when compared with control groups.

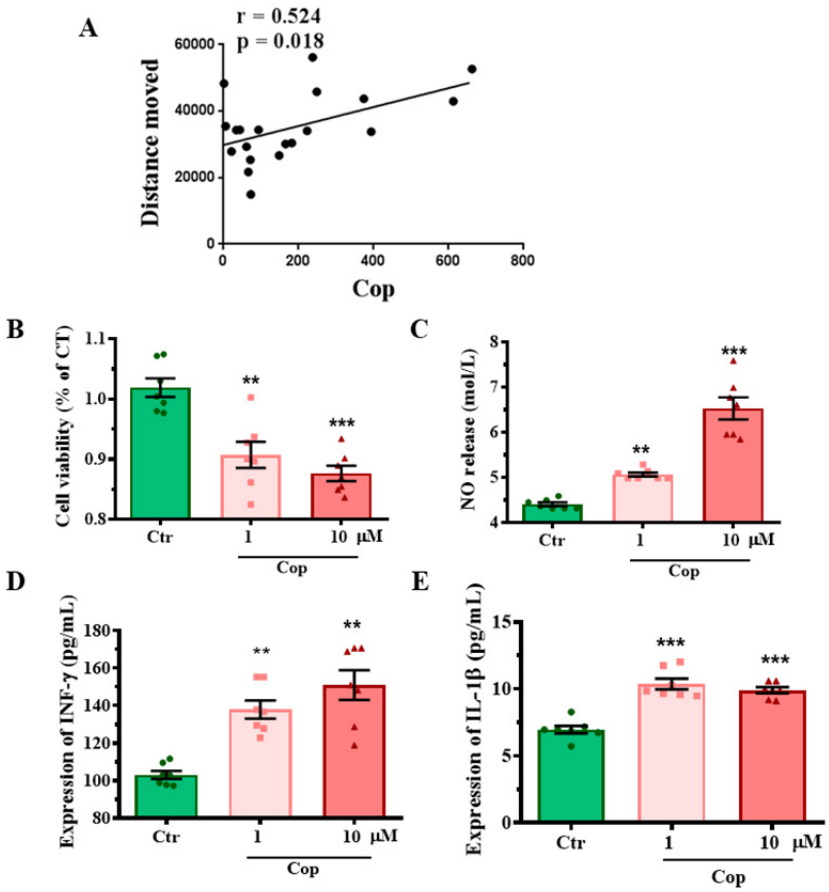

Figure 31. Coproporphyrinogen III (Cop) enhanced pro-inflammatory cytokines in BV2 microglia. (**A**) Cop was correlated with the total travel distance of mice in the open field; (**B**) Cell viability was decreased by Cop treatments; (**C**) Cop enhanced the release of nitric oxide (NO) from BV2 compared with control (Ctr), as well as interferon (IFN)-γ (**D**) and interleukin (IL)-1β (**E**) (both 1 and 10 μM). Data are presented as mean ± standard error of mean; $^{**}p < 0.05$, $^{**}p < 0.01$, $^{***}p < 0.001$; one-way ANOVA with Tukey's correction; $n = 7$ per group.

6. DISCUSSION

6.1. Stress-induced neuroimmune changes in schizophrenia (Papers I and II)

We previously found that cortical and cognitive deficits were associated with enlargement of the choroid plexus – an important cerebral neuroimmune portal – in schizophrenia patients (Zhou et al., 2020; Huang et al., 2022). Here, we observed that FES patients showed cortical thinning, cognitive impairment and higher stress perception, and PSS score was positively correlated with PANSS score. Furthermore, we found a decreased proportion of nonclassical monocytes and monocyte-related transcriptomic changes in the FES patients, including downregulated *PECAM1* and *CSF1R* and upregulated *IFITM* family members. Moreover, we discovered that monocyte-enriched genes, especially for nonclassical monocytes, were negatively associated with cerebral cortical thickness/volume as well as stress perception and cognition in HCs but not the FES patients. Nevertheless, the *CSF1R* fully moderated negative association of the superior frontal gyrus with stress perception in the HCs. Hence, we provided the first evidence that altered functions of monocytic subset and its effector receptors, such as the CSF1R, may underlie the pathophysiology of schizophrenia at early stage.

We and others have reported earlier that schizophrenia patients have monocytic dysfunctions, such as augmented monocyte counts and monocytic subcellular organelles (including the nucleolus, mitochondria, and lysosomes) (Uranova et al., 2017) as well as inflammatory fingerprints (Chen et al., 2019). However, these studies did not consider monocytes as a highly heterogeneous population that may have complicated roles in the disease onset and development of schizophrenia. Nonclassical monocytes play an important role in maintaining vascular homeostasis and are generally viewed as an anti-inflammatory subtype (Narasimhan et al., 2019). In support, monocytes and monocyte-derived microglia-like cells have been shown to promote blood vascular repair after brain ischemic injury (Mastorakos et al., 2021) or stress (Lehmann et al., 2022). For instance, a recent study reported that infiltrating monocytes instructed microglia, especially $VEGFA^{+}$ repair-associated microglia which had proliferative and proangiogenic properties, to repair injury-induced brain vasculature damage and promote cognitive recovery through monocyte-derived IL-6 (Choi et al., 2023).

Notably, we also discovered downregulation of the *PECAM1* and *CSF1R* genes in the FES patients, indicating cerebral vascular pathologies in these patients, possibly due to chronic low-grade systemic inflammation (Nguyen et al., 2018) (see also section 6.3). Our finding of the lower *CSF1R* mRNA and protein in the FES patients is in line with several previous studies (Zhang et al., 2020; Shimamoto-Mitsuyama et al., 2021). As cerebrovascular permeability is known to be compromised in psychiatric disorders (Pollak et al., 2018; Morris

et al., 2020), vascular damage may call for recruitment of circulating nonclassical monocytes into the brain, thereby resulting in nonclassical monocytopenia, along with altered mono-DEGs involved in leukocyte migration as we also found in FES patients.

Unexclusively, it may also be so that a progressive transition from classical to nonclassical monocytes may be disturbed in these patients, due to perhaps premature immune senescence or inflammaging, a phenomenon of the coexistence of adaptive and innate immune deficiencies together with increased autoimmunity and myelopoiesis during aging (Salminen, 2020). Indeed, nonclassical monocytes in a pro-inflammatory state after stimulation were found to attribute to immune senescence in a previous study (Ong et al., 2018). As already mentioned above, signs of cellular senescence in monocytes, such as increases in the area and number of lysosomes, were observed in schizophrenia patients (Uranova et al., 2017). Furthermore, lipid-inflammatory abnormality, a typical biomarker for inflammaging, was reported in the circulating blood (Campeau et al., 2022) and found to be a predictor of worse negative symptoms (Goldsmith et al., 2021) of schizophrenia patients.

Another recent report also found more severe cognitive impairments in a subset of mentally ill individuals with a high level of innate immune dysregulations (Sæther et al., 2023). Corroboratively, we found that pro-inflammatory nonclassical monocytic genes, such as *IFITM3*, encoding a late endosomal/lysosomal protein (Spence et al., 2019), were most significantly upregulated in the FES patients. Earlier studies have also shown upregulation of IFITM2/3 in the blood and postmortem brains of schizophrenia patients, especially in the PFC, HPC and cerebral cortical blood vessels (Siegel et al., 2014; Lanz et al., 2019). Meanwhile, two other most significantly down-regulated genes in our study were myeloid alarmin-related *S100A8* and *S100A9*, which by forming a heterodimer (called calprotectin) were found to act as a TLR4 ligand (Ehrchen et al., 2009). Previous studies have reported increased *S100A8/9* gene expression in peripheral blood cells and brain tissues of individuals with schizophrenia, however (Gandal et al., 2018; Gardiner et al., 2013; Lanz et al., 2019). The inconsistency with our results is possibly due to the disease chronicity and antipsychotic medications in those studies.

Taken together, the above findings postulate a provocative concept that schizophrenia may be a monocytic subset-engaged inflammaging disorder.

We previously reported that cortical thickness and cognitive impairments were impacted by allostatic load – a composite index of stress maladaptation, including immune factors such as cytokines and C-reactive protein (Zhou et al., 2021). We here found that limbic-associated cerebral cortical structures, including a PFC subarea – the superior frontal gyrus as well as the HPC-connected parahippocampal and superior temporal gyri, were smaller in FES patients than HCs. More interestingly, we found that the *CSF1R* interacted with these brain regions and moderated their negative associations with PSS in HCs but not FES patients. Our results suggest that the CSF1R may have a protective

effect on stress response in the HCs via modulating cortical limbic structures, which is lost in the FES patients.

Growing evidence has shown that impairments in social cognition (emotion processing, mentalizing, and social perception) are core features of schizophrenia (Green et al., 2019), as occurred in our FES patients as well. Schizophrenia patients are also acknowledged to have dystrophies in the limbic system, which compromise their stress-coping and social cognitive capabilities (Lieberman et al., 2018; Wannan et al., 2019). Indeed, in individuals with schizophrenia, poor neurocognitive performance is related to increased stress level (Krkovic et al., 2017).

Stress also exacerbates psychosis (Gomes et al., 2017) and anxiety (Ray et al., 2017; Juruena et al., 2020), which can further devastate cognitive deficits of schizophrenia patients (Betensky et al., 2008). In consistency, we observed stress perception in association with cerebral frontal lobe atrophy and psychotic symptoms in the FES patients. Furthermore, the *CSF1R* was negatively correlated with both the PSS and the PANSS scores in these patients. This further supports that the CSF1R-mediated stress regulation might be dysfunctional in the FES patients, as is also supported by our study linking CUS and CSF1Ri effect on animal anxiety behaviors (see section 6.2), hence contributing to psychosis and cognitive impairments possibly via neuroinflammation-mediated changes in cerebral cortical structures.

Thus, targeting inflammation to improve neurobiological machinery underlying stress coping may offer an avenue for intervention on cognitive and psychotic outcomes in individuals with schizophrenia.

6.2. Stress/CSF1Ri-induced psychiatric-like behaviors (Papers II and IV)

As discussed above, stress contributes to psychosis-associated behaviors such as anxiety and social cognitive deficit in individuals with schizophrenia, and CSF1R may regulate stress response in physiological conditions. As such, we used a CUS model and administered an inhibitor (CSF1Ri) to block Csf1r in microglia in B6N mice to depict in detail how CSF1R may regulate stress response. We also used an OBX-induced stress model to study OB-dependent animal anxiety/depressive-like behaviors.

We observed that CUS-enduring mice displayed anxiety-like behaviors, shown as more distance travelled in corners in OFT and less time spent in closed arms in EPM, in agreement with numerous previous studies (Tran et al., 2023). Importantly, we found that the CSF1Ri was anxiogenic to mice like the CUS. Our observation corroborates with a previous study reporting that *Csf1r*$^{+/-}$ mice exhibited anxiety along with cognitive and sensorimotor deficits (Chitu et al., 2015). However, other studies using CSF1Ri have not observed its effect on anxiety in mice (Green et al., 2020). This discrepancy may be due to different protocols of CSF1Ri administration, which warrant further careful investigations. In relevancy, one study reported that when CSF1Ri was administered

for 21 days, it resulted in enhanced anxiety in the EPM, while not so for 7-days and 2-months treatments (Elmore et al., 2014). Another study reported that CSF1Ri treatment for 7 but not 21 days induced temporary impairment in spatial memory but not social behavior (Torres et al., 2016). Thus, it seems that the duration of CSF1Ri administration and the timepoint for behavior tests are important.

Moreover, we found that both the CUS and the CSF1Ri induced depressive-like anhedonia in mice, as reflected by sucrose consumption in SPT. However, unlike the CUS, the CSF1Ri did not trigger both learned helplessness/despair behavior, measured as increased immobility time in TST, and social avoidance, shown as less access to a stranger mice in TCT. In other studies, CSF1Ri treatment also did not cause behavioral despair (Wang et al., 2020; Chang et al., 2023) and deficits in social preference (Badimon et al., 2020). That CSF1Ri affected anxiety and anhedonia but not despair and social behavior hints that not all psychotic and affective symptoms of psychiatric disorders may be CSF1R-dependent. Furthermore, we did not observe accumulative effects of the CSF1Ri combined with the CUS on all the above behaviors. This corroborates our clinical result that the CSF1R contributed to stress regulation in the HCs (i.e., in a physiological condition) but not in the FES patients (i.e., in a pathologically stressful condition).

As will also be discussed in section 6.4, we discovered that the murine OB was enriched with fatty acid metabolic genes compared to the PFC and olfactory microglia were exceptionally phagocytic. The OB is highly functional for exploratory and psychiatric-like behaviors in rodents (Hasegawa et al., 2022; Alvites et al., 2023). Hence, we wondered how removal of the OB would affect animal psychiatric-like behaviors. To this end, we used an OBX mouse model. We previously found the OBX induced hyperactivity in rats in the OFT, due to damage of the OB-associated limbic system and decrease of noradrenaline (Song et al., 2004). We also found that the OBX resulted in anxiety and anhedonia in rats (Song et al., 2005) . Here, we found that the OBX induced hyperlocomotion, increased rearing times and decreased sucrose consumption in mice similarly as we previously found in rats. Besides, our group also reported OBX-induced social avoidance and impaired cognition in mice (Gu et al., 2021). These results suggest that loss of olfaction disables stress coping and associated cognitive performance, which may have important implications for psychotic symptoms in patients with psychiatric disorders.

Besides CSF1Ri, other pharmacological interventions such as n-3 PUFAs have also been extensively tested in animal stress models (Hennebelle et al., 2014). Using *fat-1* mice, we found that stress-related anxiety-like behavior induced by the OBX was attenuated in the *fat-1* mice. Besides, our group also reported that the OBX-induced social avoidance and impaired cognition (Gu et al., 2021) as well as lipopolysaccharide-induced anhedonia and despair (Gu et al., 2018) were markedly restored in *fat-1* mice. Other studies have shown that *fat-1* mice are a good model to study neurological and psychiatric disorders (Das et al., 2009). For instances, they exhibited a better spatial learning

performance than WT mice via enhanced hippocampal neurogenesis (He et al., 2009) and mitigated cognitive deficits induced by lipopolysaccharide (Delpech et al., 2015) or in Alzheimer's disease model (Wu et al., 2016). These demonstrate that endogenous n-3 PUFAs and a higher ratio of n-3/n-6 PUFAs can improve the ability of mice to cope with the stress caused by the loss of the OB and improve their cognitive performance. Supplementation of n-3 PUFAs was also proven effective in improving cognitive functions and reducing severity of psychotic symptoms (Hsu et al., 2020). Thus, n-3 PUFAs are a useful supplementary therapeutic medicine to treat psychiatric disorders.

6.3. CSF1R contributes to vascular association of microglia and stress regulation (Paper II)

CSF1R signaling plays an important role in regulating brain development in both humans and rodents (Keshvari et al., 2021). Specifically, loss-of-function *CSF1R* mutations caused leukoencephalopathy, hydrocephaly, and white matter atrophy or loss of the corpus callosum, besides skeletal deficits (Guo et al., 2019), and resulted in cerebrovascular pathology in humans (Delaney et al., 2021). *Csf1r*$^{-/-}$ mice also exhibited atrophy of the neocortex along with expansion of the lateral ventricle (Erblich et al., 2011; Nandi et al., 2012). Moreover, the Csf1r signaling regulated the proliferation, survival, and differentiation of forebrain neural progenitor cells (Chitu et al., 2016). Besides neurodegenerative diseases, the aberrant Csf1r signaling has also been linked to other somatic diseases including cancer and autoimmune disorders (Hamilton, 2008; Cannarile et al., 2017).

When exploring the effects of CUS plus CSF1Ri on the mouse PFC and HPC, we revealed that the CUS compromised gene expressions of cell adhesion, angiogenesis, and tight junction molecules, reduced microglial expression of the Csf1r protein, and dampened IBA1 intensity more in VAMs compared to NVAMs, thereby implicating a less juxta-vascular association of microglial/macrophage after the CUS. Chronic stress is acknowledged to affect the BBB integrity and angiogenesis by dampening endothelial molecules and accelerating vascular inflammation in psychiatric disorders (Dion-Albert et al., 2023), and microglia near the cerebral blood vessels can monitor the BBB integrity (Ronaldson et al., 2020; Hattori, 2023). Our RNA-seq and immunohistochemistry findings on the CUS are consistent with the previous studies and suggest that the blood vessel-association of microglia/macrophages may regulate cerebrovascular integrity under stress.

In addition, we found that the CUS decreased microglial abundancy in the PFC and HPC. This may be due to the CUS-dampened Csf1r level that is pivotal for microglial survival, in line with previous reports showing stress-induced microglial apoptosis (Kreisel et al., 2014) and decrease in the Csf1r level (Wohleb et al., 2018). Meanwhile, we observed stress-induced hyper-ramification of the NVAMs, indicating enhanced surveillance of a changing surrounding environment in association with behavioral impairments as sub-

stantiated by others (Hinwood et al., 2012; Cathomas et al., 2022; Vidal-Itriago et al., 2022). Nonetheless, the VAMs were resistant to CUS-induced ramification, suggesting that their robustness may help cerebrovascular remodeling to rescue stress-induced psychiatric-like behaviors.

Importantly, the CSF1Ri also impacted the brain blood vessels by diminishing cell adhesion and angiogenic DEGs, such as *Pik3cg*, *Ang*, *Cspg4*, and *Ptk2b*, and preferentially eliminated the VAMs in the mouse brain, in line with a recent study also reporting the CSF1Ri-induced BBB leakage via dampened tight junction genes (Delaney et al., 2021). The preferential elimination of the VAMs is possibly due to the blood-route of drug delivery and/or the specific sensitivity of the VAMs to the CSF1Ri.

Additionally, the CSF1Ri induced amoeboid morphology in surviving microglia, which is indicative of enhanced phagocytic activity of microglia (Neumann et al., 2009). In consistency, we observed enhanced Vglut2 engulfment by these surviving microglia and increased expression of genes involved in endocytosis process. Besides, such morphological change implies that the surviving microglia may be microglial progenitor cells (Zhan et al., 2020), which is supported by our RNA-seq results on mitosis and cell division processes. Overall, these results are to our knowledge the first evidence revealing the involvement of the CSF1R in vascular association of microglia/macrophages in the context of stress and strongly support our clinical findings on the negative association of the CSF1R with PSS score possibly via regulating vascular functions in HCs (see section 6.1).

Intriguingly, the CSF1Ri did not facilitate the effect of the CUS on microglial parameters, including the number and morphology of the VAMs, as well as expressions of CD31 and some angiogenic genes. We speculate that since the CUS dampened both microglial abundancy and the Csf1r level in microglia, this made stressed microglia less sensitive to the CSF1Ri. Nevertheless, some brain cytoarchitecture such as OPCs may be robust in stress adaptation due to their regenerative capacity, which might be ignited by the CSF1Ri, as we observed here. Desensitization of the microglial Csf1r after the CUS also notably corroborates with our clinical observation that the negative association of the CSF1R level with the PSS was less significant in FES patients compared to the HCs (see section 6.1).

In summary, in the brains of individuals with schizophrenia, microglia/ macrophages may exist in varying functional states and only their specific subsets may contribute to vascular remodeling. Our data altogether suggest that microglial subpopulation such as the VAMs, and possibly others, may be committed to rescue psychiatric-like behaviors by promoting vascular repair and neural tissue recovery. Impairment of the VAMs by the CUS and the CSF1Ri may result in diminished cerebrovascular remodeling and profound BBB leakage, which explain their cause of psychiatric-like behaviors. Currently, clinical and preclinical studies on the angiogenic function of microglia/macrophages in psychiatric conditions are still missing, our work thereby gives a first glimpse into this theme.

6.4. Lipid metabolism, angiogenesis, and microglia in the OB (Paper III)

As discussed above, removal of the OB can result in psychiatric-like behavior and impaired cognition in mice. Likewise, the OB-related orbitofrontal gyrus was smaller in our FES patients than HCs and schizophrenia patients were reported to have a smaller volume of the OB in association with negative symptoms and cognitive deficits (Corcoran et al., 2005; Yang et al., 2021). Notably, the OB is a highly sensitive brain region to both inflammation (LaFever et al., 2022) and regeneration, hosting abundant neural stem cells in adult rodents (Tufo et al., 2022). So, we further explored the properties of the OB and olfactory microglia compared to other brain regions in mice.

By RNA-seq, we found that the most significant DEGs between the OB and the PFC were involved in lipid metabolism. The OB was reported to have the most distinct metabolic profile among brain regions, for example with higher levels of fatty acids (such as n-3 PUFAs) and phospholipids (such as phosphatidylcholines and phosphatidylethanolamines) but lower levels of prostaglandin D2 and prostaglandin E2 than other brain regions (Choi et al., 2018; Le Bon et al., 2018; Fitzner et al., 2020), whereas the CTX and HPC showed more similar lipid metabolomic content (Choi et al., 2018). Studies have shown that lipids play an important role in maintaining structural and functional plasticity of the OB (He et al., 2020; Yang et al., 2022) and impaired lipid metabolism is associated with oxidative stress and neuroinflammation, leading to neurological defects (Hamilton et al., 2007; Naudí et al., 2017; Yang et al., 2022), stress susceptibility (Chuang et al., 2010; He et al., 2020), and psychiatric disorders (Penninx et al., 2018). Therefore, our finding that fatty acid regulating DEGs were upregulated in the OB may have implications in the olfactory pathophysiology of schizophrenia.

We also observed that angiogenesis-regulating genes were more enriched in the OB. The result is strongly supported by an observation that the blood vessels in the OB had the highest branch point density and the largest diameter, as well as the lowest segmental length and thereby the smallest length over diameter ratio (indicating the lowest flow resistance of the vessel) compared to the blood vessels in the other brain regions (Miettinen et al., 2021) . Notably, normal lipid metabolism is crucial for endothelial functions. For examples, inhibition of fatty acid synthase impairs physiological and pathological angiogenesis via selectively reducing endothelial cell proliferation (Bruning et al., 2018). Enhanced n-3 PUFAs, e.g., eicosapentaenoic acid and docosahexaenoic acid, by dietary or genetic means, induced angiogenesis in mesenchymal stromal cells (Mathew et al., 2018) and promoted vessel regrowth after retinal injury (Connor et al., 2007). As well, astrocytic release of angiopoietin 2 was enhanced in *fat-1* mice, which promoted endothelial proliferation and the BBB formation (Wang et al., 2014) . Thus, the higher expressions of angiogenesis- and fatty acid-regulating DEGs in the OB indicate that these two biological

processes are closely intercalated with each other to maintain the olfactory functions.

Additionally, we found that CSF1Ri dampened the angiogenesis- and fatty acid-regulating DEGs in the OB. This is well in line with recent reports that microglia participated in regulation of lipid metabolism underlying neuronal functions and brain pathology (Bruce et al., 2018; Nugent et al., 2020; McNamara et al., 2023). Besides, chronic mild hypoxia was found to induce microglia-vascular clustering particularly in the OB as compared to the CTX (Halder et al., 2020). We also observed that the OB accommodated more $CD206^{+}IBA1^{+}$ microglia and macrophages. CD206 is a mannose receptor involved in pinocytosis and phagocytosis of macrophages including those in the brain (Régnier-Vigouroux, 2003; Tanaka et al., 2021). Transiently high expression of CD206 can be found in a subpopulation of neuroprotective microglia besides infiltrating macrophages after brain injuries (Wang et al., 2013). Importantly, $CD206^{+}$ cells are known to be associated with cerebral vasculature (Bisht et al., 2021; Drieu et al., 2022; Zheng et al., 2022). Corroboratively, we found that the $CD206^{+}IBA1^{+}$ microglia were a minor microglial subset especially enriched at the cerebral blood vessels in the adult mouse cortex compared to canonical $IBA1^{+}$ microglia. Furthermore, the $CD206^{+}IBA1^{+}$ microglia were more sensitive for CSF1Ri-induced ablation in the OB than the HPC, possibly due to the richer vasculature network in the OB (Bovetti et al., 2007; Martončíková et al., 2021; Miettinen et al., 2021) and higher level of blood vessel-association of $CD206^{+}IBA1^{+}$ microglia.

Regarding our observation of the high level of Vglut2 engulfment by olfactory microglia, as mentioned before, olfactory microglia play a critical role in maintaining structural and functional integrities of the OB in physiological and pathological conditions (Reshef et al., 2017; Seo et al., 2018; Wallace et al., 2020). Besides, $Csf1r^{-/-}$ mice displayed atrophy of the OB (Erblich et al., 2011; Nandi et al., 2012) and $Csf1r^{+/-}$ mice showed olfactory deficits (Chitu et al., 2015). Our finding that olfactory microglia engulfed more Vglut2 compared to their hippocampal counterparts provides additional supportive evidence on this line.

Overall, the above body of evidence suggests that the OB is ultra-sensitive for lipid metabolism, blood vessel integrity, and neuronal plasticity, which all underlie the pathophysiology of psychiatric disorders, and olfactory vascular-associated microglia/macrophages may be important regulators of these processes.

6.5. N-3 PUFAs play an anti-inflammatory role in OBX (Paper IV)

As the OB has active lipid metabolism, and OBX causes stress-associated psychiatric-like behaviors, we also studied lipid metabolism in *fat-1* mice in comparison to WT mice undergoing the OBX. Here, we found that the OBX disturbed the plasma lipid metabolic profile in the WT mice, which was

improved in the *fat-1* mice. These changed lipids fell into biological pathways that are closely associated with n3/n6 PUFAs and are involved in processes of inflammation and oxidative stress (Jie et al., 2007; McFadden et al., 2014; Andersen, 2022). To our knowledge, this is the first thorough report on specific lipid metabolic pathways that are associated with attenuation of OBX-induced disability of stress coping.

Our observation that the OBX-induced elevation of 15 phospholipid metabolites in the plasma was attenuated in the *fat-1* mice is substantiated by other studies showing that phospholipids, namely phosphatidylcholine and phosphatidylethanolamine, were increased in the brains of CUS-subjected mice (Faria et al., 2014), and stress-induced olfactory dysfunction may be due to disrupted lipid metabolic pathways (He et al., 2020). Our observation is also consistent with a recent report that high intake of n-6 PUFA elevated the content of phosphatidylethanolamine, one of the 15 OBX-induced phospholipids in our study, in the murine brain (Li et al., 2023).

Fat-1 mice display different basal levels of phospholipids than those in WT mice, e.g., reduced n-6 phospholipids and increased n-3 lysophosphospholipids (Kang et al., 2004; Astarita et al., 2014). A low n-6/n-3 PUFA ratio can enhance anti-inflammatory and anti-oxidative stress responses and improve endothelial functions (Yang et al., 2016). *Fat-1* mice were corroboratively reported to be protected against low-grade systemic inflammation and neuroinflammation induced by lipopolysaccharide or neurodegeneration (Das et al., 2009), and exhibited robust improvements in revascularization and angiogenesis post stroke (Wang et al., 2014). These suggest that the resistance of the *fat-1* mice to the OBX-induced stress in our study were realized via anti-inflammatory and angiogenic pathways. Indeed, among lipid regulating genes, we found anti-inflammatory genes of *KLF*, *PLA2*, and *FADS* families were increased in the HPC of the *fat-1* mice, concomitantly with dampened pro-inflammatory cytokines induced by the OBX. We also observed a positive correlation between increased Cop and hyperactive behavior in OBX-treated mice. *In vitro*, the Cop promoted microglial production of IL-1β, IFN-γ, and NO, all well-characterized biomarkers for schizophrenia (Kose et al., 2021; Hughes et al., 2022).

In *C. elegans*, *klf2* regulates *fat-1* gene expression and inhibits the transcriptional activity of NF-κB (Jha et al., 2017; Das et al., 2006). The Pla2 family is a group of enzymes that hydrolyze glycerophospholipids and a key regulatory point in lipid-driven pro-inflammatory cascades (Ruiz et al., 2015). *Pla2g6* is involved in Fc gamma receptor-mediated phagocytosis and induces arachidonic acid metabolism, which is upregulated in OBX rats (Skelin et al., 2011) and activates inflammatory response (Li et al., 2017). Additionally, Fads is involved in the peroxisome proliferator-activated receptor-mediated anti-inflammatory signaling pathway (McNamara et al., 2016).

Genes of the *KLF*, *PLA2*, and *FADS* families were also altered in the blood of our FES patients. These genes are known to be involved in schizophrenia (Jones et al., 2021; Yang et al., 2021; Guo et al., 2023; Scott et al., 2023). Moreover, increases of the phospholipids phosphatidylcholine and phosphati-

dylethanolamine in the gray matters of schizophrenia patients (Schwarz et al., 2008), and decreases of n-3 PUFAs and n-3/n-6 ratio in the peripheral blood of schizophrenia patients (Berger et al., 2019) were found, while supplementation of n-3 PUFAs was effective in reducing severity of psychotic symptoms (Hsu et al., 2020).

Overall, our study suggests that inflammation-associated lipid metabolites may reflect pathophysiological state of schizophrenia and represent as diagnosis or treatment targets for this disorder.

6.6. Limitations of our studies

Our studies have several limitations to mention. These include the small sample size in our clinical and preclinical cohorts, no comparison of potential sex differences (only male mice were studied due to the higher prevalence of schizophrenia among male human subjects), and the cross-sectional nature of our clinical study design. For transcriptomics, we used whole blood samples for humans and brain tissue samples for mice and performed bulk RNA-seq, which should be improved by more advanced approaches such as single cell RNA-seq and spatial RNAscope in the future. Moreover, we did not cross check microglial association with cerebral vasculature in OBX model, and lipid metabolomics in CUS+CSF1Ri model, which should be explored later.

7. CONCLUSIONS

Our key findings are:

I. Nonclassical monocytes were decreased, and monocyte-related genes showed significant changes in FES patients, especially for those belonging to intermediate and nonclassical monocytic subsets, with the most outstanding alterations being downregulation of *S100A* of the intermediate monocytes and upregulation of *IFITM* family members of the intermediate and nonclassical monocytes; Additionally, *CSF1R* and *PECAM1* (both signature genes of the nonclassical monocytes) were decreased in FES patients.

II. Some FES patients perceived higher stress and had decreased CSF1R level as well as atrophy of the frontal cortical subregions. Furthermore, *CSF1R* mRNA level was associated with shrinkage of the superior frontal gyrus in response to perceived stress in HCs but not FES patients. In CUS combined with CSF1Ri mouse model, CSF1Ri enhanced anxiety and downregulated angiogenesis in mice, similarly as CUS. Moreover, CSF1Ri preferentially eliminated VAMs in the mouse brain.

III. The OB accommodated more fatty acid metabolic and angiogenesis DEGs than the PFC. Furthermore, blood vessel-associated $CD206^{+}IBA1^{+}$ and Vglut2 engulfing microglia were more enriched in the OB than the other brain regions. The OB was also more sensitive to CSF1Ri treatment than the PFC in fatty acid metabolism and angiogenesis.

IV. Dysregulation of lipid metabolism, such as enhanced Cop and phospholipids, occurred in the plasma of mice subjected to OBX. OBX-induced hyperactive behavior was correlated with Cop, which provoked inflammatory responses in a BV2 microglia cell line. These changes were attenuated by endogenous n-3 PUFAs in *fat-1* mice. Furthermore, anti-inflammatory lipid genes such as *Klf2* and *Fads* were more enriched in *fat-1* mice than in WT mice. In parallel, OBX-induced pro-inflammatory cytokines were reduced in *fat-1* mice.

These key findings have several folds of indications. Firstly, we found blood nonclassical monocytic abundancy and CSF1R level were dampened in FES patients and a sub-cohort of FES patients experienced a higher level of perceived stress and displayed stress-associated region-specific cerebral cortical atrophy. These imply that the machinery of maintaining brain angiogenesis and vascular integrity may be blunted in FES, thereby contributing to cerebral cortical atrophy and enhanced stress perception. Next, we found CSF1Ri induced anxiety in mice and disrupted brain blood vessels and vascular association of microglia/macrophages, especially in the OB, which also displayed enriched genes for fatty acid metabolism and angiogenesis. These imply that interplays among inflammation, angiogenesis and lipid metabolism are important for

stress regulation, and engagement of the OB may be relevant to pathophysiology of FES. Furthermore, we found OBX-induced stress responses were rescued in *fat-1* mice that produced endogenous n-3 PUFAs, implying the importance of restoring lipid metabolism and ameliorating brain inflammation for stress regulation that is relevant to FES. These findings overall suggest that microglia modulators may benefit stress coping via regulating cerebral blood vasculature in schizophrenia (**Fig. 32**). Our studies hence provide novel knowledge on pathophysiological mechanisms mediated by microglial/monocytic subpopulations and their candidate molecules, which may be useful for improving diagnosis and treatment for schizophrenia.

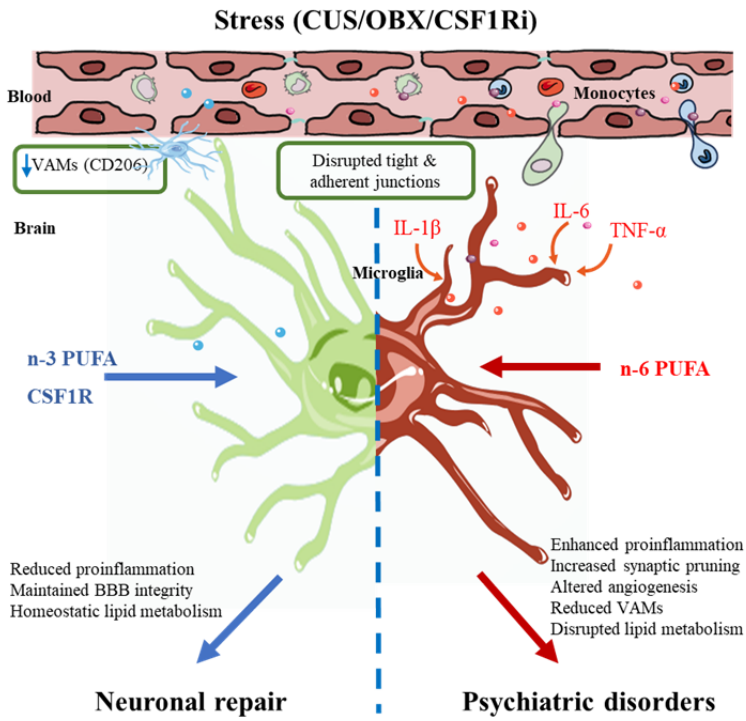

Figure 32. Microglial modulators in stressed-induced psychiatric disorders. Chronic stress and CSF1R inhibitor (CSF1Ri) compromise the cerebrovascular and blood-brain barrier (BBB) integrity by dampening tight/adherens junctions, angiogenesis, and vessel-associated microglia/macrophages (VAMs)/perivascular macrophages (PVMs). Infiltrated blood monocytes, pro-inflammatory cytokines, and n-6 polyunsaturated fatty acids (PUFAs) can enhance neuroinflammation and activate microglia, which mediate increased synaptic pruning and promote disrupted lipid metabolism, hence contributing to psychiatric disorders. On the contrary, n-3 PUFAs and colony stimulating factor 1 receptor (CSF1R) can benefit stress coping by inducing neuroprotective microglial phenotypes to reduce neuroinflammation, improve cerebrovascular and BBB integrity, and maintain normal lipid metabolism. CUS: chronic unpredictable stress; OBX: olfactory bulbectomy. The figure is prepared using Servier Medical Art under a Creative Commons Attribution 3.0 unported license.

8. REFERENCES

Abe, K., Kuo, L., Zukowska, Z. (2010). Neuropeptide Y is a mediator of chronic vascular and metabolic maladaptations to stress and hypernutrition. *Exp Biol Med (Maywood)* 235(10):1179–1184.

Al-Onaizi, M., Al-Khalifah, A., Qasem, D., ElAli, A. (2020). Role of microglia in modulating adult neurogenesis in health and neurodegeneration. *Int J Mol Sci* 21(18): 6875.

Alvites, R., Caine, A., Cherubini, G. B., Prada, J., Varejão, A. S. P., Maurício, A. C. (2023). The olfactory bulb in companion animals-anatomy, physiology, and clinical importance. *Brain Sci* 13(5):713.

Andersen, C. J. (2022). Lipid metabolism in inflammation and immune function. *Nutrients* 14(7):1414.

Araki, T., Ikegaya, Y., Koyama, R. (2021). The effects of microglia- and astrocyte-derived factors on neurogenesis in health and disease. *Eur J Neurosci* 54(5):5880–5901.

Astarita, G., McKenzie, J. H., Wang, B., Strassburg, K., Doneanu, A., Johnson, J., et al. (2014). A protective lipidomic biosignature associated with a balanced omega-6/omega-3 ratio in fat-1 transgenic mice. *PLoS One* 9(4):e96221.

Atrooz, F., Alkadhi, K. A., Salim, S. (2021). Understanding stress: Insights from rodent models. *Curr Res Neurobiol* 2:100013.

Austermann, J., Roth, J., Barczyk-Kahlert, K. (2022). The good and the bad: monocytes' and macrophages' diverse functions in inflammation. *Cells* 11(12):1979.

Badimon, A., Strasburger, H. J., Ayata, P., Chen, X., Nair, A., Ikegami, A., et al. (2020). Negative feedback control of neuronal activity by microglia. *Nature* 586(7829):417–423.

Barber, C. N., Raben, D. M. (2019). Lipid metabolism crosstalk in the brain: glia and neurons. *Front Cell Neurosci* 13:212.

Berger, M., Nelson, B., Markulev, C., Yuen, H. P., Schäfer, M. R., Mossaheb, N., et al. (2019). Relationship between polyunsaturated fatty acids and psychopathology in the neurapro clinical trial. *Front Psychiatry* 10:393.

Bernstein, D. P., Stein, J. A., Newcomb, M. D., Walker, E., Pogge, D., Ahluvalia, T., et al. (2003). Development and validation of a brief screening version of the Childhood Trauma Questionnaire. *Child Abuse Negl* 27(2):169–190.

Betensky, J. D., Robinson, D. G., Gunduz-Bruce, H., Sevy, S., Lencz, T., Kane, J. M., et al. (2008). Patterns of stress in schizophrenia. *Psychiatry Res* 160(1):38–46.

Bisht, K., Okojie, K. A., Sharma, K., Lentferink, D. H., Sun, Y. Y., Chen, H. R., et al. (2021). Capillary-associated microglia regulate vascular structure and function through PANX1-P2RY12 coupling in mice. *Nat Commun* 12(1):5289.

Bollinger, J. L., Wohleb, E. S. (2019). The formative role of microglia in stress-induced synaptic deficits and associated behavioral consequences. *Neurosci Lett* 711:134369.

Bovetti, S., Hsieh, Y. C., Bovolin, P., Perroteau, I., Kazunori, T., Puche, A. C. (2007). Blood vessels form a scaffold for neuroblast migration in the adult olfactory bulb. *J Neurosci* 27(22):5976–5980.

Bremner, J. D., Moazzami, K., Wittbrodt, M. T., Nye, J. A., Lima, B. B., Gillespie, C. F., et al. (2020). Diet, stress and mental health. *Nutrients* 12(8):2428.

Bruce, K. D., Gorkhali, S., Given, K., Coates, A. M., Boyle, K. E., Macklin, W. B., et al. (2018). Lipoprotein lipase is a feature of alternatively-activated microglia and may facilitate lipid uptake in the CNS during demyelination. *Front Mol Neurosci* 11:57.

Bruning, U., Morales-Rodriguez, F., Kalucka, J., Goveia, J., Taverna, F., Queiroz, K. C. S., et al. (2018). Impairment of angiogenesis by fatty acid synthase inhibition involves mTOR malonylation. *Cell Metab* 28(6):866–880.e815.

Cai, H. Q., Catts, V. S., Webster, M. J., Galletly, C., Liu, D., O'Donnell, M., et al. (2020). Increased macrophages and changed brain endothelial cell gene expression in the frontal cortex of people with schizophrenia displaying inflammation. *Mol Psychiatry* 25(4):761–775.

Campeau, A., Mills, R. H., Stevens, T., Rossitto, L. A., Meehan, M., Dorrestein, P., Daly, R., Nguyen, T. T., Gonzalez, D. J., Jeste, D. V., Hook, V. (2022). Multi-omics of human plasma reveals molecular features of dysregulated inflammation and accelerated aging in schizophrenia. *Mol Psychiatry* 27(2):1217–1225.

Cangalaya, C., Stoyanov, S., Fischer, K. D., Dityatev, A. (2020). Light-induced engagement of microglia to focally remodel synapses in the adult brain. *Elife* 9:e58435.

Cannarile, M. A., Weisser, M., Jacob, W., Jegg, A. M., Ries, C. H., Rüttinger, D. (2017). Colony-stimulating factor 1 receptor (CSF1R) inhibitors in cancer therapy. *J Immunother Cancer* 5(1):53.

Carbon, M., Correll, C. U. (2014). Thinking and acting beyond the positive: the role of the cognitive and negative symptoms in schizophrenia. *CNS Spectr* 19 Suppl 1:38–53.

Carmen-Orozco, R. P., Dávila-Villacorta, D. G., Cauna, Y., Bernal-Teran, E. G., Bitterfeld, L., Sutherland, G. L., et al. (2019). Blood-brain barrier disruption and angiogenesis in a rat model for neurocysticercosis. *J Neurosci Res* 97(2):137–148.

Cătălin, B., Cupido, A., Iancău, M., Albu, C. V., Kirchhoff, F. (2013). Microglia: first responders in the central nervous system. *Rom J Morphol Embryol* 54(3):467–472.

Cathomas, F., Holt, L. M., Parise, E. M., Liu, J., Murrough, J. W., Casaccia, P., et al. (2022). Beyond the neuron: role of non-neuronal cells in stress disorders. *Neuron* 110(7):1116–1138.

Cattaneo, A., Macchi, F., Plazzotta, G., Veronica, B., Bocchio-Chiavetto, L., Riva, M. A., et al. (2015). Inflammation and neuronal plasticity: a link between childhood trauma and depression pathogenesis. *Front Cell Neurosci* 9:40.

Cermenati, G., Mitro, N., Audano, M., Melcangi, R. C., Crestani, M., De Fabiani, E., et al. (2015). Lipids in the nervous system: from biochemistry and molecular biology to patho-physiology. *Biochim Biophys Acta* 1851(1):51–60.

Chang, H. X., Dai, W., Bao, J. H., Li, J. F., Zhang, J. G., Li, Y. F. (2023). Essential role of microglia in the fast antidepressant action of ketamine and hypidone hydrochloride (YL-0919). *Front Pharmacol* 14:1122541.

Charlson, F., van Ommeren, M., Flaxman, A., Cornett, J., Whiteford, H., Saxena, S. (2019). New WHO prevalence estimates of mental disorders in conflict settings: a systematic review and meta-analysis. *Lancet* 394(10194):240–248.

Chaves, C., Marque, C. R., Maia-de-Oliveira, J. P., Wichert-Ana, L., Ferrari, T. B., Santos, A. C., et al. (2015). Effects of minocycline add-on treatment on brain morphometry and cerebral perfusion in recent-onset schizophrenia. *Schizophr Res* 161(2–3):439–445.

Chen, A. Q., Fang, Z., Chen, X. L., Yang, S., Zhou, Y. F., Mao, L., et al. (2019). Microglia-derived TNF-α mediates endothelial necroptosis aggravating blood brain-barrier disruption after ischemic stroke. *Cell Death Dis* 10(7):487.

Chen, H. R., Sun, Y. Y., Chen, C. W., Kuo, Y. M., Kuan, I. S., Tiger Li, Z. R., et al. (2020). Fate mapping via CCR2-CreER mice reveals monocyte-to-microglia transition in development and neonatal stroke. *Science advances* 6(35), eabb2119.

Chen, S., Li, J., Meng, S., He, T., Shi, Z., Wang, C., et al. (2023). Microglia and macrophages in the neuro-glia-vascular unit: From identity to functions. *Neurobiol Dis* 179:106066.

Chen, S., Tian, L., Chen, N., Xiu, M. H., Wang, Z. R., Wang, Y. C., et al. (2019). More dampened monocytic Toll-like receptor 4 response to lipopolysaccharide and its association with cognitive function in Chinese Han first-episode patients with schizophrenia. *Schizophr Res* 206:300–306.

Chitu, V., Gokhan, S., Gulinello, M., Branch, C. A., Patil, M., Basu, R., et al. (2015). Phenotypic characterization of a Csf1r haploinsufficient mouse model of adult-onset leukodystrophy with axonal spheroids and pigmented glia (ALSP). *Neurobiol Dis* 74:219–228.

Chitu, V., Gokhan, Ş., Nandi, S., Mehler, M. F., Stanley, E. R. (2016). Emerging roles for CSF-1 receptor and its ligands in the nervous system. *Trends Neurosci* 39(6): 378–393.

Cho, M., Lee, T. Y., Kwak, Y. B., Yoon, Y. B., Kim, M., Kwon, J. S. (2019). Adjunctive use of anti-inflammatory drugs for schizophrenia: a meta-analytic investigation of randomized controlled trials. *Aust N Z J Psychiatry* 53(8):742–759.

Choi, B. R., Johnson, K. R., Maric, D., McGavern, D. B. (2023). Monocyte-derived IL-6 programs microglia to rebuild damaged brain vasculature. *Nat Immunol* 24(7): 1110–1123.

Choi, S. H., Langenbach, R., Bosetti, F. (2008). Genetic deletion or pharmacological inhibition of cyclooxygenase-1 attenuate lipopolysaccharide-induced inflammatory response and brain injury. *Faseb j* 22(5):1491–1501.

Choi, W. T., Tosun, M., Jeong, H. H., Karakas, C., Semerci, F., Liu, Z., et al. (2018). Metabolomics of mammalian brain reveals regional differences. *BMC Syst Biol* 12(Suppl 8):127.

Chuang, J. C., Cui, H., Mason, B. L., Mahgoub, M., Bookout, A. L., Yu, H. G., et al. (2010). Chronic social defeat stress disrupts regulation of lipid synthesis. *J Lipid Res* 51(6):1344–1353.

Cohen, S., Kamarck, T., Mermelstein, R. (1983). A global measure of perceived stress. *J Health Soc Behav* 24(4):385–396.

Collaborators, G. D. a. I. I. a. P. (2017). Global, regional, and national incidence, prevalence, and years lived with disability for 328 diseases and injuries for 195 countries, 1990–2016: a systematic analysis for the Global Burden of Disease Study 2016. *Lancet* 390(10100):1211–1259.

Colton, C. A. (2009). Heterogeneity of microglial activation in the innate immune response in the brain. *J Neuroimmune Pharmacol* 4(4):399–418.

Comer, A. L., Carrier, M., Tremblay, M., Cruz-Martín, A. (2020). The inflamed brain in schizophrenia: the convergence of genetic and environmental risk factors that lead to uncontrolled neuroinflammation. *Front Cell Neurosci* 14:274.

Connor, K. M., SanGiovanni, J. P., Lofqvist, C., Aderman, C. M., Chen, J., Higuchi, A., et al. (2007). Increased dietary intake of omega-3-polyunsaturated fatty acids reduces pathological retinal angiogenesis. *Nat Med* 13(7):868–873.

Corcoran, C., Whitaker, A., Coleman, E., Fried, J., Feldman, J., Goudsmit, N., et al. (2005). Olfactory deficits, cognition and negative symptoms in early onset psychosis. *Schizophr Res* 80(2–3):283–293.

Cornell, J., Salinas, S., Huang, H. Y., Zhou, M. (2022). Microglia regulation of synaptic plasticity and learning and memory. *Neural Regen Res* 17(4):705–716.

Croy, I., Hummel, T. (2017). Olfaction as a marker for depression. *J Neurol* 264(4):631–638.

Császár, E., Lénárt, N., Cserép, C., Környei, Z., Fekete, R., Pósfai, B., et al. (2022). Microglia modulate blood flow, neurovascular coupling, and hypoperfusion via purinergic actions. *J Exp Med* 219(3):e20211071.

Daneman, R., Prat, A. (2015). The blood-brain barrier. *Cold Spring Harb Perspect Biol* 7(1):a020412.

Das, H., Kumar, A., Lin, Z., Patino, W. D., Hwang, P. M., Feinberg, M. W., et al. (2006). Kruppel-like factor 2 (KLF2) regulates proinflammatory activation of monocytes. *Proc Natl Acad Sci U S A* 103(17): 6653–6658.

Das, U. N., Puskás, L. G. (2009). Transgenic fat-1 mouse as a model to study the pathophysiology of cardiovascular, neurological and psychiatric disorders. *Lipids Health Dis* 8:61.

De Picker, L. J., Victoriano, G. M., Richards, R., Gorvett, A. J., Lyons, S., Buckland, G. R., et al. (2021). Immune environment of the brain in schizophrenia and during the psychotic episode: a human post-mortem study. *Brain Behav Immun* 97:319–327.

De Vlaminck, K., Van Hove, H., Kancheva, D., Scheyltjens, I., Pombo Antunes, A. R., Bastos, J., et al. (2022). Differential plasticity and fate of brain-resident and recruited macrophages during the onset and resolution of neuroinflammation. *Immunity* 55(11):2085–2102.e9.

Delaney, C., Farrell, M., Doherty, C. P., Brennan, K., O'Keeffe, E., Greene, C., et al. (2021). Attenuated CSF-1R signalling drives cerebrovascular pathology. *EMBO Mol Med* 13(2):e12889.

Delpech, J. C., Madore, C., Joffre, C., Aubert, A., Kang, J. X., Nadjar, A., et al. (2015). Transgenic increase in n-3/n-6 fatty acid ratio protects against cognitive deficits induced by an immune challenge through decrease of neuroinflammation. *Neuropsychopharmacology* 40(3):525–536.

Dickens, A. M., Sen, P., Kempton, M. J., Barrantes-Vidal, N., Iyegbe, C., Nordentoft, M., et al. (2021). Dysregulated lipid metabolism precedes onset of psychosis. *Biol Psychiatry* 89(3):288–297.

Dille, M., Nikolic, A., Wahlers, N., Fahlbusch, P., Jacob, S., Hartwig, S., et al. (2022). Long-term adjustment of hepatic lipid metabolism after chronic stress and the role of FGF21. *Biochim Biophys Acta Mol Basis Dis* 1868(1):166286.

Dion-Albert, L., Cadoret, A., Doney, E., Kaufmann, F. N., Dudek, K. A., Daigle, B., et al. (2022). Vascular and blood-brain barrier-related changes underlie stress responses and resilience in female mice and depression in human tissue. *Nat Commun* 13(1):164.

Dion-Albert, L., Dudek, K. A., Russo, S. J., Campbell, M., Menard, C. (2023). Neurovascular adaptations modulating cognition, mood, and stress responses. *Trends Neurosci* 46(4):276–292.

Drexhage, R. C., Knijff, E. M., Padmos, R. C., Heul-Nieuwenhuijzen, L., Beumer, W., Versnel, M. A., et al. (2010). The mononuclear phagocyte system and its cytokine inflammatory networks in schizophrenia and bipolar disorder. *Expert Rev Neurother* 10(1):59–76.

Drieu, A., Du, S., Storck, S. E., Rustenhoven, J., Papadopoulos, Z., Dykstra, T., et al. (2022). Parenchymal border macrophages regulate the flow dynamics of the cerebrospinal fluid. *Nature* 611(7936):585–593.

Duman, R. S., Sanacora, G., Krystal, J. H. (2019). Altered connectivity in depression: GABA and glutamate neurotransmitter deficits and reversal by novel treatments. *Neuron* 102(1):75–90.

Ebrahimi, M., Yamamoto, Y., Sharifi, K., Kida, H., Kagawa, Y., Yasumoto, Y., et al. (2016). Astrocyte-expressed FABP7 regulates dendritic morphology and excitatory synaptic function of cortical neurons. *Glia* 64(1):48–62.

Ehrchen, J. M., Sunderkötter, C., Foell, D., Vogl, T., & Roth, J. (2009). The endogenous Toll-like receptor 4 agonist S100A8/S100A9 (calprotectin) as innate amplifier of infection, autoimmunity, and cancer. *J Leukoc Biol* 86(3), 557–566.

Elkhatib, S. K., Moshfegh, C. M., Watson, G. F., Case, A. J. (2020). Peripheral inflammation is strongly linked to elevated zero maze behavior in repeated social defeat stress. *Brain Behav Immun* 90:279–285.

Elmore, M. R., Najafi, A. R., Koike, M. A., Dagher, N. N., Spangenberg, E. E., Rice, R. A., et al. (2014). Colony-stimulating factor 1 receptor signaling is necessary for microglia viability, unmasking a microglia progenitor cell in the adult brain. *Neuron* 82(2):380–397.

Elmore, M. R. P., Hohsfield, L. A., Kramár, E. A., Soreq, L., Lee, R. J., Pham, S. T., et al. (2018). Replacement of microglia in the aged brain reverses cognitive, synaptic, and neuronal deficits in mice. *Aging Cell* 17(6):e12832.

Erblich, B., Zhu, L., Etgen, A. M., Dobrenis, K., Pollard, J. W. (2011). Absence of colony stimulation factor-1 receptor results in loss of microglia, disrupted brain development and olfactory deficits. *PLoS One* 6(10):e26317.

Faria, R., Santana, M. M., Aveleira, C. A., Simões, C., Maciel, E., Melo, T., et al. (2014). Alterations in phospholipidomic profile in the brain of mouse model of depression induced by chronic unpredictable stress. *Neuroscience* 273:1–11.

Feng, T., Tripathi, A., Pillai, A. (2020). Inflammatory pathways in psychiatric disorders: the case of schizophrenia and depression. *Curr Behav Neurosci Rep* 7(3):128–138.

Fillman, S. G., Cloonan, N., Catts, V. S., Miller, L. C., Wong, J., McCrossin, T., et al. (2013). Increased inflammatory markers identified in the dorsolateral prefrontal cortex of individuals with schizophrenia. *Mol Psychiatry* 18(2):206–214.

First, M. B. (2013). Diagnostic and statistical manual of mental disorders, 5th edition, and clinical utility. *J Nerv Ment Dis* 201(9):727–729.

Fischl, B. (2012). Freesurfer. *Neuroimage* 62(2):774–781.

Fischl, B., Salat, D. H., Busa, E., Albert, M., Dieterich, M., Haselgrove, C., et al. (2002). Whole brain segmentation: automated labeling of neuroanatomical structures in the human brain. *Neuron* 33(3):341–355.

Fitzner, D., Bader, J. M., Penkert, H., Bergner, C. G., Su, M., Weil, M. T., et al. (2020). Cell-type- and brain-region-resolved mouse brain lipidome. *Cell Rep* 32(11): 108132.

Forsberg, K. M. E., Zhang, Y., Reiners, J., Ander, M., Niedermayer, A., Fang, L., et al. (2018). Endothelial damage, vascular bagging and remodeling of the microvascular bed in human microangiopathy with deep white matter lesions. *Acta Neuropathol Commun* 6(1):128.

Frank, M. G., Thompson, B. M., Watkins, L. R., Maier, S. F. (2012). Glucocorticoids mediate stress-induced priming of microglial pro-inflammatory responses. *Brain Behav Immun* 26(2):337–345.

Franklin, T. B., Saab, B. J., Mansuy, I. M. (2012). Neural mechanisms of stress resilience and vulnerability. *Neuron* 75(5):747–761.

Frumer, G. R., Shin, S. H., Jung, S., Kim, J. S. (2023). Not just glia-dissecting brain macrophages in the mouse. *Glia* 10.1002/glia.24445.

Futtrup, J., Margolinsky, R., Benros, M. E., Moos, T., Routhe, L. J., Rungby, J., et al. (2020). Blood-brain barrier pathology in patients with severe mental disorders: a systematic review and meta-analysis of biomarkers in case-control studies. *Brain Behav Immun Health* 6:100102.

Galderisi, S., Mucci, A., Buchanan, R. W., Arango, C. (2018). Negative symptoms of schizophrenia: new developments and unanswered research questions. *Lancet Psychiatry* 5(8):664–677.

Gandal, M. J., Haney, J. R., Parikshak, N. N., Leppa, V., Ramaswami, G., Hartl, C., et al. (2018). Shared molecular neuropathology across major psychiatric disorders parallels polygenic overlap. *Science*, 359, 693–697.

Gao, X., Su, X., Han, X., Wen, H., Cheng, C., Zhang, S., et al. (2022). Unsaturated fatty acids in mental disorders: an umbrella review of meta-analyses. *Adv Nutr* 13(6):2217–2236.

Gardiner, E. J., Cairns, M. J., Liu, B., Beveridge, N. J, Carr, V., Kelly, B., et al. (2013). Gene Expression Analysis Reveals Schizophrenia-Associated Dysregulation of Immune Pathways in Peripheral Blood Mononuclear Cells. *J Psychiatr Res* 47:425–37.

Geissmann, F., Manz, M. G., Jung, S., Sieweke, M. H., Merad, M., et al. (2010). Development of monocytes, macrophages, and dendritic cells. *Science* 327:656–661.

Giordano G.M., Bucci P., Mucci A., Pezzella P., Galderisi S. (2021) Gender differences in clinical and psychosocial features among persons with schizophrenia: a mini review. *Front Psychiatry* 12:789179.

Glinka, M. E., Samuels, B. A., Diodato, A., Teillon, J., Feng Mei, D., Shykind, B. M., et al. (2012). Olfactory deficits cause anxiety-like behaviors in mice. J *Neurosci* 32(19):6718–6725.

Godoy, L. D., Rossignoli, M. T., Delfino-Pereira, P., Garcia-Cairasco, N., de Lima Umeoka, E. H. (2018). A comprehensive overview on stress neurobiology: basic concepts and clinical implications. *Front Behav Neurosci* 12:127.

Godoy, M. D., Voegels, R. L., Pinna Fde, R., Imamura, R., Farfel, J. M. (2015). Olfaction in neurologic and neurodegenerative diseases: a literature review. *Int Arch Otorhinolaryngol* 19(2):176–179.

Gogoleva, V. S., Drutskaya, M. S., Atretkhany, K. S. (2019). The role of microglia in the homeostasis of the central nervous system and neuroinflammation. *Mol Biol (Mosk)* 53(5):790–798.

Goldsmith, D. R., Massa, N., Miller, B. J., Miller, A. H., Duncan, E. (2021). The interaction of lipids and inflammatory markers predict negative symptom severity in patients with schizophrenia. *NPJ Schizophr* 7(1):50.

Gomes, F. V., Grace, A. A. (2017). Adolescent stress as a driving factor for schizophrenia development-a basic science perspective. *Schizophr Bull* 43(3):486–489.

Grabert, K., Michoel, T., Karavolos, M. H., Clohisey, S., Baillie, J. K., Stevens, M. P., et al. (2016). Microglial brain region-dependent diversity and selective regional sensitivities to aging. *Nat Neurosci* 19(3):504–516.

Green, K. N., Crapser, J. D., Hohsfield, L. A. (2020). To kill a microglia: a case for CSF1R inhibitors. *Trends Immunol* 41(9):771–784.

Green, M. F., Horan, W. P., Lee, J. (2019). Nonsocial and social cognition in schizophrenia: current evidence and future directions. *World Psychiatry* 18(2):146–161.

Greene, C., Hanley, N., Campbell, M. (2020). Blood-brain barrier associated tight junction disruption is a hallmark feature of major psychiatric disorders. *Transl Psychiatry* 10(1):373.

Greene, C., Kealy, J., Humphries, M. M., Gong, Y., Hou, J., Hudson, N., et al. (2018). Dose-dependent expression of claudin-5 is a modifying factor in schizophrenia. *Mol Psychiatry* 23(11):2156–2166.

Grier, B. D., Belluscio, L., Cheetham, C. E. (2016). Olfactory sensory activity modulates microglial-neuronal interactions during dopaminergic cell loss in the olfactory bulb. *Front Cell Neurosci* 10:178.

Gu, M., Li, X., Yan, L., Zhang, Y., Yang, L., Li, S., et al. (2021). Endogenous ω-3 fatty acids in Fat-1 mice attenuated depression-like behaviors, spatial memory impairment and relevant changes induced by olfactory bulbectomy. *Prostaglandins Leukot Essent Fatty Acids* 171:102313.

Gu, M., Li, Y., Tang, H., Zhang, C., Li, W., Zhang, Y., et al. (2018). Endogenous mmega (n)-3 fatty acids in *Fat-1* mice attenuated depression-like behavior, imbalance between microglial M1 and M2 phenotypes, and dysfunction of neurotrophins induced by lipopolysaccharide administration. *Nutrients* 10(10):1351.

Guilliams, M., Mildner, A., Yona, S. (2018). Developmental and functional heterogeneity of monocytes. *Immunity* 49(4):595–613.

Guo, L.-K., Su, Y., Zhang, Y.-Y.-N., Yu, H., Lu, Z., Li, W.-Q., et al. (2023). Prediction of treatment response to antipsychotic drugs for precision medicine approach to schizophrenia: randomized trials and multiomics analysis. *Military Medical Research* 10(1):24.

Guo, L., Bertola, D. R., Takanohashi, A., Saito, A., Segawa, Y., Yokota, T., et al. (2019). Bi-allelic CSF1R mutations cause skeletal dysplasia of dysosteosclerosis-pyle disease spectrum and degenerative encephalopathy with brain malformation. *Am J Hum Genet* 104(5):925–935.

Halbreich, U. (2021). Stress-related physical and mental disorders: a new paradigm. *BJPsych Advances* 27(3):145–152.

Halder, S. K., Milner, R. (2019). A critical role for microglia in maintaining vascular integrity in the hypoxic spinal cord. *Proc Natl Acad Sci U S A* 116(51):26029–26037.

Halder, S. K., Milner, R. (2020). Mild hypoxia triggers transient blood-brain barrier disruption: a fundamental protective role for microglia. *Acta Neuropathol Commun* 8(1):175.

Hamilton, J. A. (2008). Colony-stimulating factors in inflammation and autoimmunity. *Nat Rev Immunol* 8(7):533–544.

Hamilton, J. A., Hillard, C. J., Spector, A. A., Watkins, P. A. (2007). Brain uptake and utilization of fatty acids, lipids and lipoproteins: application to neurological disorders. *J Mol Neurosci* 33(1):2–11.

Han, B., Wang, J. H., Geng, Y., Shen, L., Wang, H. L., Wang, Y. Y., et al. (2017). Chronic stress contributes to cognitive dysfunction and hippocampal metabolic abnormalities in *APP/PS1* mice. *Cell Physiol Biochem* 41(5):1766–1776.

Han, F., Nakano, T., Yamamoto, Y., Shioda, N., Lu, Y. M., Fukunaga, K. (2009). Improvement of depressive behaviors by nefiracetam is associated with activation of CaM kinases in olfactory bulbectomized mice. *Brain Res* 1265:205–214.

Han, J., Zhu, K., Zhang, X. M., Harris, R. A. (2019). Enforced microglial depletion and repopulation as a promising strategy for the treatment of neurological disorders. *Glia* 67(2):217–231.

Harrison, J. E., Weber, S., Jakob, R., Chute, C.G. (2021). ICD-11: an international classification of diseases for the twenty-first century. *BMC Med Inform Decis Mak* 21(Suppl 6):206.

Haruwaka, K., Ikegami, A., Tachibana, Y., Ohno, N., Konishi, H., Hashimoto, A., et al. (2019). Dual microglia effects on blood brain barrier permeability induced by systemic inflammation. *Nat Commun* 10(1):5816.

Hasegawa, Y., Ma, M., Sawa, A., Lane, A. P., Kamiya, A. (2022). Olfactory impairment in psychiatric disorders: does nasal inflammation impact disease psychophysiology? *Transl Psychiatry* 12(1):314.

Hatakeyama, M., Ninomiya, I., Kanazawa, M. (2020). Angiogenesis and neuronal remodeling after ischemic stroke. *Neural Regen Res* 15(1):16–19.

Hattori, Y. (2023). The microglia-blood vessel interactions in the developing brain. *Neurosci Res* 187:58–66.

He, C., Qu, X., Cui, L., Wang, J., Kang, J. X. (2009). Improved spatial learning performance of *fat-1* mice is associated with enhanced neurogenesis and neuritogenesis by docosahexaenoic acid. *Proc Natl Acad Sci U S A* 106(27):11370–11375.

He, H., Mack, J. J., Güç, E., Warren, C. M., Squadrito, M. L., Kilarski, W. W., et al. (2016). Perivascular macrophages limit permeability. *Arterioscler Thromb Vasc Biol* 36(11):2203–2212.

He, Y., Wang, Y., Wu, Z., Lan, T., Tian, Y., Chen, X., et al. (2020). Metabolomic abnormalities of purine and lipids implicated olfactory bulb dysfunction of CUMS depressive rats. *Metab Brain Dis* 35(4):649–659.

Hennebelle, M., Champeil-Potokar, G., Lavialle, M., Vancassel, S., Denis, I. (2014). Omega-3 polyunsaturated fatty acids and chronic stress-induced modulations of glutamatergic neurotransmission in the hippocampus. *Nutr Rev* 72(2):99–112.

Hinwood, M., Morandini, J., Day, T. A., Walker, F. R. (2012). Evidence that microglia mediate the neurobiological effects of chronic psychological stress on the medial prefrontal cortex. *Cereb Cortex* 22(6):1442–1454.

Hjorthøj, C., Stürup, A. E., McGrath, J. J., Nordentoft, M. (2017). Years of potential life lost and life expectancy in schizophrenia: a systematic review and meta-analysis. *Lancet Psychiatry* 4(4):295–301.

Hodo, T. W., de Aquino, M. T. P., Shimamoto, A., Shanker, A. (2020). Critical neurotransmitters in the neuroimmune network. *Front Immunol* 11:1869.

Holm, M., Taipale, H., Tanskanen, A., Tiihonen, J., Mitterdorfer-Rutz, E. (2021). Employment among people with schizophrenia or bipolar disorder: A population-based study using nationwide registers. *Acta Psychiatr Scand* 143(1):61–71.

Holtzman, C. W., Trotman, H. D., Goulding, S. M., Ryan, A. T., Macdonald, A. N., Shapiro, D. I., et al. (2013). Stress and neurodevelopmental processes in the emergence of psychosis. *Neuroscience* 249:172–191.

Hsu, M.-C., Huang, Y.-S., Ouyang, W.-C. (2020). Beneficial effects of omega-3 fatty acid supplementation in schizophrenia: possible mechanisms. *Lipids in Health and Disease* 19(1):159.

Hu, X., Leak, R. K., Shi, Y., Suenaga, J., Gao, Y., Zheng, P., et al. (2015). Microglial and macrophage polarization—new prospects for brain repair. *Nat Rev Neurol* 11(1):56–64.

Huang, J., Tong, J., Zhang, P., Zhou, Y., Li, Y., Tan, S., et al. (2022). Elevated salivary kynurenic acid levels related to enlarged choroid plexus and severity of clinical phenotypes in treatment-resistant schizophrenia. *Brain Behav Immun* 106:32–39.

Hughes, H. K., Yang, H., Lesh, T. A., Carter, C. S., Ashwood, P. (2022). Evidence of innate immune dysfunction in first-episode psychosis patients with accompanying mood disorder. *J Neuroinflammation* 19(1):287.

Hurwitz, T., Kopala, L., Clark, C., Jones, B. (1988). Olfactory deficits in schizophrenia. *Biol Psychiatry* 23(2):123–128.

Ikezu, S., Yeh, H., Delpech, J. C., Woodbury, M. E., Van Enoo, A. A., Ruan, Z., et al. (2021). Inhibition of colony stimulating factor 1 receptor corrects maternal inflammation-induced microglial and synaptic dysfunction and behavioral abnormalities. *Mol Psychiatry* 26(6):1808–1831.

Iwata, M., Ota, K. T., Li, X. Y., Sakaue, F., Li, N., Dutheil, S., et al. (2016). Psychological stress activates the inflammasome via release of adenosine triphosphate and stimulation of the purinergic type 2X7 receptor. *Biol Psychiatry* 80(1):12–22.

Mildner, A., Schmidt, H., Nitsche, M., Merkler, D., Hanisch, U. K., Mack, M., et al. (2007). Microglia in the adult brain arise from Ly-6ChiCCR2+ monocytes only under defined host conditions. *Nat Neurosci* 10:1544–1553.

Jeppesen, R., Christensen, R. H. B., Pedersen, E. M. J., Nordentoft, M., Hjorthøj, C., Köhler-Forsberg, O., et al. (2020). Efficacy and safety of anti-inflammatory agents in treatment of psychotic disorders - a comprehensive systematic review and meta-analysis. *Brain Behav Immun* 90:364–380.

Jha, P., Das, H. (2017). KLF2 in regulation of NF-κB-mediated immune cell function and inflammation. *Int J Mol Sci* 18(11):2383.

Jiang, W. J., Zhong, B. L., Liu, L. Z., Zhou, Y. J., Hu, X. H., Li, Y. (2018). Reliability and validity of the chinese version of the childhood trauma questionnaire-short form for inpatients with schizophrenia. *PLoS One* 13(12):e0208779.

Jie, R., Chung, S. H. (2007). Anti-inflammatory effect of alpha-linolenic acid and its mode of action through the inhibition of nitric oxide production and inducible nitric oxide synthase gene expression via NF-kappaB and mitogen-activated protein kinase pathways. *J Agric Food Chem* 55(13):5073–5080.

Jones, H. J., Borges, M. C., Carnegie, R., Mongan, D., Rogers, P. J., Lewis, S. J., et al. (2021). Associations between plasma fatty acid concentrations and schizophrenia: a two-sample mendelian randomisation study. *Lancet Psychiatry* 8(12):1062–1070.

Jurga, A. M., Paleczna, M., Kuter, K. Z. (2020). Overview of general and discriminating markers of differential microglia phenotypes. *Front Cell Neurosci* 14:198.

Juruena, M. F., Eror, F., Cleare, A. J., Young, A. H. (2020). The rRole of early life stress in HPA axis and anxiety. *Adv Exp Med Biol* 1191:141–153.

Kadakia, A., Catillon, M., Fan, Q., Williams, G. R., Marden, J. R., Anderson, A., et al. (2022). The economic burden of schizophrenia in the united states. *J Clin Psychiatry* 83(6):22m14458.

Kalin, N. H. (2019). Prefrontal cortical and limbic circuit alterations in psychopathology. *Am J Psychiatry* 176(12):971–973.

Kang, J. X., Wang, J., Wu, L., Kang, Z. B. (2004). Transgenic mice: *fat-1* mice convert n-6 to n-3 fatty acids. *Nature* 427(6974):504.

Kapellos, T. S., Bonaguro, L., Gemünd, I., Reusch, N., Saglam, A., Hinkley, E. R., et al. (2019). Human monocyte subsets and phenotypes in major chronic inflammatory diseases. *Front Immunol* 10:2035.

Katsel, P., Roussos, P., Pletnikov, M., Haroutunian, V. (2017). Microvascular anomaly conditions in psychiatric disease. schizophrenia - angiogenesis connection. *Neurosci Biobehav Rev* 77:327–339.

Katz, R. J., Roth, K. A., Carroll, B. J. (1981). Acute and chronic stress effects on open field activity in the rat: implications for a model of depression. *Neurosci Biobehav Rev* 5(2):247–251.

Kay, S. R., Fiszbein, A., Opler, L. A. (1987) The positive and negative syndrome scale (PANSS) for schizophrenia. *Schizophr Bull* 13(2):261–276.

Kealy, J., Greene, C., Campbell, M. (2020). Blood-brain barrier regulation in psychiatric disorders. *Neurosci Lett* 726:133664.

Keller, A., Malaspina, D. (2013). Hidden consequences of olfactory dysfunction: a patient report series. *BMC Ear Nose Throat Disord* 13(1):8.

Keri, S., Szabo, C., Kelemen, O. (2017). Antipsychotics influence toll-like receptor (TLR) expression and its relationship with cognitive functions in schizophrenia. *Brain Behav Immun* 62:256–264.

Keshvari, S., Caruso, M., Teakle, N., Batoon, L., Sehgal, A., Patkar, O. L., et al. (2021). CSF1R-dependent macrophages control postnatal somatic growth and organ maturation. *PLoS Genet* 17(6):e1009605.

Kim, E. J., Pellman, B., Kim, J. J. (2015). Stress effects on the hippocampus: a critical review. *Learn Mem* 22(9):411–416.

Kivimäki, M., Bartolomucci, A., Kawachi, I. (2023). The multiple roles of life stress in metabolic disorders. *Nat Rev Endocrinol* 19(1):10–27.

Köhler, O., Benros, M., Nordentoft, M., Mors, P., Krogh, J. (2014). Effect of anti-inflammatory treatment on depression, depressive symptoms and side effects: a systematic review and meta-analysis of randomized clinical trials. *European Psychiatry* 30(12):342–342.

Kose, M., Pariante, C. M., Dazzan, P., Mondelli, V. (2021). The role of peripheral inflammation in clinical outcome and brain imaging abnormalities in psychosis: a systematic review. *Front Psychiatry* 12:612471.

Kreisel, T., Frank, M. G., Licht, T., Reshef, R., Ben-Menachem-Zidon, O., Baratta, M. V., et al. (2014). Dynamic microglial alterations underlie stress-induced depressive-like behavior and suppressed neurogenesis. *Mol Psychiatry* 19(6):699–709.

Krkovic, K., Moritz, S., Lincoln, T. M. (2017). Neurocognitive deficits or stress overload: Why do individuals with schizophrenia show poor performance in neurocognitive tests? *Schizophr Res* 183:151–156.

Kuehl, F. A., Jr., Egan, R. W. (1980). Prostaglandins, arachidonic acid, and inflammation. *Science* 210(4473):978–984.

Kugler, E. C., Greenwood, J., MacDonald, R. B. (2021). The "neuro-glial-vascular" unit: the role of glia in neurovascular unit formation and dysfunction. *Front Cell Dev Biol* 9:732820.

Kumar, S., Bandyopadhyay, U. (2005). Free heme toxicity and its detoxification systems in human. *Toxicol Lett* 157(3):175–188.

Kyrou, I., Tsigos, C. (2009). Stress hormones: physiological stress and regulation of metabolism. *Curr Opin Pharmacol* 9(6):787–793.

LaFever, B. J., Imamura, F. (2022). Effects of nasal inflammation on the olfactory bulb. *J Neuroinflammation* 19(1):294.

Lanz, T. A., Reinhart, V., Sheehan, M. J., Rizzo, S. J. S., Bove, S. E., James, L. C., et al. (2019). Postmortem transcriptional profiling reveals widespread increase in inflammation in schizophrenia: a comparison of prefrontal cortex, striatum, and hippocampus among matched tetrads of controls with subjects diagnosed with schizophrenia, bipolar or major depressive disorder. *Transl Psychiatry* 9(1):151.

Laskaris, L. E., Di Biase, M. A., Everall, I., Chana, G., Christopoulos, A., Skafidas, E., et al. (2016). Microglial activation and progressive brain changes in schizophrenia. *Br J Pharmacol* 173(4):666–680.

Lau, C. I., Wang, H. C., Hsu, J. L., Liu, M. E. (2013). Does the dopamine hypothesis explain schizophrenia? *Rev Neurosci* 24(4):389–400.

Le Bon, A. M., Deprêtre, N., Sibille, E., Cabaret, S., Grégoire, S., Soubeyre, V., et al. (2018). Comprehensive study of rodent olfactory tissue lipid composition. *Prostaglandins Leukot Essent Fatty Acids* 131:32–43.

Lehmann, M. L., Samuels, J. D., Kigar, S. L., Poffenberger, C. N., Lotstein, M. L., Herkenham, M. (2022). CCR2 monocytes repair cerebrovascular damage caused by chronic social defeat stress. *Brain Behav Immun* 101:346–358.

Lehmann, M. L., Weigel, T. K., Poffenberger, C. N., Herkenham, M. (2019). The behavioral sequelae of social defeat require microglia and are driven by oxidative stress in mice. *J Neurosci* 39(28):5594–5605.

Leung, D. Y., Lam, T. H., Chan, S. S. (2010). Three versions of perceived stress scale: validation in a sample of Chinese cardiac patients who smoke. *BMC Public Health* 10:513.

Li, J., Huang, H., Fan, R., Hua, Y., Ma, W. (2023). Lipidomic analysis of brain and hippocampus from mice fed with high-fat diet and treated with fecal microbiota transplantation. *Nutrition & Metabolism* 20(1):12.

Li, M., Li, C., Liu, W. X., Liu, C., Cui, J., Li, Q., et al. (2017). Dysfunction of PLA2G6 and CYP2C44-associated network signals imminent carcinogenesis from chronic inflammation to hepatocellular carcinoma. *J Mol Cell Biol* 9(6):489–503.

Li X., Zhou W., Yi Z. (2022) A glimpse of gender differences in schizophrenia. *Gen Psychiatr* 35(4):e100823.

Lieberman, J. A., Girgis, R. R., Brucato, G., Moore, H., Provenzano, F., Kegeles, L., et al. (2018). Hippocampal dysfunction in the pathophysiology of schizophrenia: a selective review and hypothesis for early detection and intervention. *Mol Psychiatry* 23(8):1764–1772.

Liu, L. L., Li, J. M., Su, W. J., Wang, B., Jiang, C. L. (2019). Sex differences in depressive-like behaviour may relate to imbalance of microglia activation in the hippocampus. *Brain Behav Immun* 81:188–197.

López-González, I., Pinacho, R., Vila, È., Escanilla, A., Ferrer, I., Ramos, B. (2019). Neuroinflammation in the dorsolateral prefrontal cortex in elderly chronic schizophrenia. *Eur Neuropsychopharmacol* 29(3):384–396.

Lou, N., Takano, T., Pei, Y., Xavier, A. L., Goldman, S. A., Nedergaard, M. (2016). Purinergic receptor P2RY12-dependent microglial closure of the injured blood-brain barrier. *Proc Natl Acad Sci U S A* 113(4):1074–1079.

Machlitt-Northen, S., Keers, R., Munroe, P. B., Howard, D. M., Pluess, M. (2022). Gene-environment correlation over time: a longitudinal analysis of polygenic risk scores for schizophrenia and major depression in three british cohorts studies. *Genes (Basel)* 13(7):1136.

Mancuso, M. R., Kuhnert, F., Kuo, C. J. (2008). Developmental angiogenesis of the central nervous system. *Lymphat Res Biol* 6(3–4):173–180.

Marchi, N., Rasmussen, P., Kapural, M., Fazio, V., Kight, K., Mayberg, M. R., et al. (2003). Peripheral markers of brain damage and blood-brain barrier dysfunction. *Restor Neurol Neurosci* 21(3–4):109–121.

Martončíková, M., Alexovič Matiašová, A., Ševc, J., Račeková, E. (2021). Relationship between blood vessels and migration of neuroblasts in the olfactory neurogenic region of the rodent brain. *Int J Mol Sci* 22(21):11506.

Mastorakos, P., Mihelson, N., Luby, M., Burks, S. R., Johnson, K., Hsia, A. W., et al. (2021). Temporally distinct myeloid cell responses mediate damage and repair after cerebrovascular injury. *Nat Neurosci* 24(2):245–258.

Masuda, T., Croom, D., Hida, H., Kirov, S. A. (2011). Capillary blood flow around microglial somata determines dynamics of microglial processes in ischemic conditions. *Glia* 59(11):1744–1753.

Masuda, T., Sankowski, R., Staszewski, O., Prinz, M. (2020). Microglia heterogeneity in the single-cell era. *Cell Rep* 30(5):1271–1281.

Mathew, S. A., Bhonde, R. R. (2018). Omega-3 polyunsaturated fatty acids promote angiogenesis in placenta derived mesenchymal stromal cells. *Pharmacol Res* 132:90–98.

Mattei, D., Ivanov, A., Ferrai, C., Jordan, P., Guneykaya, D., Buonfiglioli, A., et al. (2017). Maternal immune activation results in complex microglial transcriptome signature in the adult offspring that is reversed by minocycline treatment. *Transl Psychiatry* 7(5):e1120.

Maydych, V. (2019). The interplay between stress, inflammation, and emotional attention: relevance for depression. *Front Neurosci* 13:384.

Mazza, M. G., Capellazzi, M., Lucchi, S., Tagliabue, I., Rossetti, A., Clerici, M. (2020). Monocyte count in schizophrenia and related disorders: a systematic review and meta-analysis. *Acta Neuropsychiatr* 32(5):229–236.

McCutcheon, R. A., Reis Marques, T., Howes, O. D. (2020). Schizophrenia-an overview. *JAMA Psychiatry* 77(2):201–210.

McEwen, B. S. (2006). Protective and damaging effects of stress mediators: central role of the brain. *Dialogues Clin Neurosci* 8(4):367–381.

McEwen, B. S., Eiland, L., Hunter, R. G., Miller, M. M. (2012). Stress and anxiety: structural plasticity and epigenetic regulation as a consequence of stress. *Neuropharmacology* 62(1):3–12.

McFadden, J. W., Aja, S., Li, Q., Bandaru, V. V., Kim, E. K., Haughey, N. J., et al. (2014). Increasing fatty acid oxidation remodels the hypothalamic neurometabolome to mitigate stress and inflammation. *PLoS One* 9(12):e115642.

McHugh, K., Calcagno, P., Ferdousi, M., Sanchez, C., Roche, M., Finn, D. P., et al. (2019). P.127 Alterations in the central opioid system following acute swim stress and olfactory bulbectomy in the rat. *European Neuropsychopharmacology* 29:S105.

McNamara, R. K. (2016). Role of Omega-3 fatty acids in the etiology, treatment, and prevention of depression: current status and future directions. *J Nutr Intermed Metab* 5:96–106.

McNamara, N. B., Munro, D. A. D., Bestard-Cuche, N., Uyeda, A., Bogie, J. F. J., Hoffmann, A., et al. (2023). Microglia regulate central nervous system myelin growth and integrity. *Nature* 613(7942):120–129.

Mehrabadi, A. R., Korolainen, M. A., Odero, G., Miller, D. W., Kauppinen, T. M. (2017). Poly(ADP-ribose) polymerase-1 regulates microglia mediated decrease of endothelial tight junction integrity. *Neurochem Int* 108:266–271.

Miettinen, A., Zippo, A. G., Patera, A., Bonnin, A., Shahmoradian, S. H., Biella, G. E. B., et al. (2021). Micrometer-resolution reconstruction and analysis of whole mouse brain vasculature by synchrotron-based phase-contrast tomographic microscopy. *BioRxiv*.

Mifsud, K. R., Reul, J. (2018). Mineralocorticoid and glucocorticoid receptor-mediated control of genomic responses to stress in the brain. *Stress* 21(5):389–402.
Moberly, A. H., Schreck, M., Bhattarai, J. P., Zweifel, L. S., Luo, W., Ma, M. (2018). Olfactory inputs modulate respiration-related rhythmic activity in the prefrontal cortex and freezing behavior. *Nat Commun* 9(1):1528.
Mocking, R. J. T., Assies, J., Ruhé, H. G., Schene, A. H. (2018). Focus on fatty acids in the neurometabolic pathophysiology of psychiatric disorders. *J Inherit Metab Dis* 41(4):597–611.
Monteiro, S., Roque, S., de Sá-Calçada, D., Sousa, N., Correia-Neves, M., Cerqueira, J. J. (2015). An efficient chronic unpredictable stress protocol to induce stress-related responses in C57BL/6 mice. *Front Psychiatry* 6:6.
Morales-Medina, J. C., Iannitti, T., Freeman, A., Caldwell, H. K. (2017). The olfactory bulbectomized rat as a model of depression: the hippocampal pathway. *Behav Brain Res* 317:562–575.
Morales-Medina, J. C., Juarez, I., Venancio-García, E., Cabrera, S. N., Menard, C., Yu, W., Flores, G., et al. (2013). Impaired structural hippocampal plasticity is associated with emotional and memory deficits in the olfactory bulbectomized rat. *Neuroscience* 236:233–243.
Morris, G., Puri, B. K., Olive, L., Carvalho, A., Berk, M., Walder, K., et al. (2020). Endothelial dysfunction in neuroprogressive disorders-causes and suggested treatments. *BMC Med* 18(1):305.
Müller, N. (2018). Inflammation in schizophrenia: pathogenetic aspects and therapeutic considerations. *Schizophr Bull* 44(5):973–982.
Muller, N., Wagner, J. K., Krause, D., Weidinger, E., Wildenauer, A., Obermeier, M., et al. (2012). Impaired monocyte activation in schizophrenia. *Psychiatry Res* 198(3):341–346.
Nandam, L. S., Brazel, M., Zhou, M., Jhaveri, D. J. (2019). Cortisol and major depressive disorder-translating findings from humans to animal models and back. *Front Psychiatry* 10:974.
Nandi, S., Gokhan, S., Dai, X. M., Wei, S., Enikolopov, G., Lin, H., et al. (2012). The CSF-1 receptor ligands IL-34 and CSF-1 exhibit distinct developmental brain expression patterns and regulate neural progenitor cell maintenance and maturation. *Dev Biol* 367(2):100–113.
Narasimhan, P. B., Marcovecchio, P., Hamers, A. A. J., Hedrick, C. C. (2019). Non-classical monocytes in health and disease. *Annu Rev Immunol* 37:439–456.
Naudí, A., Cabré, R., Dominguez-Gonzalez, M., Ayala, V., Jové, M., Mota-Martorell, N., et al. (2017). Region-specific vulnerability to lipid peroxidation and evidence of neuronal mechanisms for polyunsaturated fatty acid biosynthesis in the healthy adult human central nervous system. *Biochim Biophys Acta Mol Cell Biol Lipids* 1862(5):485–495.
Neumann, H., Kotter, M. R., Franklin, R. J. (2009). Debris clearance by microglia: an essential link between degeneration and regeneration. *Brain* 132(Pt 2):288–295.
Nguyen, T. T., Dev, S. I., Chen, G., Liou, S. C., Martin, A. S., Irwin, M. R., et al. (2018). Abnormal levels of vascular endothelial biomarkers in schizophrenia. *Eur Arch Psychiatry Clin Neurosci* 268(8):849–860.
Nicholas, R. S., Wing, M. G., Compston, A. (2001). Nonactivated microglia promote oligodendrocyte precursor survival and maturation through the transcription factor NF-kappa B. *Eur J Neurosci* 13(5):959–967.

Nikolakopoulou, A. M., Dutta, R., Chen, Z., Miller, R. H., Trapp, B. D. (2013). Activated microglia enhance neurogenesis via trypsinogen secretion. *Proc Natl Acad Sci U S A* 110(21):8714–8719.

Nimmerjahn, A., Kirchhoff, F., Helmchen, F. (2005). Resting microglial cells are highly dynamic surveillants of brain parenchyma in vivo. *Science* 308(5726):1314–1318.

Nitta, M., Kishimoto, T., Müller, N., Weiser, M., Davidson, M., Kane, J. M., et al. (2013). Adjunctive use of nonsteroidal anti-inflammatory drugs for schizophrenia: a meta-analytic investigation of randomized controlled trials. *Schizophr Bull* 39(6):1230–1241.

Noerman, S., Klåvus, A., Järvelä-Reijonen, E., Karhunen, L., Auriola, S., Korpela, R., et al. (2020). Plasma lipid profile associates with the improvement of psychological well-being in individuals with perceived stress symptoms. *Sci Rep* 10(1):2143.

Nollet, M. (2021). Models of depression: unpredictable chronic mild stress in mice. *Curr Protoc* 1(8):e208.

Nugent, A. A., Lin, K., van Lengerich, B., Lianoglou, S., Przybyla, L., Davis, S. S., et al. (2020). TREM2 regulates microglial cholesterol metabolism upon chronic phagocytic challenge. *Neuron* 105(5):837–854.e839.

Ong, S. M., Hadadi, E., Dang, T. M., Yeap, W. H., Tan, C. T., Ng, T. P., et al. (2018). The pro-inflammatory phenotype of the human non-classical monocyte subset is attributed to senescence. *Cell Death Dis* 9(3):266.

Ortiz de Montellano, P. R. (2008) Hemes in biology. *John Wiley & Sons, Inc* 1–10.

Paolicelli, R. C., Bolasco, G., Pagani, F., Maggi, L., Scianni, M., Panzanelli, P., et al. (2011). Synaptic pruning by microglia is necessary for normal brain development. *Science* 333(6048):1456–1458.

Paolicelli, R. C., Sierra, A., Stevens, B., Tremblay, M. E., Aguzzi, A., Ajami, B., et al. (2022). Microglia states and nomenclature: a field at its crossroads. *Neuron* 110(21):3458–3483.

Park, L., Uekawa, K., Garcia-Bonilla, L., Koizumi, K., Murphy, M., Pistik, R., et al. (2017). Brain perivascular macrophages initiate the neurovascular dysfunction of alzheimer Aβ peptides. *Circ Res* 121(3):258–269.

Passos, S., Carvalho, L. P., Costa, R. S., Campos, T. M., Novais, F. O., Magalhães, A., et al. (2015). Intermediate monocytes contribute to pathologic immune response in leishmania braziliensis infections. *J Infect Dis* 211(2):274–282.

Pedragosa, J., Salas-Perdomo, A., Gallizioli, M., Cugota, R., Miró-Mur, F., Briansó, F., et al. (2018). CNS-border associated macrophages respond to acute ischemic stroke attracting granulocytes and promoting vascular leakage. *Acta Neuropathol Commun* 6(1):76.

Peng, Z.-x., Wang, Y., Gu, X., Xue, Y., Wu, Q., Zhou, J.-y., et al. (2015). Metabolic transformation of breast cancer in a MCF-7 xenograft mouse model and inhibitory effect of volatile oil from Saussurea lappa Decne treatment. *Metabolomics* 11(3):636–656.

Penninx, B., Lange, S. M. M. (2018). Metabolic syndrome in psychiatric patients: overview, mechanisms, and implications. *Dialogues Clin Neurosci* 20(1):63–73.

Piirainen, S., Chithanathan, K., Bisht, K., Piirsalu, M., Savage, J. C., Tremblay, M. E., et al. (2021). Microglia contribute to social behavioral adaptation to chronic stress. *Glia* 69(10):2459–2473.

Pillinger, T., Beck, K., Stubbs, B., Howes, O. D. (2017). Cholesterol and triglyceride levels in first-episode psychosis: systematic review and meta-analysis. *Br J Psychiatry* 211(6):339–349.

Pittenger, C., Duman, R. S. (2008). Stress, depression, and neuroplasticity: a convergence of mechanisms. *Neuropsychopharmacology* 33(1):88–109.
Planchez, B., Surget, A., Belzung, C. (2019). Animal models of major depression: drawbacks and challenges. *J Neural Transm (Vienna)* 126(11):1383–1408.
Pollak, T. A., Drndarski, S., Stone, J. M., David, A. S., McGuire, P., Abbott, N. J. (2018). The blood-brain barrier in psychosis. *Lancet Psychiatry* 5(1):79–92.
Pruessner, M., Iyer, S. N., Faridi, K., Joober, R., Malla, A. K. (2011). Stress and protective factors in individuals at ultra-high risk for psychosis, first episode psychosis and healthy controls. *Schizophr Res* 129(1):29–35.
Raphael, W., Sordillo, L. M. (2013). Dietary polyunsaturated fatty acids and inflammation: the role of phospholipid biosynthesis. *International Journal of Molecular Sciences* 14(10):21167–21188.
Ray, A., Gulati, K., Rai, N. (2017). Stress, anxiety, and immunomodulation: a pharmacological analysis. *Vitam Horm* 103:1–25.
Régnier-Vigouroux, A. (2003). The mannose receptor in the brain. *Int Rev Cytol* 226:321–342.
Reshef, R., Kudryavitskaya, E., Shani-Narkiss, H., Isaacson, B., Rimmerman, N., Mizrahi, A., et al. (2017). The role of microglia and their CX3CR1 signaling in adult neurogenesis in the olfactory bulb. *Elife* 6: e30809.
Ribeiro Xavier, A. L., Kress, B. T., Goldman, S. A., Lacerda de Menezes, J. R., Nedergaard, M. (2015). A distinct population of microglia supports adult neurogenesis in the subventricular zone. *J Neurosci* 35(34):11848–11861.
Rice, R. A., Spangenberg, E. E., Yamate-Morgan, H., Lee, R. J., Arora, R. P., Hernandez, M. X., et al. (2015). Elimination of microglia improves functional outcomes following extensive neuronal loss in the hippocampus. *J Neurosci* 35(27):9977–9989.
Rinwa, P., Kumar, A. (2013). Quercetin suppress microglial neuroinflammatory response and induce antidepressent-like effect in olfactory bulbectomized rats. *Neuroscience* 255:86–98.
Ronaldson, P. T., Davis, T. P. (2020). Regulation of blood-brain barrier integrity by microglia in health and disease: a therapeutic opportunity. *J Cereb Blood Flow Metab* 40(1_suppl):S6-s24.
Rosin, J. M., Vora, S. R., Kurrasch, D. M. (2018). Depletion of embryonic microglia using the CSF1R inhibitor PLX5622 has adverse sex-specific effects on mice, including accelerated weight gain, hyperactivity and anxiolytic-like behaviour. *Brain Behav Immun* 73:682–697.
Ruiz, M., Jové, M., Schlüter, A., Casasnovas, C., Villarroya, F., Guilera, C., et al. (2015). Altered glycolipid and glycerophospholipid signaling drive inflammatory cascades in adrenomyeloneuropathy. *Human Molecular Genetics* 24(24):6861.
Sæther, L. S., Ueland, T., Haatveit, B., Maglanoc, L. A., Szabo, A., Djurovic, S., et al. (2023). Inflammation and cognition in severe mental illness: patterns of covariation and subgroups. *Mol Psychiatry* 28(3):1284–1292.
Saijo, K., Glass, C. (2011). Microglial cell origin and phenotypes in health and disease. *Nat Rev Immunol* 11: 775–787.
Salminen, A. (2020). Activation of immunosuppressive network in the aging process. *Ageing Res Rev* 57:100998.
Sarabdjitsingh, R. A., Loi, M., Joëls, M., Dijkhuizen, R. M., van der Toorn, A. (2017). Early life stress-induced alterations in rat brain structures measured with high resolution MRI. *PLoS One* 12(9):e0185061.

Saraswathi, V., Wu, G., Toborek, M., Hennig, B. (2004). Linoleic acid-induced endothelial activation: role of calcium and peroxynitrite signaling. *J Lipid Res* 45(5):794–804.

Schmidl, C., Renner, K., Peter, K., Eder, R., Lassmann, T., Balwierz, P. J., Itoh, M., et al. (2014). Transcription and enhancer profiling in human monocyte subsets. *Blood* 123(17):e90–99.

Schmidt, L., Phelps, E., Friedel, J., Shokraneh, F. (2019). Acetylsalicylic acid (aspirin) for schizophrenia. *Cochrane Database Syst Rev* 8(8):Cd012116.

Schwarz, E., Prabakaran, S., Whitfield, P., Major, H., Leweke, F. M., Koethe, D., McKenna, P., et al. (2008). High throughput lipidomic profiling of schizophrenia and bipolar disorder brain tissue reveals alterations of free fatty acids, phosphatidylcholines, and ceramides. *J Proteome Res* 7(10):4266–4277.

Scott, M. R., Zong, W., Ketchesin, K. D., Seney, M. L., Tseng, G. C., Zhu, B., et al. (2023). Twelve-hour rhythms in transcript expression within the human dorsolateral prefrontal cortex are altered in schizophrenia. *PLoS Biol* 21(1):e3001688.

Sellgren, C. M., Gracias, J., Watmuff, B., Biag, J. D., Thanos, J. M., Whittredge, P. B., et al. (2019). Increased synapse elimination by microglia in schizophrenia patient-derived models of synaptic pruning. *Nat Neurosci* 22(3):374–385.

Seo, Y., Kim, H. S., Kang, K. S. (2018). Microglial involvement in the development of olfactory dysfunction. *J Vet Sci* 19(3):319–330.

Shi, C., Kang, L., Yao, S., Ma, Y., Li, T., Liang, Y., et al. (2015). The MATRICS consensus cognitive battery (MCCB): co-norming and standardization in china. *Schizophr Res* 169(1–3):109–115.

Shimamoto-Mitsuyama, C., Nakaya, A., Esaki, K., Balan, S., Iwayama, Y., Ohnishi, T., et al. (2021). Lipid pathology of the corpus callosum in schizophrenia and the potential role of abnormal gene regulatory networks with reduced microglial marker expression. *Cereb Cortex* 31(1):448–462.

Si, T., Yang, J., Shu, L., Wang, X., Kong, Q., Zhou, M., et al. (2004). The Reliability,Validity of PANSS and its Implication. *J Chinese Mental Health* 01:45–47.

Siegel, B. I., Sengupta, E. J., Edelson, J. R., Lewis, D. A., Volk, D. W. (2014). Elevated viral restriction factor levels in cortical blood vessels in schizophrenia. *Biol Psychiatry* 76(2):160–167.

Skelin, I., Kovačević, T., Sato, H., Diksic, M. (2011). Upregulated arachidonic acid signalling in the olfactory bulbectomized rat model of depression. *Neurochemistry International* 58(4):483–488.

Snijders, G., van Zuiden, W., Sneeboer, M. A. M., Berdenis van Berlekom, A., van der Geest, A. T., Schnieder, T., et al. (2021). A loss of mature microglial markers without immune activation in schizophrenia. *Glia* 69(5):1251–1267.

Song, C., Leonard, B. E. (2005). The olfactory bulbectomised rat as a model of depression. *Neurosci Biobehav Rev* 29(4–5):627–647.

Song, C., Phillips, A. G., Leonard, B. E., Horrobin, D. F. (2004). Ethyl-eicosapentaenoic acid ingestion prevents corticosterone-mediated memory impairment induced by central administration of interleukin-1|[beta]| in rats. *Mol Psychiatry* 9(6):630–638.

Song, C., Shieh, C. H., Wu, Y. S., Kalueff, A., Gaikwad, S., Su, K. P. (2016). The role of omega-3 polyunsaturated fatty acids eicosapentaenoic and docosahexaenoic acids in the treatment of major depression and alzheimer's disease: acting separately or synergistically? *Progress in Lipid Research* 62:41–54.

Spence, J. S., He, R., Hoffmann, H. H., Das, T., Thinon, E., Rice, C. M., et al. (2019). IFITM3 directly engages and shuttles incoming virus particles to lysosomes. *Nat Chem Biol* 15(3):259–268.

Spiller, K. J., Restrepo, C. R., Khan, T., Dominique, M. A., Fang, T. C., Canter, R. G., et al. (2018). Microglia-mediated recovery from ALS-relevant motor neuron degeneration in a mouse model of TDP-43 proteinopathy. *Nat Neurosci* 21(3):329–340.

Steiner, J., Mawrin, C., Ziegeler, A., Bielau, H., Ullrich, O., Bernstein, H. G., et al. (2006). Distribution of HLA-DR-positive microglia in schizophrenia reflects impaired cerebral lateralization. *Acta Neuropathol* 112(3):305–316.

Stephens, M. A., Wand, G. (2012). Stress and the HPA axis: role of glucocorticoids in alcohol dependence. *Alcohol Res* 34(4):468–483.

Studerus, E., Ittig, S., Beck, K., Del Cacho, N., Vila-Badia, R., Butjosa, A., et al. (2021). Relation between self-perceived stress, psychopathological symptoms and the stress hormone prolactin in emerging psychosis. *J Psychiatr Res* 136:428–434.

Sugama, S., Kakinuma, Y. (2020). Stress and brain immunity: microglial homeostasis through hypothalamus-pituitary-adrenal gland axis and sympathetic nervous system. *Brain Behav Immun Health* 7:100111.

Sugama, S., Takenouchi, T., Hashimoto, M., Ohata, H., Takenaka, Y., Kakinuma, Y. (2019). Stress-induced microglial activation occurs through β-adrenergic receptor: noradrenaline as a key neurotransmitter in microglial activation. *J Neuroinflammation* 16(1):266.

Sweeney, M. D., Sagare, A. P., Zlokovic, B. V. (2018). Blood-brain barrier breakdown in alzheimer disease and other neurodegenerative disorders. *Nat Rev Neurol* 14(3):133–150.

Takahashi, K., Nakagawasai, O., Nemoto, W., Kadota, S., Isono, J., Odaira, T., et al. (2018). Memantine ameliorates depressive-like behaviors by regulating hippocampal cell proliferation and neuroprotection in olfactory bulbectomized mice. *Neuropharmacology* 137:141–155.

Tam, S. J., Watts, R. J. (2010). Connecting vascular and nervous system development: angiogenesis and the blood-brain barrier. *Annu Rev Neurosci* 33:379–408.

Tan, Y. L., Yuan, Y., Tian, L. (2020). Microglial regional heterogeneity and its role in the brain. *Mol Psychiatry* 25(2):351–367.

Tanaka, S., Ohgidani, M., Hata, N., Inamine, S., Sagata, N., Shirouzu, N., et al. (2021). CD206 expression in induced microglia-like cells from peripheral blood as a surrogate biomarker for the specific immune microenvironment of neurosurgical diseases including glioma. *Front Immunol* 12:670131.

Tandon, R., Gaebel, W., Barch, D. M., Bustillo, J., Gur, R. E., Heckers, S., et al. (2013). Definition and description of schizophrenia in the DSM-5. *Schizophr Res* 150(1):3–10.

Tasset, I., Medina, F. J., Peña, J., Jimena, I., Del, C. M. M., Salcedo, M., et al. (2010). Olfactory bulbectomy induced oxidative and cell damage in rat: protective effect of melatonin. *Physiological Research* 59(1):105–112.

Tay, T. L., Béchade, C., D'Andrea, I., St-Pierre, M. K., Henry, M. S., Roumier, A., et al. (2017). Microglia gone rogue: impacts on psychiatric disorders across the lifespan. *Front Mol Neurosci* 10:421.

Tian, Y., Zhu, P., Liu, S., Jin, Z., Li, D., Zhao, H., et al. (2019). IL-4-polarized BV2 microglia cells promote angiogenesis by secreting exosomes. *Adv Clin Exp Med* 28(4):421–430.

Torres, L., Danver, J., Ji, K., Miyauchi, J. T., Chen, D., Anderson, M. E., et al. (2016). Dynamic microglial modulation of spatial learning and social behavior. *Brain Behav Immun* 55:6–16.

Tran, I., Gellner, A. K. (2023). Long-term effects of chronic stress models in adult mice. *J Neural Transm* (Vienna) 10.1007/s00702-023-02598-6.

Trow, J. E., Jones, A. M., McDonald, R. J. (2019). Comparison of the effects of repeated exposures to predictable or unpredictable stress on the behavioural expression of fear in a discriminative fear conditioning to context task. *Physiol Behav* 208:112556.

Tufo, C., Poopalasundaram, S., Dorrego-Rivas, A., Ford, M. C., Graham, A., Grubb, M. S. (2022). Development of the mammalian main olfactory bulb. *Development* 149(3):dev200210.

Uher, R., Zwicker, A. (2017). Etiology in psychiatry: embracing the reality of poly-gene-environmental causation of mental illness. *World Psychiatry* 16(2):121–129.

Umpierre, A. D., Wu, L. J. (2021). How microglia sense and regulate neuronal activity. *Glia* 69(7):1637–1653.

Uno, Y., Coyle, J. T. (2019). Glutamate hypothesis in schizophrenia. *Psychiatry Clin Neurosci* 73(5):204–215.

Uranova, N. A., Bonartsev, P. D., Androsova, L. V., Rakhmanova, V. I., Kaleda, V. G. (2017). Impaired monocyte activation in schizophrenia: ultrastructural abnormalities and increased IL-1β production. *Eur Arch Psychiatry Clin Neurosci* 267(5):417–426.

Vafadari, B., Mitra, S., Stefaniuk, M., Kaczmarek, L. (2019). Psychosocial stress induces schizophrenia-like behavior in mice with reduced MMP-9 activity. *Front Behav Neurosci* 13:195.

van Berckel, B. N., Bossong, M. G., Boellaard, R., Kloet, R., Schuitemaker, A., Caspers, E., et al. (2008). Microglia activation in recent-onset schizophrenia: a quantitative (R)-[11C]PK11195 positron emission tomography study. *Biol Psychiatry* 64(9):820–822.

van der Spek, A., Stewart, I. D., Kühnel, B., Pietzner, M., Alshehri, T., Gauß, F., et al. (2023). Circulating metabolites modulated by diet are associated with depression. *Mol Psychiatry* 10.1038/s41380-023-02180-2.

van Os, J., Kapur, S. (2009). Schizophrenia. *Lancet* 374(9690):635–645.

van Os, J., Rutten, B. P., Poulton, R. (2008). Gene-environment interactions in schizophrenia: review of epidemiological findings and future directions. *Schizophr Bull* 34(6):1066–1082.

Van Hove, H., Martens, L., Scheyltjens, I., De Vlaminck, K., Pombo Antunes, A. R., De Prijck, S., et al. (2019). A single-cell atlas of mouse brain macrophages reveals unique transcriptional identities shaped by ontogeny and tissue environment. *Nature neuroscience* 22(6): 1021–1035.

van Riezen, H., Schnieden, H., Wren, A. (1976). Behavioural changes following olfactory bulbectomy in rats: a possible model for the detection of antidepressant drugs [proceedings]. *Br J Pharmacol* 57(3):426p–427p.

Vidal-Itriago, A., Radford, R. A. W., Aramideh, J. A., Maurel, C., Scherer, N. M., Don, E. K., et al. (2022). Microglia morphophysiological diversity and its implications for the CNS. *Front Immunol* 13:997786.

Villani, A. C., Satija, R., Reynolds, G., Sarkizova, S., Shekhar, K., Fletcher, J., et al. (2017). Single-cell RNA-seq reveals new types of human blood dendritic cells, monocytes, and progenitors. *Science* 356(6335).

Wallace, J., Lord, J., Dissing-Olesen, L., Stevens, B., Murthy, V. N. (2020). Microglial depletion disrupts normal functional development of adult-born neurons in the olfactory bulb. *Elife* 9:e50531.

Wang, C., Yue, H., Hu, Z., Shen, Y., Ma, J., Li, J., et al. (2020). Microglia mediate forgetting via complement-dependent synaptic elimination. *Science* 367(6478):688–694.

Wang, D., Li, S. P., Fu, J. S., Zhang, S., Bai, L., Guo, L. (2016). Resveratrol defends blood-brain barrier integrity in experimental autoimmune encephalomyelitis mice. *J Neurophysiol* 116(5):2173–2179.

Wang, D., Noda, Y., Tsunekawa, H., Zhou, Y., Miyazaki, M., Senzaki, K., et al. (2007). Behavioural and neurochemical features of olfactory bulbectomized rats resembling depression with comorbid anxiety. *Behav Brain Res* 178(2):262–273.

Wang, G., Zhang, J., Hu, X., Zhang, L., Mao, L., Jiang, X., et al. (2013). Microglia/macrophage polarization dynamics in white matter after traumatic brain injury. *J Cereb Blood Flow Metab* 33(12):1864–1874.

Wang, H., He, Y., Sun, Z., Ren, S., Liu, M., Wang, G., et al. (2022). Microglia in depression: an overview of microglia in the pathogenesis and treatment of depression. *J Neuroinflammation* 19(1):132.

Wang, J., Lai, S., Li, G., Zhou, T., Wang, B., Cao, F., et al. (2020). Microglial activation contributes to depressive-like behavior in dopamine D3 receptor knockout mice. *Brain Behav Immun* 83:226–238.

Wang, J., Shi, Y., Zhang, L., Zhang, F., Hu, X., Zhang, W., et al. (2014). Omega-3 polyunsaturated fatty acids enhance cerebral angiogenesis and provide long-term protection after stroke. *Neurobiol Dis* 68:91–103.

Wannan, C. M. J., Cropley, V. L., Chakravarty, M. M., Bousman, C., Ganella, E. P., Bruggemann, J. M., et al. (2019). Evidence for network-based cortical thickness reductions in schizophrenia. *Am J Psychiatry* 176(7):552–563.

Want, E. J., Wilson, I. D., Gika, H., Theodoridis, G., Plumb, R. S., Shockcor, J., et al. (2010). Global metabolic profiling procedures for urine using UPLC-MS. *Nat Protoc* 5(6):1005–1018.

Watanabe, S., Kanada, S., Takenaka, M., Hamazaki, T. (2004). Dietary n-3 fatty acids selectively attenuate LPS-induced behavioral depression in mice. *Physiology & Behavior* 81(4):605–613.

Weber, M. D., Frank, M. G., Tracey, K. J., Watkins, L. R., Maier, S. F. (2015). Stress induces the danger-associated molecular pattern HMGB-1 in the hippocampus of male sprague dawley rats: a priming stimulus of microglia and the NLRP3 inflammasome. *J Neurosci* 35(1):316–324.

Weber, M. D., Godbout, J. P., Sheridan, J. F. (2017). Repeated social defeat, neuroinflammation, and behavior: monocytes carry the signal. *Neuropsychopharmacology* 42(1):46–61.

Weber, M. D., McKim, D. B., Niraula, A., Witcher, K. G., Yin, W., Sobol, C. G., et al. (2019). The influence of microglial elimination and repopulation on stress sensitization induced by repeated social defeat. *Biol Psychiatry* 85(8):667–678.

Weber, N. S., Gressitt, K. L., Cowan, D. N., Niebuhr, D. W., Yolken, R. H., Severance, E. G. (2018). Monocyte activation detected prior to a diagnosis of schizophrenia in the US military new onset psychosis project (MNOPP). *Schizophr Res* 197:465–469.

Willis, C. L., Garwood, C. J., Ray, D. E. (2007). A size selective vascular barrier in the rat area postrema formed by perivascular macrophages and the extracellular matrix. *Neuroscience* 150(2):498–509.

Willner, P. (2017). The chronic mild stress (CMS) model of depression: history, evaluation and usage. *Neurobiol Stress* 6:78–93.
Winship, I. R., Dursun, S. M., Baker, G. B., Balista, P. A., Kandratavicius, L., Maia-de-Oliveira, J. P., et al. (2019). An overview of animal models related to schizophrenia. *Can J Psychiatry* 64(1):5–17.
Wohleb, E. S., Franklin, T., Iwata, M., Duman, R. S. (2016). Integrating neuroimmune systems in the neurobiology of depression. *Nat Rev Neurosci* 17(8):497–511.
Wohleb, E. S., McKim, D. B., Shea, D. T., Powell, N. D., Tarr, A. J., Sheridan, J. F., et al. (2014a). Re-establishment of anxiety in stress-sensitized mice is caused by monocyte trafficking from the spleen to the brain. *Biol Psychiatry* 75(12):970–981.
Wohleb, E. S., McKim, D. B., Sheridan, J. F., Godbout, J. P. (2014b). Monocyte trafficking to the brain with stress and inflammation: a novel axis of immune-to-brain communication that influences mood and behavior. *Front Neurosci* 8:447.
Wohleb, E. S., Terwilliger, R., Duman, C. H., Duman, R. S. (2018). Stress-induced neuronal colony stimulating factor 1 provokes microglia-mediated neuronal remodeling and depressive-like behavior. *Biol Psychiatry* 83(1):38–49.
Wong, K. L., Tai, J. J., Wong, W. C., Han, H., Sem, X., Yeap, W. H., et al. (2011). Gene expression profiling reveals the defining features of the classical, intermediate, and nonclassical human monocyte subsets. *Blood* 118(5):e16–31.
Wu, K., Gao, X., Shi, B., Chen, S., Zhou, X., Li, Z., et al. (2016). Enriched endogenous n-3 polyunsaturated fatty acids alleviate cognitive and behavioral deficits in a mice model of Alzheimer's disease. *Neuroscience* 333:345–355.
Wu, Q., Xia, D. M., Lan, F., Wang, Y. K., Tan, X., Sun, J. C., et al. (2019). UPLC-QTOF/MS-based metabolomics reveals the mechanism of chronic unpredictable mild stress-induced hypertension in rats. *Biomed Chromatogr* 33(10):e4619.
Xia, Y., Zhang, Z., Lin, W., Yan, J., Zhu, C., Yin, D., et al. (2020). Modulating microglia activation prevents maternal immune activation induced schizophrenia-relevant behavior phenotypes via arginase 1 in the dentate gyrus. *Neuropsychopharmacology* 45(11):1896–1908.
Xie, Y., Li, J., Kang, R., Tang, D. (2020). Interplay between lipid metabolism and autophagy. *Front Cell Dev Biol* 8:431.
Yamanaka, G., Morichi, S., Takamatsu, T., Watanabe, Y., Suzuki, S., Ishida, Y., et al. (2009). Links between Immune Cells from the Periphery and the Brain in the Pathogenesis of Epilepsy: A Narrative Review. *Int J Mol Sci* 22(9):4395.
Yan, L., Jayaram, M., Chithanathan, K., Zharkovsky, A., Tian, L. (2021). Sex-specific microglial activation and SARS-CoV-2 receptor expression induced by chronic unpredictable stress. *Front Cell Neurosci* 15:750373.
Yang, D., Wang, X., Zhang, L., Fang, Y., Zheng, Q., Liu, X., et al. (2022). Lipid metabolism and storage in neuroglia: role in brain development and neurodegenerative diseases. *Cell Biosci* 12(1):106.
Yang, J., Yang, N., Zhao, H., Qiao, Y., Li, Y., Wang, C., et al. (2022). Adipose transplantation improves olfactory function and neurogenesis via PKCα-involved lipid metabolism in Seipin Knockout mice, *Research Square*.
Yang, K., Hua, J., Etyemez, S., Paez, A., Prasad, N., Ishizuka, K., et al. (2021). Volumetric alteration of olfactory bulb and immune-related molecular changes in olfactory epithelium in first episode psychosis patients. *Schizophr Res* 235:9–11.
Yang, L. G., Song, Z. X., Yin, H., Wang, Y. Y., Shu, G. F., Lu, H. X., et al. (2016). Low n-6/n-3 PUFA ratio improves lipid metabolism, inflammation, oxidative stress

and endothelial function in rats using plant oils as n-3 fatty acid source. *Lipids* 51(1):49–59.
Yang, Q. Q., Zhou, J. W. (2019). Neuroinflammation in the central nervous system: symphony of glial cells. *Glia* 67(6):1017–1035.
Yang, T., Guo, R., Zhang, F. (2019). Brain perivascular macrophages: recent advances and implications in health and diseases. *CNS Neurosci Ther* 25(12):1318–1328.
Yang, X., Li, M., Jiang, J., Hu, X., Qing, Y., Sun, L., et al. (2021). Dysregulation of phospholipase and cyclooxygenase expression is involved in Schizophrenia. *EBioMedicine* 64:103239.
Yu, F., Wang, Y., Stetler, A. R., Leak, R. K., Hu, X., Chen, J. (2022). Phagocytic microglia and macrophages in brain injury and repair. *CNS Neurosci Ther* 28(9):1279–1293.
Yu, X., Ji, C., Shao, A. (2020). Neurovascular unit dysfunction and neurodegenerative disorders. *Front Neurosci* 14:334.
Yuan, N., Chen, Y., Xia, Y., Dai, J., Liu, C. (2019). Inflammation-related biomarkers in major psychiatric disorders: a cross-disorder assessment of reproducibility and specificity in 43 meta-analyses. *Transl Psychiatry* 9(1):233.
Zawada, A. M., Rogacev, K. S., Rotter, B., Winter, P., Marell, R. R., Fliser, D., et al. (2011). SuperSAGE evidence for CD14++CD16+ monocytes as a third monocyte subset. *Blood* 118(12):e50–61.
Zhan, L., Fan, L., Kodama, L., Sohn, P. D., Wong, M. Y., Mousa, G. A., et al. (2020). A MAC2-positive progenitor-like microglial population is resistant to CSF1R inhibition in adult mouse brain. *Elife* 9:e51796.
Zhang, J., Chang, L., Pu, Y., Hashimoto, K. (2020). Abnormal expression of colony stimulating factor 1 receptor (CSF1R) and transcription factor PU.1 (SPI1) in the spleen from patients with major psychiatric disorders: a role of brain-spleen axis. *J Affect Disord* 272:110–115.
Zhang, L., Zheng, H., Wu, R., Kosten, T. R., Zhang, X. Y., Zhao, J. (2019). The effect of minocycline on amelioration of cognitive deficits and pro-inflammatory cytokines levels in patients with schizophrenia. *Schizophr Res* 212:92–98.
Zhang, L., Zheng, H., Wu, R., Zhu, F., Kosten, T. R., Zhang, X. Y., et al. (2018). Minocycline adjunctive treatment to risperidone for negative symptoms in schizophrenia: association with pro-inflammatory cytokine levels. *Prog Neuropsychopharmacol Biol Psychiatry* 85:69–76.
Zhao, X., Eyo, U. B., Murugan, M., Wu, L. J. (2018). Microglial interactions with the neurovascular system in physiology and pathology. *Dev Neurobiol* 78(6):604–617.
Zhao, Y., Xiao, W., Chen, K., Zhan, Q., Ye, F., Tang, X., et al. (2019). Neurocognition and social cognition in remitted first-episode schizophrenia: correlation with VEGF serum levels. *BMC Psychiatry* 19(1):403.
Zheng, L., Guo, Y., Zhai, X., Zhang, Y., Chen, W., Zhu, Z., et al. (2022). Perivascular macrophages in the CNS: From health to neurovascular diseases. *CNS Neurosci Ther* 28(12):1908–1920.
Zhou, G., Soufan, O., Ewald, J., Hancock, R. E. W., Basu, N., Xia, J. (2019). NetworkAnalyst 3.0: a visual analytics platform for comprehensive gene expression profiling and meta-analysis. *Nucleic Acids Res* 47(W1):W234–w241.
Zhou, Y., Huang, J., Zhang, P., Tong, J., Fan, F., Gou, M., et al. (2021). Allostatic load effects on cortical and cognitive deficits in essentially normotensive, normoweight patients with schizophrenia. *Schizophr Bull* 47(4):1048–1057.

Zhou, Y. F., Huang, J. C., Zhang, P., Fan, F. M., Chen, S., Fan, H. Z., et al. (2020). Choroid plexus enlargement and allostatic load in schizophrenia. *Schizophr Bull* 46(3):722–731.

Ziegler-Heitbrock, L., Ancuta, P., Crowe, S., Dalod, M., Grau, V., Hart, D. N., et al. (2010). Nomenclature of monocytes and dendritic cells in blood. *Blood* 116(16): e74–80.

9. SUMMARY IN ESTONIAN

Stressiga seotud immuunmehhanismid skisofreenia puhul: regioonispetsiiflise mikrogliia-neurovaskulaarsüsteemi interaktsiooni olulisus

Psühhiaatrilised häired on tööealise elanikkonna hulgas üks peamiseid puude ja surma põhjuseid, suurendades ülemaailmselt märkimisväärset majanduslikku ja tervishoiukoormust. Psühhiaatrilisi häireid võivad esile kutsuda mitmesugused organismi sisemised ja välised tegurid, mis koostoimides mõjutavad aju talitlust ja selle kaudu käitumist. Psühhosotsiaalne stress on laialt tunnustatud skisofreenia tekke ja arengu riskitegur. Teiste bioloogiliste mehhanismide hulgas häirib krooniline stress aju vereringet ja süvendab neuropõletikku. Veresoontega seotud mikrogliia ja monotsüütidest pärinevad makrofaagid on neuropõletiku kõige olulisemateks regulaatoriteks. Selleks, et paremini mõista mikrogliia ja monotsüütide funktsiooni kroonilisest stressist lähtudes, viisime läbi terve rea kliinilisi ja prekliinilisi uuringuid skisofreenia esmasepisoodi (FES) patsientide rühmas, samuti hiirtel, kellel oli rakendatud kroonilist ettearvamatut stressi ja haistesibula purustamisest (OBX) tingitud stressi. Kliiniliste uuringute käigus leidsime, et FES patsientidel, kellel esines kõrgenenud tajutud stressi tase, neil avaldus ajukoore mahu vähenemine otsmikusagaras. Samuti oli neil patsientidel veres vähenenud mitteklassikaliste monotsüütide arv ning mikrogliia retseptori CSF1R tase. Loommudelites leidsime, et CSF1R-i inhibiitor põhjustas ärevust ja häiris mikrogliia/makrofaagide vaskulaarset seostumist. Peale selle leidsime, et haistesibulas oli rohkesti veresoontega seotud mikrogliiat/ makrofaage ning antud piirkond oli rikastatud rasvhapete metabolismi ja angiogeneesi geenidega. Lisaks ilmnes, et endogeenseid n-3 PUFA-sid tootvatel fat-1 hiirtel ei avaldu OBX-indutseeritud stressireaktsioonid. Need leiud viitavad sellele, et mikrogliia modulaatorid võivad tänu ajuveresoonkonna efektiivsemale reguleerimisele aidata skisofreenia haigetel stressiga paremini toime tulla. Meie uuringud annavad uudseid teadmisi mikrogliia/monotsüütiliste alampopulatsioonide ja nende kandidaatmolekulide kohta, mis võivad olla kasulikud, et paremini mõista skisofreenia kujunemise ja haigustunnuste püsimise patofüsioloogilisi mehhanisme ja seeläbi töötada välja uusi ravivõimalusi.

ACKNOWLEDGEMENTS

Firstly, I would like to express my deepest gratitude and appreciation to my supervisor Professor Li Tian for her invaluable guidance and support throughout my dissertation. Her expertise, insightful feedback, and constructive criticism have helped shape and refine my research, enabling me to grow as a scholar. Her wealth of knowledge, patience, and willingness to engage in countless discussions have been instrumental in expanding my understanding of the subject matter.

Additionally, I am immensely thankful to my co-supervisors, Professors Cai Song and Eero Vasar, for their support of my study, especially Professor Cai Song for her valuable guidance and support on me since the beginning of my academic journey.

I am very grateful for the medical staff and students at Beijing Huilongguan Hospital whose commitment to participants' recruitment and clinical investigations are of utmost importance for shaping my thesis work. I also give my special thanks to colleagues in Guangdong Ocean University for their support on my thesis work. I highly appreciate all co-authors of my published papers, who played a remarkably important part in creating these stories.

I am truly thankful for Fang-Ling Xuan and Keerthana Chithanathan, who were always there helping me with commitment, friendship, and enthusiasm. I learned a lot from you and will remember this journey with wonderful memories.

I would like to thank Professor Alexander Zharkovsky for his kind support and collaboration on my research projects. I give my special thanks to Dr. Mohan Jayaram for supervising me with animal experiments and encouraging words. I also extend my sincere thanks to those colleagues in the Department of Physiology who created a warm, welcoming, and kind atmosphere for me. Their support and camaraderie have enriched my research experience and made it an unforgettable journey.

I would like to humbly express my unstoppable gratitude to all volunteers who participated in clinical studies and laboratory mice that were sacrificed in preclinical studies. This project could not have happened without their vulnerability.

I would also like to reveal my great appreciation to the peer reviewers Liina Haring and Martti Laan for taking their precious time to give me useful and valuable suggestions on this thesis. Likewise, I am truly glad to extend my genuine acknowledgments to Urtė Neniškytė for being my opponent and helping me to finalize this academic period.

Last but not least, I would like to full-heartedly thank my family and friends for their unwavering support, understanding, and encouragement throughout my life. Their belief in my abilities and willingness to offer a listening ear during challenging moments of my life have been gemstones to me.

SUPPLEMENTARY MATERIALS

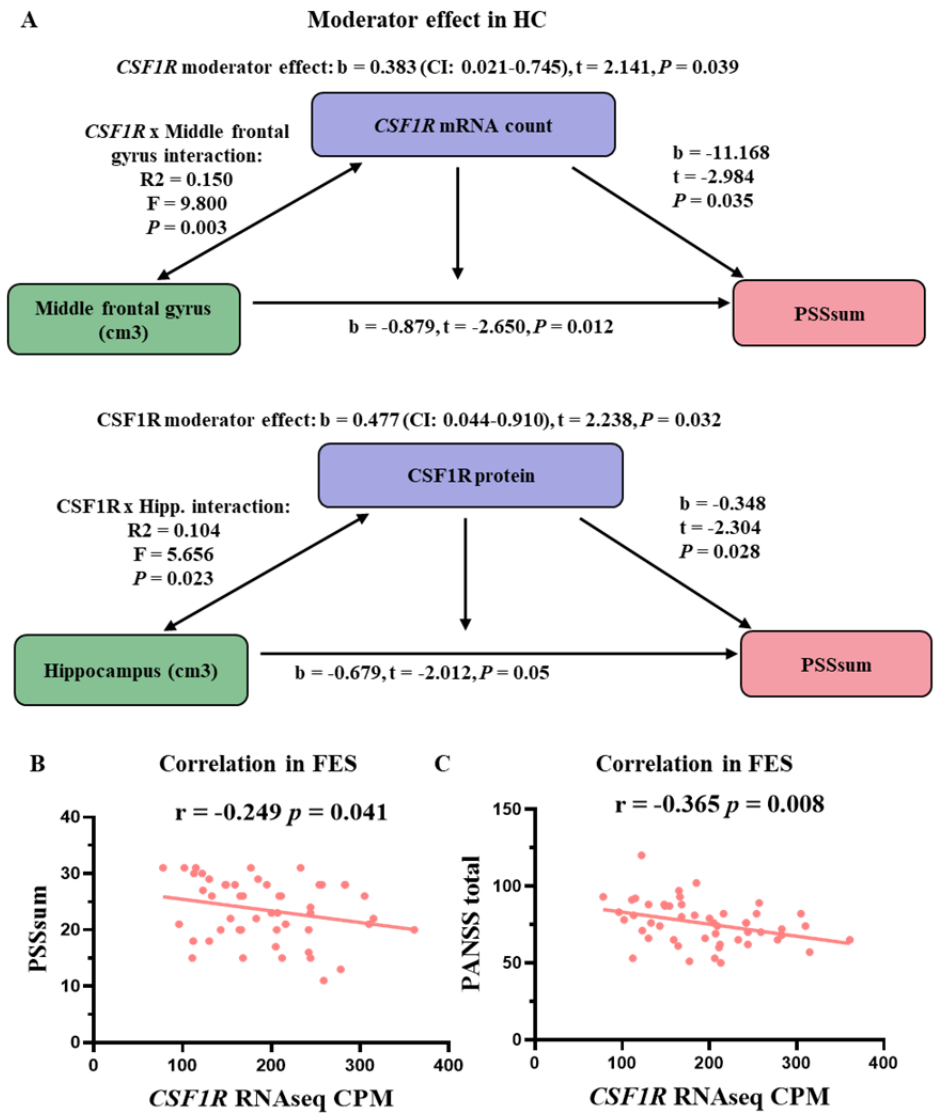

Figure S1. Colony stimulating factor 1 receptor (CSF1R) facilitated negative associations of brain structures with perceived stress scale (PSS) scores in healthy controls (HCs) and was negatively associated with stress perception and psychosis in first episode schizophrenia (FES) patients. (**A**) In HCs, blood CSF1R mRNA and protein moderated the negative associations of the volumes of the middle frontal gyrus and hippocampus (HPC) (independent variables) with the PSS score (dependent variable), respectively, controlled by age, sex, and ICV (n = 41). (**B&C**) In FES patients, blood *CSF1R* mRNA counts (count per million, CPM) were negatively correlated with PSS scores and PANSS total scores (n = 51) (Spearman's correlation).

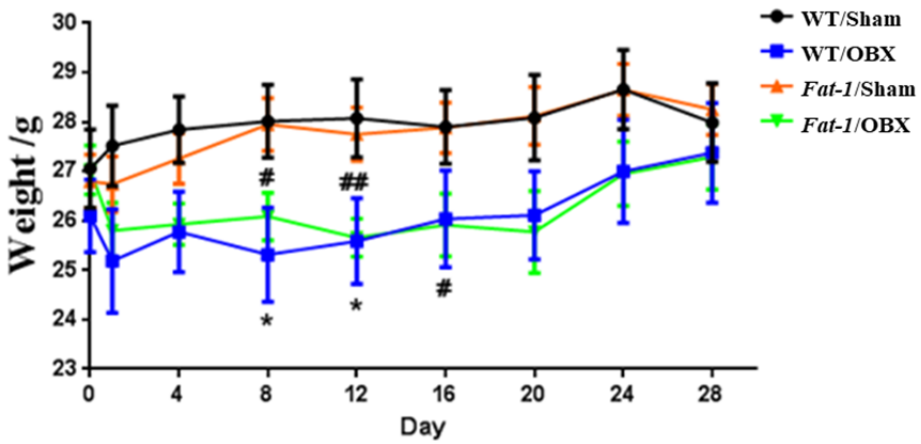

Figure S2. Body weights of mice post olfactory bulbectomy (OBX) operation (*p < 0.05 wild type (WT)/OBX *vs* WT/Sham; #p < 0.05, ##p < 0.01 Fat-1/OBX *vs* Fat-1/Sham, repeated ANOVA, n = 5 per group).

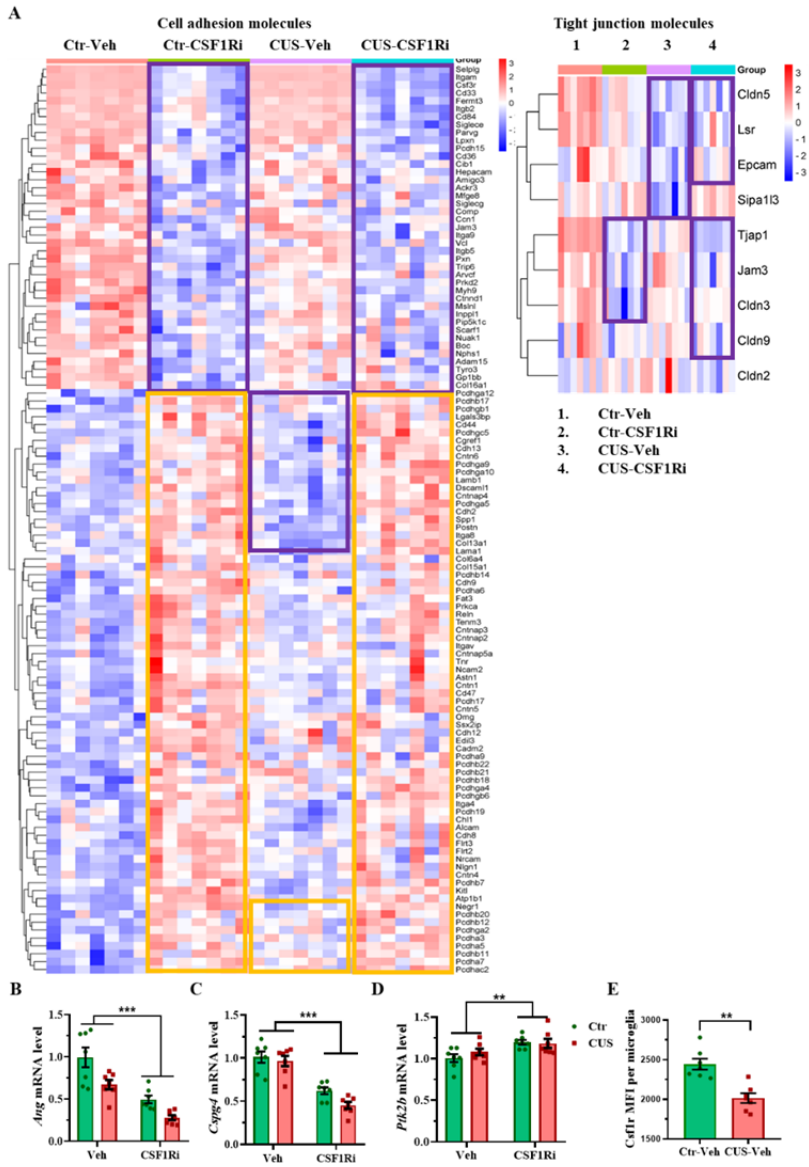

Figure S3. Chronic unpredictable stress (CUS) or CSF1R inhibitor (CSF1Ri) affected expression of differentially expressed gene (DEG)s mediating cell adhesion and colony stimulating factor 1 receptor (Csf1r) in the mouse prefrontal cortex (PFC). (**A**) RNA-seq heatmap of cell adhesion and tight junction molecules differentially expressed among 4 groups in the PFC, most of which were downregulated after CSF1Ri or CUS-CSF1Ri combination. Downregulated (in purple frame) and upregulated (in orange frame) genes are highlighted in the heatmap (n = 7). The mRNA expression of (**B**) *Ang*, (**C**) *Cspg4* and (**D**) *Ptk2b*. (**E**) Csf1r MFI expressed on each hippocampal microglia. Data are presented as mean ± standard error of mean; Two-way ANOVA with Bonferroni's correction (n = 9-10).

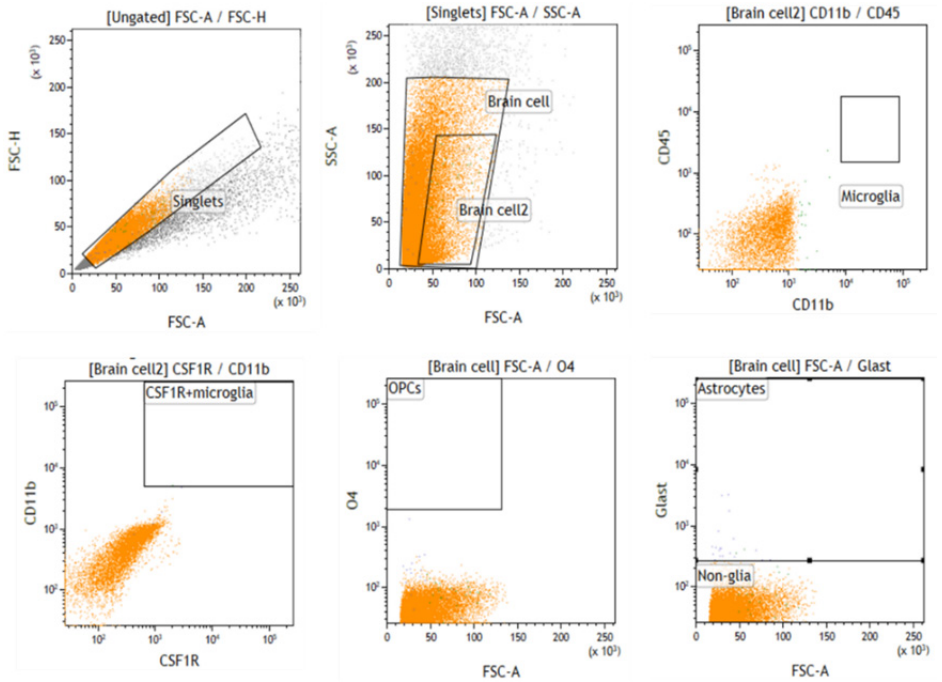

Figure S4. Representative dot plots of negative controls for murine glial populations used in flow cytometric analysis. Representative plots showing negative staining by isotype control antibodies for flow markers of microglia (CD11b-iso & CD45-iso), colony stimulating factor 1 receptor $(CSF1R)^{+}$ microglia (CSF1R-iso), oligodendrocyte precursor cell (OPCs) (O4-iso), and astrocytes (Glast-iso) analyzed by flow cytometry.

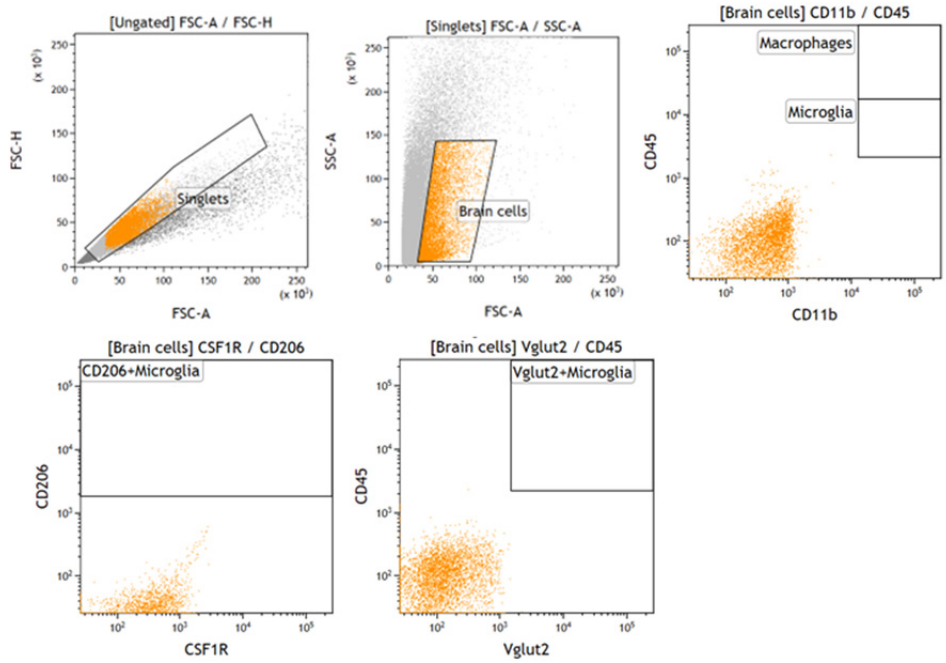

Figure S5. Representative dot plots of negative controls for Vglut2 in murine microglia used in flow cytometric analysis. Representative plots showing negative staining by isotype control antibodies for flow markers of microglia (CD11b-iso & CD45-iso), $CD206^{+}$ microglia (CD206-iso) and Vglut2 (Vglut2-iso) analyzed by flow cytometry.

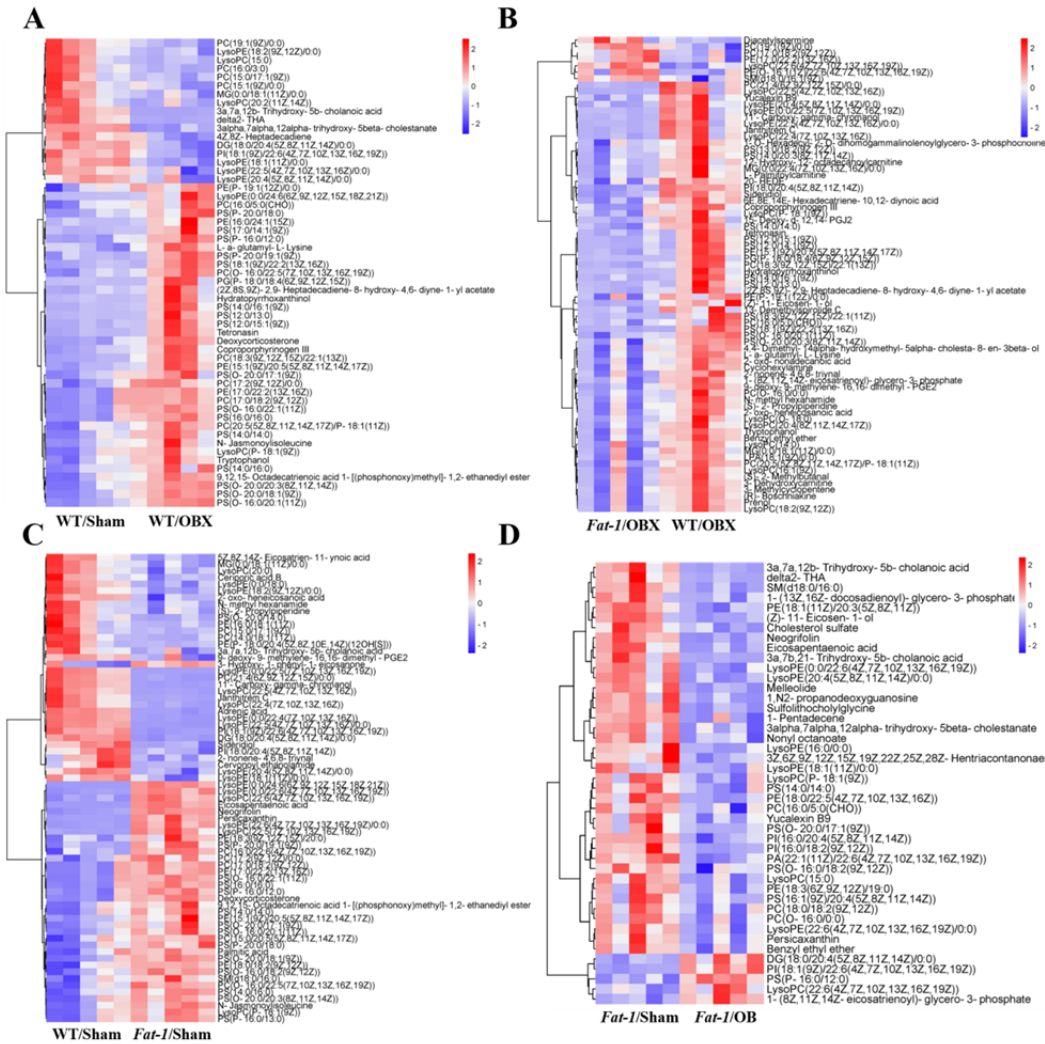

Figure S6. Heat maps of serum lipid metabolites in mice of wild type (WT)/olfactory bulbectomy (OBX), WT/Sham, Fat-1/OBX, and Fat-1/Sham groups. (**A**) WT/Sham *vs* WT/OBX, (**B**) Fat-1/OBX *vs* WT/OBX, (**C**) WT/Sham *vs* Fat-1/ Sham, (**D**) Fat-1/Sham *vs* Fat-1/OBX (*n* = 5 per group).

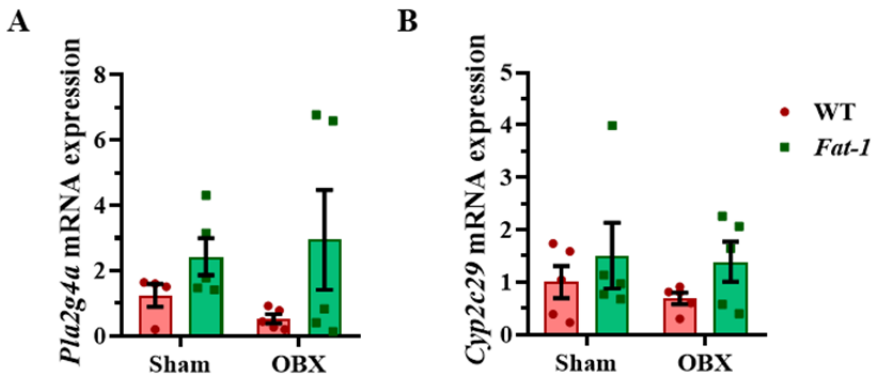

Figure S7. Inflammatory mediators involved in lipid metabolic pathways in wild type (WT)/olfactory bulbectomy (OBX), WT/Sham, Fat-1/OBX, and Fat-1/Sham mice. (**A&B**) mRNA expressions of P*la2g4a* and *Cyp2c29*. Data are presented as mean ± standard error of mean, two-way ANOVA with Tukey's correction, $n = 5$ per group.

ORIGINAL PUBLICATIONS

CURRICULUM VITAE

Name: Ling Yan
Date of Birth: September 26, 1990, China
Address: Ravila 14b, 50411, Tartu, Estonia
E-mail: ling.yan@ut.ee, lingy517@gmail.com

Education:

2021–present	**PhD.** in Neurosciences, University of Tartu, Faculty of Medicine, Estonia
2016–2019	**MSc.** in Food Science and Engineering, Guangdong Ocean University, Institute of Marine Drugs and Nutrition, China
2008–2012	**BSc.** in Pharmacy, Binzhou Medical University, Faculty of Pharmacy, China

Career:

2012–2016	**Associate Scientist** in Huaxia Shengsheng Pharmaceutical Industry (Beijing) Co., Ltd.
2019–2021	**Specialist** in Institute of Biomedicine and Translational Medicine, University of Tartu.

Professional Courses and Conferences

2023	Competence course in laboratory animal science, Tartu
2022	MIND & BRAIN – 61st International Neuropsychiatric Congress, online
2021	MIND & BRAIN – 60st International Neuropsychiatric Congress, online
2018	8th MBI Symposium – Confirmation of Symposium Presentation, China
2016	Brain and immune interactions: behavior, stress, brain disease, drugs and nutrition, China

List of Pubication

1. **Yan L**, Gu MQ, Yang ZY, Xia J, Li P, Vasar E, Tian L, Song C. (2021) Endogenous n-3 PUFAs attenuated olfactory bulbectomy-induced behavioral and metabolomic abnormalities in Fat-1 mice. Brain Behavior and Immunity. 96:143–153. doi: 10.1016/j.bbi.2021.05.024.
2. **Yan L***, Li Y*, Feng W, Chithanathan K, Li W, Huang J, Li H, Chen W, Tian B, Wang Z, Tan S, Zharkovsky A, Hong LE, Tan Y, Tian L. (2023) CSF1R regulates schizophrenia-related stress response and vascular association of microglia/macrophages. BMC Medicine. 21(1):286. doi: 10.1186/s12916-023-02959-8
3. **Yan L***, Xuan FL**,** Chen S, Gou M, Chen W, Li Y, Wang Z, Wang L, Xie T, Fan F, Zharkovsky A, Tan Y, Tian L. (2023) Replenished Microglia

Partially Rescue Schizophrenia-Related Stress Response. Frontiers in Cellular Neuroscience. 17:1254923. doi: 10.3389/fncel.2023.1254923.
4. **Yan L**, Jayaram M, Chithanathan K, Zharkovsky A, Tian L. (2021) Sex-specific microglial activation and SARS-CoV-2 receptor expression induced by chronic unpredictable stress. Frontiers in Cellular Neuroscience. 15:750373. doi: 10.3389/fncel.2021.750373.
5. Xuan FL, **Yan L***, Li Y, Fan F, Deng H, Gou M, Chithanathan K, Heinla I, Yuan L, Seppa K, Zharkovsky A, Kalda A, Hong LE, Hu GF, Tan Y, Tian L. (2022) Glial receptor PLXNB2 regulates schizophrenia-related stress perception via the amygdala. Frontiers in Immunology. 13:1005067. doi:10.3389/fimmu.2022.1005067.
6. Li K, **Yan L***, Zhang Y, Yang Z, Zhang C, Li Y, Kalueff AV, Li W, Song C. (2020) Seahorse treatment improves depression-like behavior in mice exposed to CUMS through reducing inflammation/oxidants and restoring neurotransmitter and neurotrophin function. Journal of Ethnopharmacology, 250:112487. doi: 10.1016/j.jep.2019.112487.
7. Zhang Y, Yin J, Yan H, **Yan L**, Li Y, Zhang C, Li Y, Liu B, Lin J, Zhang L, Hu Song C. (2023) Correlations between omega-3 fatty acids and inflammatory/glial abnormalities: the involvement of membrane and neurotransmitter dysfunction in Schizophrenia. Frontiers in Cellular Neuroscience. 17:1163764. doi: 10.3389/fncel.2023.1163764
8. Chen S, Fan F, Xuan FL, **Yan L**, Xiu M, Fan H, Cui Y, Zhang P, Yu T, Yang F, Tian B, Hong LE, Tan Y, Tian L. (2022) Monocytic subsets impact cerebral cortex and cognition: differences between healthy subjects and patients with first-episode schizophrenia. Frontiers in Immunology. 13:900284. doi: 10.3389/fimmu.2022.900284.
9. Chithanathan K, Jürgenson M, Guha M, **Yan L**, Žarkovskaja T, Pook M, Magilnick N, Boldin MP, Rebane A, Tian L, Zharkovsky A (2022) Paradoxical attenuation of neuroinflammatory response upon LPS challenge in miR-146b deficient mice. Frontiers in Immunology. 13:996415. doi: 10.3389/fimmu.2022.996415.
10. Pan S, Zhou Y, **Yan L**, Xuan F, Tong J, Li Y, Huang J, Feng W, Chen S, Cui Y, Yang F, Tan S, Wang Z, Tian B, Hong LE, Tan YL, Tian L. (2022) TGF-β1 is associated with deficits in cognition and cerebral cortical thickness in first-episode schizophrenia. Journal of Psychiatry and Neuroscience. 47(2):E86–E98. doi: 10.1503/jpn.210121.
11. Chithanathan K, Somelar K, Jürgenson M, Žarkovskaja T, Periyasamy K, **Yan L**, Magilnick N, Boldin MP, Rebane A, Tian L, Zharkovsky A. (2022) Enhanced Cognition and Neurogenesis in miR-146b Deficient Mice. Cells. 11(13):2002. doi: 10.3390/cells11132002.
12. Gu M, Li X, **Yan L**, Zhang Y, Yang L, Li S, Song C. (2021) Endogenous ω-3 fatty acids in Fat-1 mice attenuated depression-like behaviors, spatial memory impairment and relevant changes induced by olfactory bulbectomy. Prostaglandins, Leukotrienes & Essential Fatty Acids. 171:102313. doi: 10.1016/j.plefa.2021.102313.

13. Peng Z, Zhang C, **Yan L**, Zhang Y, Yang Z, Wang J, Song C. (2020) EPA is More Effective than DHA to Improve Depression-Like Behavior, Glia Cell Dysfunction and Hippcampal Apoptosis Signaling in a Chronic Stress-Induced Rat Model of Depression. International journal of molecular sciences. 21(5):1769. doi: 10.3390/ijms21051769.
14. Liu D, **Yan L**, Ma L, Huang Y, Pan X, Liu W, Lv Z. (2015) Diphenyl derivatives from coastal saline soil fungus *Aspergillus iizukae*. Archives of Pharmacal Research. 38(6):1038–1043. doi: 10.1007/s12272-014-0371-z.
15. **Yan L**, Yang Z, Huang W, Zhang Y, Yang W, Liu Y, Zhang Y, Cui Y, Song C. (2019) Anti-inflammatory and Nitric Oxide (NO) Release Effects of Hippocampus erectus Ethanol Extracts on Lipopolysaccharide-induced BV2 Microglia. Journal of Guangdong Ocean University. 39(01):90–96. (Chinese) doi: 10.3969/j.issn.1673-9159.2019.01.014
16. Liu D, **Yan L**, Han J. (2012) Extraction, Identification and Content Determination of Polysaccharides from the Leaves of Prunus pseudocerasus Lindl. Journal of Anhui Agricultural Sciences. 40(21):10861–10562.
17. Liu D, Liu W, **Yan L**. (2012) Antioxidative effect of Prunus pseudocerasus Lindl. polysaccharide in vitro. Chinese Journal of Biochemical Pharmaceutics. 33(5):571–574.

ELULOOKIRJELDUS

Nimi: Ling Yan
Sünniaeg: 26. september 1990, Hiina
Aadress: Ravila 14b, Tautu 50411, Eesti
E-mail: ling.yan@ut.ee, lingy517@gmail.com

Haridustee:

2021–present	**PhD.** neuroteadused, Tartu Ülikool, Meditsiiniteaduste valdkond, Eesti
2016–2019	**MSc.** toiduainete teaduse ja inseneri erialal, Guangdongi ookeaniülikool, mereravimite ja toitumise instituut, Hiina
2008–2012	**BSc.** farmaatsia erialal, Binzhou meditsiiniülikool, farmaatsiateaduskond, Hiina

Teenistuskäik:

2012–2016	**Abiteadlane**, Huaxia Shengsheng farmaatsiatööstuse (Peking) co., Ltd.
2019–2021	**Spetsialist**, Tartu Ülikooli Bio- ja siirdemeditsiini instituut.

Erialane enesetäiendus:

2023	Laboriloomateaduse pädevuskursus, Tartu
2022	MIND & BRAIN – 61. rahvusvaheline neuropsühhiaatria kongress, veebipõhine
2021	MIND & BRAIN – 60. rahvusvaheline neuropsühhiaatria kongress, veebipõhine
2018	8. MBI sümpoosion – sümpoosioni esitluse kinnitamine, Hiina
2016	Aju ja immuunsüsteemi koostoimed: käitumine, stress, ajuhaigused, ravimid ja toitumine, Hiina

Publikatsioonid:

1. **Yan L**, Gu MQ, Yang ZY, Xia J, Li P, Vasar E, Tian L, Song C. (2021) Endogenous n-3 PUFAs attenuated olfactory bulbectomy-induced behavioral and metabolomic abnormalities in Fat-1 mice. Brain Behavior and Immunity. 96:143-153. doi: 10.1016/j.bbi.2021.05.024.
2. **Yan L***, Li Y*, Feng W, Chithanathan K, Li W, Huang J, Li H, Chen W, Tian B, Wang Z, Tan S, Zharkovsky A, Hong LE, Tan Y, Tian L. (2023) CSF1R regulates schizophrenia-related stress response and vascular association of microglia/macrophages. BMC Medicine. 21(1):286. doi: 10.1186/s12916-023-02959-8
3. **Yan L***, Xuan FL***,** Chen S, Gou M, Chen W, Li Y, Wang Z, Wang L, Xie T, Fan F, Zharkovsky A, Tan Y, Tian L. (2023) Replenished Microglia Partially Rescue Schizophrenia-Related Stress Response. Frontiers in Cellular Neuroscience. 17:1254923. doi: 10.3389/fncel.2023.1254923.

4. **Yan L**, Jayaram M, Chithanathan K, Zharkovsky A, Tian L. (2021) Sex-specific microglial activation and SARS-CoV-2 receptor expression induced by chronic unpredictable stress. Frontiers in Cellular Neuroscience. 15:750373. doi: 10.3389/fncel.2021.750373.
5. Xuan FL, **Yan L***, Li Y, Fan F, Deng H, Gou M, Chithanathan K, Heinla I, Yuan L, Seppa K, Zharkovsky A, Kalda A, Hong LE, Hu GF, Tan Y, Tian L. (2022) Glial receptor PLXNB2 regulates schizophrenia-related stress perception via the amygdala. Frontiers in Immunology. 13:1005067. doi:10. 3389/fimmu.2022.1005067.
6. Li K, **Yan L***, Zhang Y, Yang Z, Zhang C, Li Y, Kalueff AV, Li W, Song C. (2020) Seahorse treatment improves depression-like behavior in mice exposed to CUMS through reducing inflammation/oxidants and restoring neurotransmitter and neurotrophin function. Journal of Ethnopharmacology, 250:112487. doi: 10.1016/j.jep.2019.112487.
7. Zhang Y, Yin J, Yan H, **Yan L**, Li Y, Zhang C, Li Y, Liu B, Lin J, Zhang L, Hu Song C. (2023) Correlations between omega-3 fatty acids and inflammatory/glial abnormalities: the involvement of membrane and neurotransmitter dysfunction in Schizophrenia. Frontiers in Cellular Neuroscience. 17:1163764. doi: 10.3389/fncel.2023.1163764
8. Chen S, Fan F, Xuan FL, **Yan L**, Xiu M, Fan H, Cui Y, Zhang P, Yu T, Yang F, Tian B, Hong LE, Tan Y, Tian L. (2022) Monocytic subsets impact cerebral cortex and cognition: differences between healthy subjects and patients with first-episode schizophrenia. Frontiers in Immunology. 13:900284. doi: 10.3389/fimmu.2022.900284.
9. Chithanathan K, Jürgenson M, Guha M, **Yan L**, Žarkovskaja T, Pook M, Magilnick N, Boldin MP, Rebane A, Tian L, Zharkovsky A (2022) Paradoxical attenuation of neuroinflammatory response upon LPS challenge in miR-146b deficient mice. Frontiers in Immunology. 13:996415. doi: 10.3389/fimmu.2022.996415.
10. Pan S, Zhou Y, **Yan L**, Xuan F, Tong J, Li Y, Huang J, Feng W, Chen S, Cui Y, Yang F, Tan S, Wang Z, Tian B, Hong LE, Tan YL, Tian L. (2022) TGF-β1 is associated with deficits in cognition and cerebral cortical thickness in first-episode schizophrenia. Journal of Psychiatry and Neuroscience. 47(2):E86–E98. doi: 10.1503/jpn.210121.
11. Chithanathan K, Somelar K, Jürgenson M, Žarkovskaja T, Periyasamy K, **Yan L**, Magilnick N, Boldin MP, Rebane A, Tian L, Zharkovsky A. (2022) Enhanced Cognition and Neurogenesis in miR-146b Deficient Mice. Cells. 11(13):2002. doi: 10.3390/cells11132002.
12. Gu M, Li X, **Yan L**, Zhang Y, Yang L, Li S, Song C. (2021) Endogenous ω-3 fatty acids in Fat-1 mice attenuated depression-like behaviors, spatial memory impairment and relevant changes induced by olfactory bulbectomy. Prostaglandins, Leukotrienes & Essential Fatty Acids. 171:102313. doi: 10.1016/j.plefa.2021.102313.
13. Peng Z, Zhang C, **Yan L**, Zhang Y, Yang Z, Wang J, Song C. (2020) EPA is More Effective than DHA to Improve Depression-Like Behavior, Glia

Cell Dysfunction and Hippcampal Apoptosis Signaling in a Chronic Stress-Induced Rat Model of Depression. International journal of molecular sciences. 21(5):1769. doi: 10.3390/ijms21051769.
14. Liu D, **Yan L**, Ma L, Huang Y, Pan X, Liu W, Lv Z. (2015) Diphenyl derivatives from coastal saline soil fungus *Aspergillus iizukae*. Archives of Pharmacal Research. 38(6):1038–1043. doi: 10.1007/s12272-014-0371-z.
15. **Yan L**, Yang Z, Huang W, Zhang Y, Yang W, Liu Y, Zhang Y, Cui Y, Song C. (2019) Anti-inflammatory and Nitric Oxide (NO) Release Effects of Hippocampus erectus Ethanol Extracts on Lipopolysaccharide-induced BV2 Microglia. Journal of Guangdong Ocean University. 39(01):90–96. (Chinese) doi: 10.3969/j.issn.1673-9159.2019.01.014
16. Liu D, **Yan L**, Han J. (2012) Extraction, Identification and Content Determination of Polysaccharides from the Leaves of Prunus pseudocerasus Lindl. Journal of Anhui Agricultural Sciences. 40(21):10861–10562.
17. Liu D, Liu W, **Yan L**. (2012) Antioxidative effect of Prunus pseudocerasus Lindl. polysaccharide in vitro. Chinese Journal of Biochemical Pharmaceutics. 33(5):571–574.

DISSERTATIONES NEUROSCIENTIAE UNIVERSITATIS TARTUENSIS

1. **Sirli Raud.** Cholecystokinin$_2$ receptor deficient mice: changes in function of GABA-ergic system. Tartu, 2005.
2. **Kati Koido.** Single-nucleotide polymorphism profiling of 22 candidate genes in mood and anxiety disorders. Tartu, 2005.
3. **Dzhamilja Safiulina.** The studies of mitochondria in cultured cerebellar granule neurons: characterization of mitochondrial function, volume homeostasis and interaction with neurosteroids. Tartu, 2006.
4. **Tarmo Areda.** Behavioural and neurogenetic study of mechanisms related to cat odour induced anxiety in rodents. Tartu, 2006.
5. **Aleksei Nelovkov.** Behavioural and neurogenetic study of molecular mechanisms involved in regulation of exploratory behaviour in rodents. Tartu, 2006.
6. **Annika Vaarmann**. The studies on cystatin B deficient mice: neurochemical and behavioural alterations in animal model of progressive myoclonus epilepsy of Unverricht-Lundborg type. Tartu, 2007.
7. **Urho Abramov.** Sex and environmental factors determine the behavioural phenotype of mice lacking CCK_2 receptors: implications for the behavioural studies in transgenic lines. Tartu, 2008.
8. **Hendrik Luuk.** Distribution and behavioral effects of WFS1 protein in the central nervous system. Tartu, 2009.
9. **Anne Must.** Studies on molecular genetics of male completed suicide in Estonian population. Tartu, 2009.
10. **Kaido Kurrikoff**. Involvement of cholecystokinin in chronic pain mechanisms and endogenous antinociception. Tartu, 2009.
11. **Anu Aonurm-Helm.** Depression-like phenotype and altered intracellular signalling in neural cell adhesion molecule (NCAM)-deficient mice. Tartu, 2010.
12. **Silva Sütt.** Role of endocannabinoid system and *Wfs1* in regulation of emotional behaviour: behavioural, pharmacological and genetic studies. Tartu, 2010.
13. **Mari-Anne Philips.** Characterization of *Myg1* gene and protein: expression patterns, subcellular localization, gene deficient mouse and functional polymorphisms in human. Tartu, 2010.
14. **Ranno Rätsep.** Genetics of psoriasis and vitiligo, focus on IL10 family cytokines. Tartu, 2010.
15. **Kairit Joost.** Selective screening of metabolic diseases in Estonia: the application of new diagnostic methods. Tartu, 2012, 143 p.
16. **Monika Jürgenson.** A complex phenotype in mice with partial or complete deficiency of the NCAM protein. Tartu, 2012, 117 p.

17. **Ene Reimann.** Description of the cytokines and cutaneous neuroendocrine system in the development of vitiligo. Tartu, 2012, 117 p.
18. **Jürgen Innos.** Behavioural, pharmacological and neurochemical characterisation of limbic system-associated membrane protein (LSAMP) deficient mice. Tartu, 2013, 113 p.
19. **Kaili Anier.** The role of DNA methylation in the development of cocaine-induced behavioural sensitisation. Tartu, 2013, 147 p.
20. **Maarika Liik.** Cognitive functioning, perceived cognition, subjective complaints and symptoms of depression in patients with epilepsy: neuropsychological assessment and spet brain imaging study. Tartu, 2014, 124 p.
21. **Sten Ilmjärv.** Estimating differential expression from multiple indicators. Tartu, 2015, 125 p.
22. **Paula Reemann.** The effects of microenvironment on skin cells. Tartu, 2015, 146 p.
23. **Tanel Visnapuu.** Pharmacological and behavioral characterization of the monoaminergic and GABA-ergic systems of Wfs1-deficient mice. Tartu, 2015, 107 p.
24. **Indrek Heinla.** Behavioural and genetic comparison of B6 and 129Sv mouse lines focusing on the anxiety profile and the expression of *Lsamp* gene. Tartu, 2016, 115 p.
25. **Liina Haring.** Cognitive functioning after first psychotic episode. Tartu, 2017, 146 p.
26. **Triin Tekko.** Neurodevelopmental Approach in the Study of the Function of *Wfs1* and *Lsamp*, Potential Targets in the Regulation of Emotional Behaviour. Tartu, 2018, 194 p.
27. **Alina Altpere.** Targeting of mechanisms of elevated anxiety in female Wfs1-deficient mice. Tartu, 2018, 98 p.
28. **Maarja Toots.** Pharmacological challenge in rodent models of Wolfram syndrome with emphasis on diabetic phenotype. Tartu, 2018, 114 p.
29. **Katyayani Singh.** Neuropsychiatric endophenotypes – focusing on IgLON adhesion molecules in the mouse brain. Tartu, 2019, 148 p.
30. **Kattri-Liis Eskla.** Therapeutic strategies for ischemia reperfusion injury. Tartu, 2019, 138 p.
31. **Hardo Lilleväli**. Hyperphenylalaninaemias and neurophysiological disorders associated with the condition. Tartu, 2020, 134 p.
32. **Roman Balõtšev**. Interaction between the immune and metabolic systems in different stages of schizophrenia spectrum disorders. Tartu, 2020, 164 p.
33. **Mari Urb**. DNA methylation in the predisposition, expression and abstinence of cocaine addiction. Tartu, 2020, 147 p.
34. **Liisa Leppik.** Alterations in metabolomic profile of lipids, amino acids and biogenic amines in the early course of schizophrenia spectrum disorders. Tartu, 2021, 173 p.
35. **Kadri Seppa.** The neuroprotective effect of GLP-1 receptor agonist liraglutide in a rat model of Wolfram syndrome. Tartu, 2021, 154 p.

36. **Akbar Zeb.** The novel mechanisms of Parkin-dependent mitophagy. Tartu, 2022, 146 p.
37. **Aleksandr Bregin.** Alterations of emotional behaviour induced by the genetic invalidation of the limbic system associated membrane protein (Lsamp) – potential implications for neuropsychiatric disorders. Tartu, 2022, 176 p.
38. **Jane Varul.** Different stress coping strategies of 129Sv and C57/Bl6 mouse strains – evidence from behavioural, pharmacological, metabolomics and gene expression studies. Tartu, 2022, 177 p.
39. **Maria Kaare.** The involvement of NEGR1 and LSAMP in the psychiatric disorders are mediated through monoaminergic neurotransmission and changes in the systemic metabolism. Tartu, 2023, 164 p.
40. **Maria Piirsalu.** Effects of inflammation and diet on the metabolic profile and selected genetic parameters of Bl6 and 129Sv mouse lines. Tartu, 2023, 183 p.
41. **Taavi Vanaveski.** Modelling the quantitative nature of neuropsychiatric disorders in animal models: metabolic, behavioural, and genetic profiles. Tartu, 2023, 165 p.
42. **Keiu Heinla.** Effects of GLP-1 receptor agonists on pituitary and adrenal hormones. Tartu, 2023, 119 p.